STUDIES ON INITIATING SPECIES IN RADIATION-INDUCED IONIC POLYMERIZATION OF NITROETHYLENE

HITOSHI YAMAOKA

Department of Polymer Chemistry
Kyoto University

STUDIES ON INITIATING SPECIES IN RADIATION-INDUCED IONIC POLYMERIZATION OF NITROETHYLENE

HITOSHI YAMAOKA

Department of Polymer Chemistry

Kyoto University

PREFACE

The present thesis is a collection of studies done under the direction of Professor Seizo Okamura during 1964-1968. The studies on the present theme are still being carried out; however, the results obtained are put on record as an indication of the author's achievement so far.

The studies are mostly concerned with chemical reactions induced by ionizing radiation. They are grouped into three parts as follows:

1. Radiation-induced polymerization of nitroethylene,
2. Mass spectrometric study on negative ion-molecule reactions of nitroethylene,
3. Mass spectrometric study on primary processes of radiation-induced reaction.

The first deals with the reaction mechanism of radiation-induced polymerization of nitroethylene, paying particular attention to the initiation process of polymerization. The second is concerned with negative ion formations and negative ion-molecule reactions of nitroethylene for the purpose of elucidating the initiating species of polymerization. This was carried out with the help of Dr. Sugiura at Takasaki Radiation Chemistry Research Establishment, Japan

Atomic Energy Research Institute. The last is on processes of collision-induced dissociation of acetylene ions in order to study the dissociative states of molecular ions. This was done under the guidance of Professor Durup at the Laboratory of Physical Chemistry, University of Paris.

It is a great pleasure for the author to have the opportunity to record here his profound gratitude to Professor Seizo Okamura and Professor Koichiro Hayashi of Hokkaido University for their valuable advice and continuous encouragement throughout the work. The author wishes to extend his appreciation to Dr. Toshio Sugiura and Professor Jean Durup for their constant guidance and helpful suggestions.

The author is also thankful to Messrs. Ryuji Uchida, Katsuo Nishiyama, Tetsuo Shiga, Ryozo Mazume, Isamu Obama, and Hiroaki Mori for their active collaboration in the course of experiments, and to Professor Ffrancon Williams of University of Tennessee, Dr. Hiroshi Yoshida, Messrs. Hideo Kamiyama, Kanae Hayashi, Kozo Tsuji, and Katsuji Ueno for their helpful discussions.

Hitoshi Yamaoka

Department of Polymer Chemistry
Kyoto University
November 1969

CONTENTS

P A R T 1

GENERAL INTRODUCTION

Experimental evidence of radiation-induced ionic polymerization was first provided in 1957 by Worrall et al.[1] They reported that purified isobutene readily polymerized at -78°C through cationic mechanism by the irradiation of high energy electrons. In 1958, Okamura et al.[2] found that the solution polymerization of styrene at -78°C also proceeded through cationic mechanism by the use of suitable solvents such as chlorinated hydrocarbons. Similar experiments were carried out quite independently by Chapiro[3] and Abkin.[4] In those days, one of the experimental requirements for radiation-induced ionic polymerization was generally thought to decrease the polymerization temperature in order to sustain the lifetime of ionic initiating species.

In recent years, however, conclusive evidence for the occurrence of ionic polymerization at room temperature or above has been accumulated in the polymerization of extremely dried systems.[5] The pioneering study on the polymerization of extremely dried α-methylstyrene was reported in 1960 by Williams and his co-corkers.[6] They have extensively developed the same line of work to the polymerization kinetics of various monomer systems. Furthermore, Ueno et al.[7] and Metz et al.[8] found that the bulk polymerization of styrene at room temperature was critically dependent on the technique of drying the monomer. More recently,

Cordischi et al.[9] reported that the polymerization of 1,2-cyclohexene oxide was enhanced by the use of careful purification methods.

Extensive studies on the polymerization of extremely dried monomers have also provided information about the propagation rate constant of radiation-induced ionic polymerization. The estimation method of the propagation rate constant was first proposed for the polymerization of cyclopentadiene by the competitive kinetic method based on the retarding effect of ammonia.[10] The rate constants of α-methylstyrene[11] and styrene[12] were also determined by a similar method. Another attempt to estimate the propagation rate constant was made by electroconductivity measurements during the continuous irradiation of polymerization systems by Ka. Hayashi et al.[13] The propagation rate constants obtained in the above-mentioned investigations were generally much larger than those in conventional ionic polymerizations. It was therefore suggested that the radiation-induced ionic polymerization was largely caused by free ions.

Compared with the studies of cationic polymerizations mentioned above, much less information is available on the radiation-induced anionic polymerization. Okamura et al.[14] first observed the anionic propagation in solution polymerizations of acrylonitrile and methylmethacrylate in amines at

$-78^{\circ}C$. However, the reaction mechanism is not yet clear, although some researchers have since carried out studies on radiation-induced anionic polymerization, mostly using acrylonitrile.[5)]

One of the main purposes of the present thesis is to elucidate the reaction mechanism of radiation-induced anionic polymerization using nitroethylene which is known, as a monomer, to be extremely susceptible to anionic polymerization.

The kinetics of radiation-induced polymerization of nitroethylene is studied and the consideration on the reaction mechanism of this polymerization is made in Part 2 of the present thesis.

The solution polymerization in tetrahydrofuran at $-78^{\circ}C$ is carried out to obtain the general features of radiation-induced polymerization of nitroethylene. By the effects of additives and the copolymerization with acrylonitrile, the anionic propagation in this system is confirmed in Chapter 1.

In order to compare the propagation rate constant of nitroethylene with the results of radiation-induced cationic polymerization of various monomers, the bulk polymerization in extremely dried systems is investigated at room temperature. The experimental results are described in Chapters 2 and 3. In Chapter 2, the additive effect of

hydrogen bromide as a polymerization retarder is examined, and an attempt to estimate the propagation rate constant is made. In Chapter 3, the dose rate dependence on the rate of polymerization is studied. The obtained results show a good agreement with the kinetic scheme based on the propagation by free anions. The propagation rate constant is also estimated in this Chapter.

For the purpose of studying the initiating species of polymerization, the electron spin resonance measurements of irradiated 2-methyltetrahydrofuran glass containing a small amount of nitroethylene are carried out at -196°C, and also the negative ions formed by the electron impact from nitroethylene are measured by means of a mass spectrometer. On the basis of these spectrometric observations, the nature of initiating species of polymerization is discussed in Chapter 4.

Since the initiating species of polymerization appears to be easily trapped in glassy systems containing monomers, the postpolymerization in the glassy mixture of nitroethylene and 2-methyltetrahydrofuran is studied in Chapter 5. The experimental results of postpolymerization show a reasonable correlation with those of electron spin resonance measurements. It is suggested from the results obtained in Chapters 4 and 5 that the anion radicals of nitroethylene

formed by the capture of electrons are responsible for the initiation process of the radiation-induced polymerization of nitroethylene.

In Chapter 6, the reaction mechanism of nitroethylene polymerization is considered in order to clarify the characteristics of radiation-induced polymerization. Compared with catalytic polymerizations, the distinctive features of radiation-induced polymerization appear to be as follows:

(1) Coexistence of radicals and ionic polymerizations, and the contribution of ion radicals to the initiation process.

(2) Propagation by free ions.

The former is shown experimentally in the copolymerization of p-chlorostyrene with styrene by changing the polymerization conditions such as polymerization temperature and the addition of scavengers. The latter is shown by the summarized results of radiation-induced polymerization of several monomers in extremely dried systems. These characteristics are also observed in the radiation-induced polymerization of nitroethylene.

It has been recognized that the chemical reactions of high-energy radiation in the gas or condensed phase are initiated by transient intermediates which are produced in

reaction systems by radiation. One of the appropriate approaches to investigate these transient intermediates seems to be attained by the application of mass spectrometry. From the viewpoint of studying the radiation-induced polymerization, it is also expected that mass spectrometric observation can provide some useful information on the initiation process of polymerization in condensed phases, although the important differences between gas and condensed phases arise in the primary physical and chemical acts of energy absorption, and hence in the nature and spatial distribution of primary chemical species.

Part 3 of the present thesis deals with negative ion-molecule reactions of nitroethylene. It is suggested in Part 2 that the radiation-induced polymerization of nitroethylene is initiated by negative intermediates. Therefore, it appears to be very interesting to study the formation of negative ions and the negative ion-molecule reactions of nitroethylene.

In Chapter 7, the formation of negative ions from nitroethylene is investigated. One of the most important results is that the parent negative ion of nitroethylene, the appearance potential of which is about 0 eV, is observed at even lower source pressures. This indicates that the nitroethylene molecule has an ability to capture thermal electrons easily

by a nondissociative resonance capture process.

Chapter 8 is mostly concerned with the dimer negative ion formation of nitroethylene by ion-molecule reaction. By measurements of the appearance potential and the source pressure dependence about the dimer negative ion, it is shown that the precursor of the dimer ion is the parent negative ion of nitroethylene and that the dimer negative ion is formed by the ion-molecule reaction between the parent ion and the neutral molecule. Furthermore, the rate constant of this reaction is estimated and compared with the theoretical value derived from simple collision theory.

In Chapter 9, the formation process of the parent and the dimer negative ions at higher electron energies is studied, for chemical reactions in irradiated system are usually induced by ionizing radiation with high energies. The experimental results suggest that the collisional stabilization process of the product ions is very important at higher electron energies.

It has been admitted that the role of ionic fragmentation processes in radiation chemistry is very significant. However, detailed studies of these processes have mostly been limited to diatomic molecules such as hydrogen and nitrogen molecules. One of the easiest methods to investigate the ionic fragmentation processes is to excite fast ground-state

ions into the dissociative states of molecule ions by collision with atomic or molecular targets. In the case of collision-induced dissociation of hydrogen molecule ions, experimental evidence for the occurrence of two different processes were observed as below:

(i) electronic excitation to a dissociative state, and

(ii) adiabatic dissociation following momentum transfer.

In Part 4, the fragmentation processes of acetylene molecule ions induced by collision with rare gas atoms are investigated by means of a mass spectrometer. The main purpose of this Part is to provide information on the ionic fragmentation of polyatomic molecules. The third possible type of dissociation process, which is not observed in the case of hydrogen molecule ions, is found in the present study; (iii) collision-induced dissociation of ions in a metastable state.

In Chapter 10, the dissociation processes of molecular acetylene ions into C_2H^+ fragment ions are investigated as functions of relevant parameters such as initial state of the molecular ions, their incident velocity, their time of flight, and the kind of target. In this dissociation, two different processes (processes (i) and (iii)) are discriminated, and the findings are discussed on several possible dissociation processes.

In order to compare the dissociation mode of H^+ formation with that of C_2H^+ ions, the dissociation process of acetylene molecular ions into H^+ fragment ions is studied in Chapter 11. The experimental results indicate that this process is caused by the vibrational excitation of electronically-ground-state acetylene ions(process (ii)).

In Chapter 12, the collision-induced dissociations of acetylene molecular ions into C_2^+, CH_2^+, CH^+, and C^+ fragment ions are studied. Although the detailed discussion on these fragmentations is not extended, siginificant evidence is obtained even at this stage. On the basis of the obtained results, some features of these dissociation processes are mentioned.

The investigations which constitute the contents of the present thesis are, of cource, as yet incomplete. The scope is, therefore, mostly limited to the discription of fundamental experiments which should be followed up by further detailed studies. The experimental results will be explained successively in the following Chapters.

References

1) W. H. T. Davison, S. H. Pinner, and R. Worrall, Chem. and Ind., 1274 (1957).

2) S. Okamura, T. Higashimura, and S. Futami, Isotopes and Radiation, 1, 216 (1958).

3) A. Chapiro and V. Stannett, J. Chim. Phys., 56, 830 (1959).

4) A. P. Sheinker, M. K. Yakovleva, E. V. Kristal'nyi, and A. D. Abkin, Doklady Akad. Nauk S. S. S. R., 124, 632 (1959).

5) F. Williams, "Fundamental Processes in Radiation Chemistry" (P. Ausloos ed.), p. 515, Interscience, New York, 1968.

6) T. H. Bates, J. V. F. Best, and F. Williams, Nature, 188, 469 (1960).

7) K. Ueno, K. Hayashi, and S. Okamura, Polymer, 7, 431 (1966).

8) R. C. Potter, C. L. Johnson, D. J. Metz, and R. H. Bretton, J. Polymer Sci. A-1, 4, 419 (1966).

9) D. Cordischi, A. Mele, and R. Rufo, Trans. Faraday Soc., 64, 2794 (1968).

10) M. A. Bonin, W. R. Busler, and F. Williams, J. Am. Chem. Soc., 87, J. Am. Chem. Soc., 87, 199 (1965).

11) E. Hubmann, R. B. Taylor, and F. Williams, Trans. Faraday Soc., 62, 88 (1966).

12) K. Ueno, F. Williams, K. Hayashi, and S. Okamura, Trans. Faraday Soc., 63, 1478 (1967).

13) Ka. Hayashi, Y. Yamazawa, T. Takagaki, F. Williams, K. Hayashi, and S. Okamura, Trans. Faraday Soc., 63, 1489 (1967).

14) S. Okamura, K. Hayashi, M. Nishii, and Y. Nakamura, Annual Report of Japan Assoc. Rad. Res. Polymers, 1, 101 (1958 / 1959); Isotopes and Radiation, 3, 344 (1960).

P A R T 2

RADIATION-INDUCED POLYMERIZATION OF NITROETHYLENE

Chapter 1

Solution Polymerization at Low Temperature

1. Introduction

Nitroethylene is well known to be very reactive in anionic polymerization, since the strongly electro-withdrawing character of the nitro group makes the double bond extremely susceptible to a wide variety of basic reagents.

Catalytic polymerizations of nitroethylene have been studied by several groups of workers since 1919. Wieland and Sakellarios[1] first observed the polymerization to be catalyzed by alkali. Jones,[2] Blomquist,[3] Buckley,[4] Noma,[5] and Horner[6] also investigated the polymerization by the use of various catalysts. However, these investigators were interested mainly in the synthesis of polynitroethylene. Only one series of detailed studies on the kinetics has so far been reported by Katchalsky et al.[7-9] They elucidated the mechanism of the polymerization by weak nucleophilic reagents, and observed the formation of "living polymer" at

sufficiently low temperatures. On the other hand, in the field of radiation-induced polymerization, no detailed investigation on nitroethylene has been made, except the qualitative works by Sokolov[10] and Tabata.[11]

The present study deals with the radiation-induced solution polymerization of nitroethylene at -78°C. The kinetics of the polymerization, the effects of additives and the copolymerization with acrylonitrile have been studied, and the results are discussed in relation to the mechanism of the polymerization.

2. Experimental

2.1. Materials

1. Synthesis of monomer

The synthetic route of the monomer was as follows:

$$CH_3NO_2 + HCHO \xrightarrow{K_2CO_3} \left\{ \begin{array}{l} CH_2(OH)CH_2NO_2 \\ (CH_2OH)_2CHNO_2 \\ (CH_2OH)_3CNO_2 \end{array} \right\}$$

$$\xrightarrow{\text{distillation}} CH_2(OH)CH_2NO_2 \qquad \text{(i)}$$

$$CH_2(OH)CH_2NO_2 + \begin{array}{c} CO \\ \diagup \\ \text{C}_6\text{H}_4 \\ \diagdown \\ CO \end{array} O \longrightarrow CH_2{=}CHNO_2 \qquad \text{(ii)}$$

2-Nitroethanol was prepared from nitromethane and paraformaldehyde in 4 : 1 molar ratio according to the method of Gorsky and Makarov[12] (Process (i)).

Nitroethylene was prepared by the dehydration of 2-nitroethanol following the procedure of Buckley and Scaife[4] (Process (ii)). The product was distilled twice under reduced pressure. A middle fraction boiling between 38-39°C/80 mmHg was collected and dried over Drierite (anhydrous calcium sulfate). Physical properties of the monomer were as follows: m.p. -70°C, b.p. 38-39°C/80 mmHg, n^{18} 1.4337, d_{20}^{20} 1.112.

2.2. Solvents and additives

Tetrahydrofuran (THF), diethyl ether, nitroethane and toluene were used as solvents. THF was predried over Drierite and then dried over sodium metal for a week. Before use, it was distilled twice over metallic sodium. Diethyl ether was washed with a 5% aqueous sodium hydroxide solution, and an aqueous alkaline solution of potassium permanganate and finally water, dried over metallic sodium, and then distilled twice over metallic sodium. Nitroethane was washed with an aqueous mixture-solution of sodium bicarbonate and sodium sulfite, and water. Then, it was dried over barium oxide and distilled just before use. Toluene was washed with

concentrated sulfuric acid, water, 10 % aqueous sodium hydroxide solution and water, dried over calcium chloride, and distilled twice over metallic sodium.

Acrylonitrile as a comonomer was washed with a 5 % aqueous sodium hydroxide solution and a saturated aqueous solution of sodium chloride, and dried by a freeze-drying method. It was then dried over calcium chloride, and distilled twice just before use.

1,1-Diphenyl-2-picryl-hydrazyl (DPPH), benzoquinone (BQ) and hydrogen chloride (HCl) were used as additives. Commercial DPPH and BQ were purified by recrystallization. HCl was prepared by a procedure whereby concentrated sulfuric acid was added dropwise to baked sodium chloride. HCl thus obtained was dried by passing it through a spiral tube, cooled at $-78^{\circ}C$, following which it was bubbled into THF. The concentration of HCl was determined by titration of 1/10N-NaOH solution in THF by the use of pH meter.

2.3. Polymerization

Samples for irradiation were prepared in cylindrical glass ampoules of about 30-ml. capacity. These amouples, in which given amounts of monomer and solvent were introduced, were degassed by successive freezing and thawing, and finally sealed off in vacuum ($< 10^{-4}$ mmHg). The

samples were irradiated at -78°C, using solid carbon dioxide-methanol as the coolant, by gamma-rays from a 500 curie cobalt-60 radiation source at Osaka Laboratory, Japan Atomic Energy Research Institute. The dose rates in the various positions were determined with the Fricke dosimeter using the G value of 15.6 for the oxidation of ferrous sulfate.

2.4. Polymer

After irradiation, the polymer was precipitated by pouring the sample into a vigorously stirred 1 : 1 water + methanol mixture, previously acidified with concentrated hydrogen chloride in order to prevent further polymerization. The polymer was isolated by filtering and then washed successively with water, ethyl alcohol and ether, before drying to constant weight in vacuum at room temperature. The polymer conversion was determined gravimetrically.

The viscosity number of the polymer was measured in dimethyl formamide solution at 20°C. The average molecular weight $\overline{M}_w$ was estimated from the following equation[9]:

$$[\eta] = 1.7 \times 10^{-3} \overline{M}_w^{0.56}$$

The degree of polymerization was calculated on the assumption that $\overline{M}_w/\overline{M}_n$ is equal to 2.0 for a most probable distribution.

In the case of copolymerization with acrylonitrile, the copolymer conversion was usually kept to less than 10 %. The composition of the copolymer was determined by elementary analysis.

3. Results

3.1. Effect of Solvents

In order to study the effect of solvents in the radiation-induced polymerization of nitroethylene, the solution polymerization in various solvents was carried out at -78°C. The results of the polymerization in diethyl ether are shown in Table 1-1. Although the polymer yield increased with the increase in monomer concentration, the polymerization system became heterogeneous and the polymer precipitated above 3 % polymer conversion. Therefore, detailed kinetic studies in diethyl ether were prevented by the heterogeneous nature of the reaction.

As presented in Table 1-2, no polymer was found in nitroethane solution even at the irradiation beyond 3×10^6 r. Similarly the polymerization did not take place in the toluene solution.

In the case of THF solution, the polymerization easily

Table 1-1. Polymerization of nitroethylene in diethyl ether.

Monomer concentration (mol/l)	Dose rate $\times 10^{-4}$ (r/hr)	Total dose $\times 10^{-6}$ (r)	Conversion (%)	$R_p \times 10^7$ (mol/l·sec)
0.77	1.99	2.45	1.4	0.23
1.03	1.99	2.45	1.5	0.34
2.21	1.99	2.45	2.2	1.05
3.87	1.99	2.45	3.6	3.02

Temp. -78°C.

Table 1-2. Polymerization of nitroethylene in nitroethane.

Monomer concentration (mol/l)	Dose rate $\times 10^{-4}$ (r/hr)	Total dose $\times 10^{-6}$ (r)	Conversion (%)
0.52	0.81	3.44	0
1.03	0.81	3.44	0
2.21	0.81	3.44	0
3.87	0.81	3.44	0

Temp. -78°C.

occurred and proceeded homogeneously in the conversion range below 30 %. The rate of polymerization was over 10 times as large as that in diethyl ether. Consequently, THF was chosen as a solvent in the present study. The detailed results will be presented in Section 3.2.

Further, bulk polymerization of nitroethylene was carried out at -78°C in solid state. As shown in Table 1-3, the polymerization in solid state was observed, although the G value for monomer consumption, G(-monomer), was very small. Similar results were reported by Tabata.[11)]

Table 1-3. Solid state polymerization of nitroethylene in bulk.

Dose rate $\times 10^{-4}$ (r/hr)	Total dose $\times 10^{-6}$ (r)	Conversion (%)	G(-M)
2.80	9.38	0.9	14
2.80	9.38	1.1	17

Temp. -78°C

3.2. Polymerization in THF solution

In the case of the polymerization in THF solution at -78°C, the relation between the polymer conversion and the

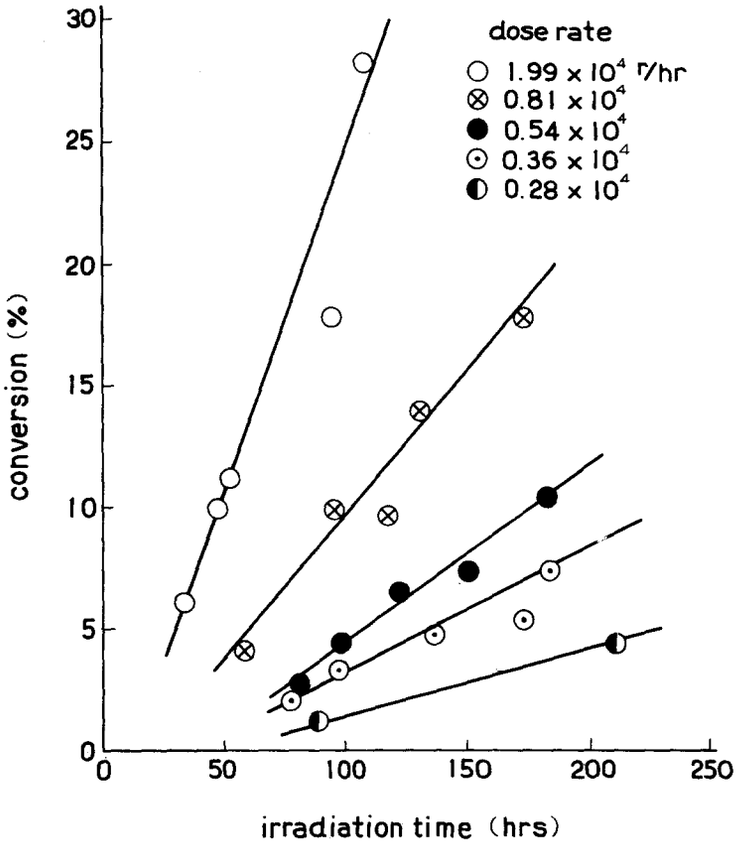

Figure 1-1. Relation between conversion and irradiation time.

Monomer conc. 2.21 mol/l, polym. temp. -78°C.

irradiation time at various dose rates is shown in Figure 1-1. The polymer conversion increased linearly with the increase of irradiation time in all cases beyond the region of the induction period. The rate of polymerization at each dose rate was obtained from the slope of the linear part in Figure 1-1. The dependence of the dose rate on the rate of polymerization is represented in Figure 1-2. This result indicates that the rate of polymerization is proportional to the first power of the dose rate.

Figure 1-3 shows the first order plot of monomer consumption. The fact that this relation is linear at each dose rate suggests that the concentration of active species is of stationary state over the whole range of polymerization.

The molecular weight of the polymer obtained is shown in Figures 1-4 and 1-5. Figure 1-4 indicates that the molecular weight does not depend on the polymer yield up to 30 % conversion. Also, the molecular weight is nearly independent of the dose rate as presented in Figure 1-5.

The effects of the monomer concentration on the rate of polymerization and the molecular weight of the polymer are shown in Figures 1-6 and 1-7. The rate of polymerization was proportional to the monomer concentration, and also the molecular weight, which did not change with the variation of dose rate as mentioned above, increased linearly with

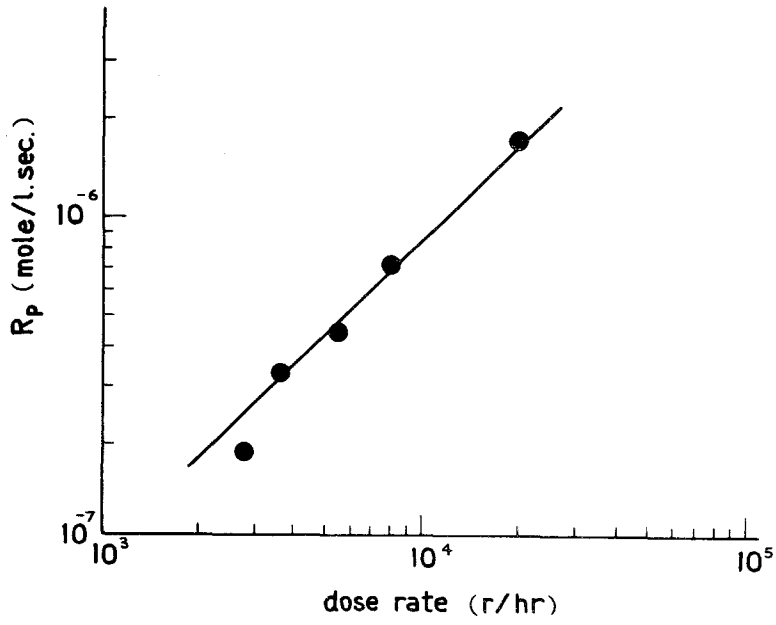

Figure 1-2. Effect of dose rate on the rate of polymerization.

Monomer conc. 2.21 mol/l, polym. temp. -78°C.

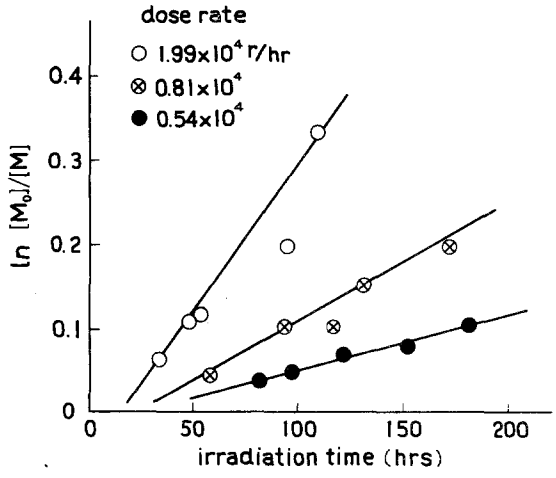

Figure 1-3. Plot of $\ln[M_o]/[M]$ vs. irradiation time.

Initial monomer conc. 2.21 mol/l,
polym. temp. -78°C.

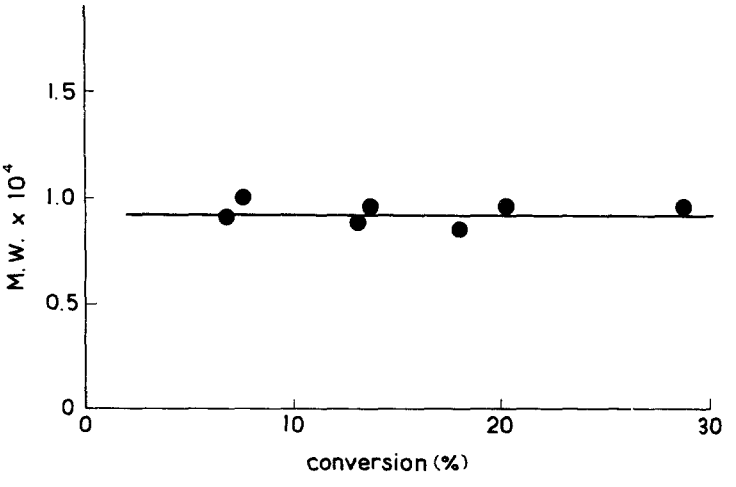

Figure 1-4. Relation between the molecular weight of polymer and conversion.
Monomer conc. 2.21 mol/l, polym. temp. -78°C.

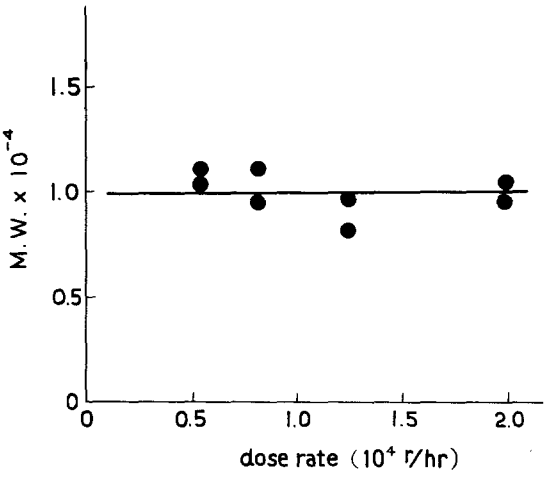

Figure 1-5. Effect of dose rate on the molecular weight of polymer.
Monomer conc. 2.21 mol/l, polym. temp. -78°C.

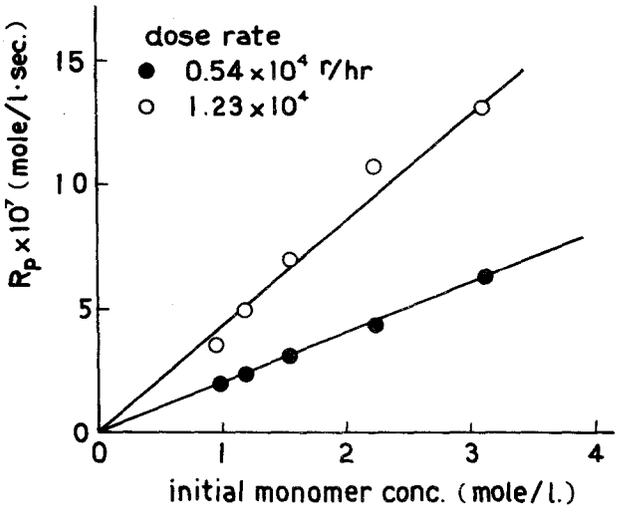

Figure 1-6. Effect of monomer concentration on the rate of polymerization.

Polym. temp. -78°C.

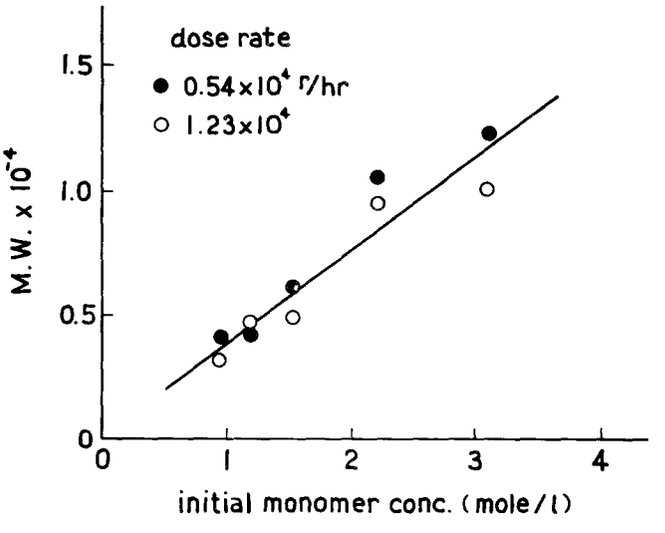

Figure 1-7. Effect of monomer concentration on the molecular weight of polymer.

Polym. temp. -78°C.

the increase in monomer concentration.

It is generally considered that the G-value for chain initiation, G_i, can be derived from the quotient G(-monomer) $/\overline{DP}_n$ in the case of the absence of chain transfer reaction. The G_i values for changing the conversion, the dose rate and the monomer concentration were calculated, and these results are shown in Figures 1-8, 1-9, and 1-10, respectively. The estimated G_i values, which lie in the range between 5 and 6, are substantially constant on the variation of the conversion, the dose rate and the monomer concentration.

In order to examine the possibility for the formation of "living polymer", the polymerization system was kept for a few day at $-78^{\circ}C$ after irradiation. Both the conversion and the molecular weight of the polymer scarcely changed with the keeping time as presented in Table 1-4. These facts indicate that the "living polymer" does not exist in the present conditions for polymerization.

3.3. Effects of Additives and Copolymerization

For the purpose of elucidating the reaction mechanism, the effects of additives, such as DPPH, BQ, and HCl, were studied. The results obtained are summarized in Table 1-5. In the cases of DPPH and BQ, the polymer yield decreased gradually with the increase in concentration of additives.

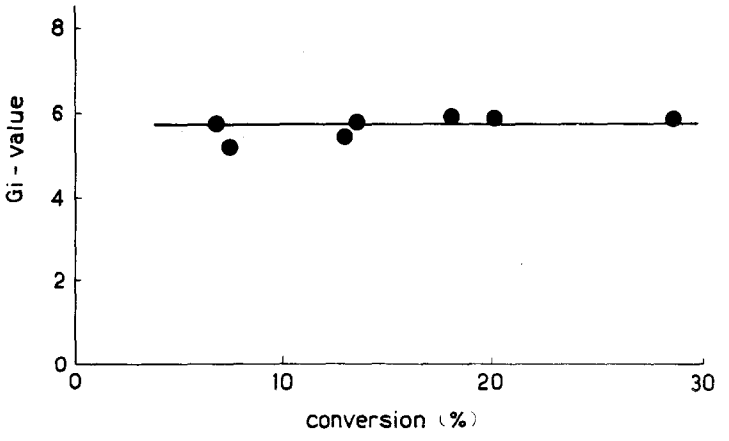

Figure 1-8. Effect of conversion on G_i-value.
Monomer conc. 2.21 mol/l, polym. temp. -78°C,
dose rate 1.99×10^4 r/hr.

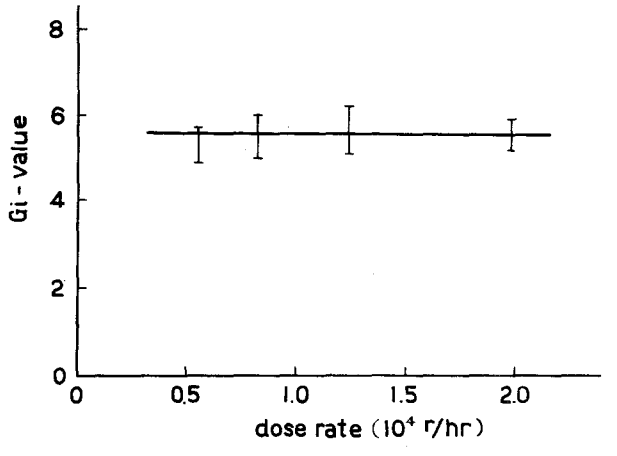

Figure 1-9. Effect of dose rate on G_i-value.
Monomer conc. 2.21 mol/l, polym. temp. -78°C.

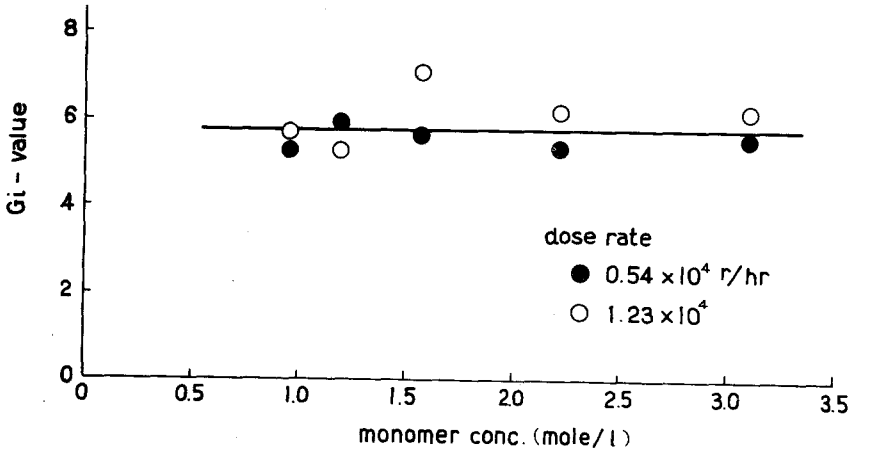

Figure 1-10. Effect of monomer concentration on G_i-value.
Polym. temp. -78°C.

Table 1-4. Post polymerization of nitroethylene.

Time for standing (hr)	Conversion (%)	G(-M)	MW	G_i
0	10.5	280	8600	4.7
24	10.6	280	7300	5.5
53	11.3	300	7500	5.8
100	11.2	300	9800	4.5

Temp. $-78^{\circ}C$, monomer concentration in THF 2.21 mol/l, dose rate 1.99×10^4 r/hr, total dose 0.95×10^6 r.

On the other hand, the polymerization inhibited completely by the addition of HCl even at the concentration of 1.1×10^{-4} mol/l.

As another attempt to elucidate the reaction mechanism, the copolymerization of nitroethylene with acrylonitrile was carried out in THF solution at $-78^{\circ}C$. As shown in Figure 1-11, the nitroethylene component in the copolymer was abundant in the whole range of the feed monomer composition. From these results, the monomer reactivity ratios were determined to be r_1 (nitroethylene) = 63 ± 15 and r_2 (acrylonitrile) = 0.01 ± 0.01. The copolymer yield

Table 1-5. Effect of additives.

Additive	Additive concentration (mol/l)	Total dose $\times 10^{-6}$ (r)	Conversion (%)
DPPH	8.9×10^{-3}	1.80	7.1
	4.4×10^{-3}	1.80	10.1
	8.9×10^{-4}	1.80	11.7
	4.4×10^{-4}	1.80	13.6
	8.9×10^{-5}	1.80	15.1
	none	1.80	17.8
BQ	8.0×10^{-3}	1.80	5.3
	8.0×10^{-4}	1.80	12.5
	8.0×10^{-5}	1.80	13.8
	none	1.80	16.8
HCl	1.1×10^{-2}	1.20	0
	5.5×10^{-3}	1.20	0
	1.1×10^{-4}	1.20	0
	none	1.20	15.0

Temp. $-78^{\circ}C$, monomer concentration in THF 2.21 mol/l, dose rate 1.99×10^{4} r/hr.

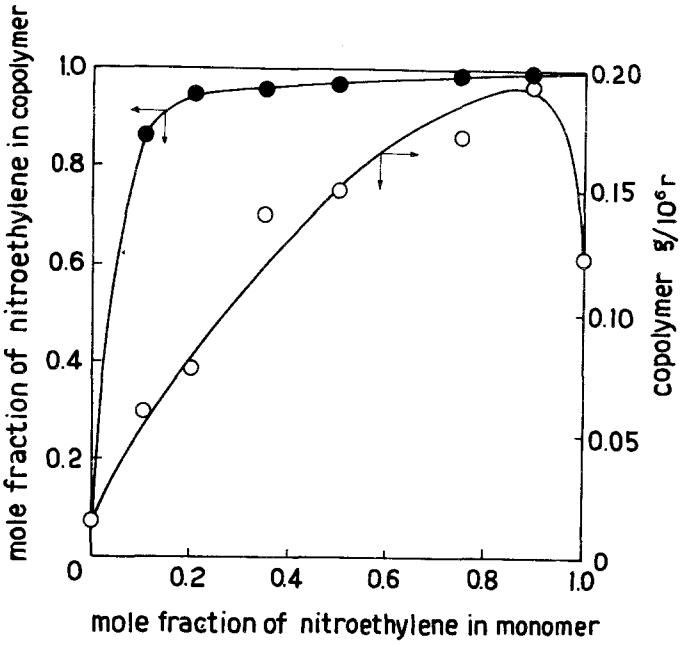

Figure 1-11. Copolymerization of nitroethylene with acrylonitrile.
Monomer conc. 14.3 vol %, polym. temp. -78°C.

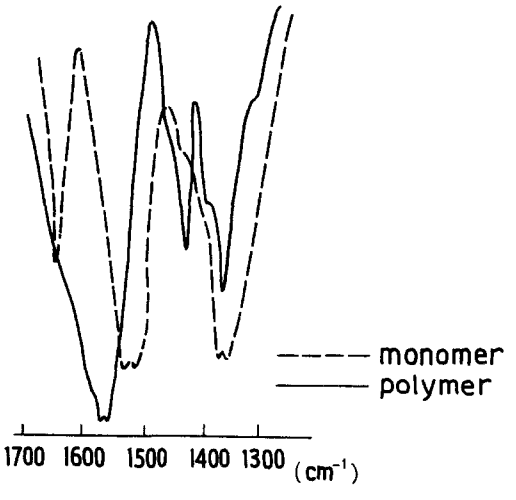

Figure 1-12. Infrared absorption spectra of monomer and polymer.

per the irradiation dosage of 10^6 r showed a maximum at about 90 % nitroethylene component in the feed monomer.

3.4. Polymer Structure

Figure 1-12 shows the infrared absorption spectra of the monomer and the polymer obtained in THF solution. Only the middle-frequency region of these two spectra is included in Figure 1-12, since other regions of two spectra are essentially identical. Two absorption peaks due to nitro group at near 1350 and 1500-1550 cm^{-1} were observed in both spectra. The peak due to double bond at 1650 cm^{-1}, which exhibited as a characteristic peak in the spectrum of monomer, was not found in that of the polymer. Alternatively the peak at 1450 cm^{-1} identified as methylene group, which was absent in the spectrum of the monomer, was confirmed in that of the polymer. These results indicate evidently that the polymer of nitroethylene was produced by opening the double bond with gamma-ray irradiation. Further, it was found from the results of X-ray diffraction analysis that the polymer obtained was completely amorphous.

4. Discussion

In the field of catalytic polymerization, it is generally believed that nitroethylene is highly susceptible to anionic polymerization as previously described. From the results of copolymerization[13] and the studies on reactivity of various bases to monomers,[14] Pepper[15] discussed that the order of susceptibility to anionic polymerization seemed to be qualitatively as follows:

nitroethylene > acrylonitrile > methyl methacrylate > styrene > butadiene.

In the present study, the polymerization was inhibited completely by the addition of a small quantity of HCl. Further, the results of the copolymerization with acrylonitrile showed that the propagating species produced from nitroethylene were more reactive than those from acrylonitrile. These facts indicate that the radiation-induced polymerization of nitroethylene at -78°C proceeds by an anionic mechanism.

In order to discuss the polymerization mechanism, the following kinetic scheme is assumed.

Ionization	$A \longrightarrow\!\!\!\!\!\!\sim\!\!\!\!\!\!\rightarrow A\cdot^{+} + e^{-}$	(a)
Initiation	$e^{-} + M \longrightarrow M\cdot^{-}$	(b)
	$M\cdot^{-} + M \longrightarrow \cdot M\text{-}M^{-}\ (M_2^{-})$	(b')
Propagation	$M_{n-1}^{-} + M \xrightarrow{k_p} M_n^{-}$	(c)
Transfer	$M_n^{-} + M \xrightarrow{k_m} M_n + M^{-}$	(d)
	$M_n^{-} + S \xrightarrow{k_s} M_n + S^{-}$	(e)
Termination	$M_n^{-} + A\cdot^{+} \xrightarrow{k_t} M_n\ (\text{or } M_n\text{-}A)$	(f)
	$M_n^{-} + X \xrightarrow{k_{tx}} M_n + X^{-}$	(g)

where k_p, k_m, k_s, k_t, and k_{tx} are the rate constants for propagation, monomer transfer, solvent transfer, termination by charge recombination and termination by reaction with impurities X, respectively. Assuming the nitroethylene molecule has an ability to capture predominantly electrons released in the system, the rate-determining step of initiation is the reaction (a). This assumption is supported by the fact that the G_i value is independent of the monomer concentration as presented in Figure 1-10. Then, the rate of initiation, R_i, is given by the equation (1).

$$R_i = I\ G_i\ [A] / 100 \qquad (1)$$

where I is the dose rate, and A is the substance to release electrons by the irradiation. For termination reactions, the linear dependence of the dose rate on the rate of polymerization indicates that the termination takes place between the propagating anion and impurities (reaction (g)) The termination by charge recombination (reaction (f)) would lead to a square-root dependence of the dose rate on the rate of polymerization. Since the concentration of active species remains constant during the whole cource of polymerization, the stationary state assumption holds in the present system. Consequently, the rate of polymerization, R_p, is represented by the following equation:

$$R_p = k_p[M^-][M] = \left[\frac{k_p}{k_{tx}[X]} \frac{G_i[A]}{100}\right] I\,[M] \qquad (2)$$

The results of Figures 1-2 and 1-6 are in good agreement with the equation (2). In the present study, the chain transfers both to the monomer and to the solvent (reactions (d),(e)) can be reasonably neglected, because the degree of polymerization is linearly proportional to the monomer concentration. Therefore, the degree of polymerization is given by the equation (3).

$$\overline{DP}_n = \frac{k_p}{k_{tx}[X]}\,[M] \qquad (3)$$

As an attempt to estimate the substance A, the following calculation was carried out. The equation (2) can be rewritten in the form:

$$[A] = \frac{R_p}{\frac{k_p}{k_{tx}[X]} \quad \frac{IG_i}{100}[M]} \qquad (4)$$

Since the value of $k_p/k_{tx}[X]$ is obtained from the slope of Figure 1-7 and other values in right-side term are known, the value of A, which is expressed by the dimension of density, can be calculated. In the cases of changing the dose rate and the monomer concentration, the results are summarized in Tables 1-6 and 1-7, respectively. The calculated [A] shows a reasonable agreement with the average density of the system. From these results it is suggested that the substance A means the whole polymerization system containing the monomer and the solvent, and consequently all of the energy absorbed in the system participates effectively in the initiation of polymerization.

In the experiments of the additives, it is not yet clear as to why DPPH and BQ, which are typical radical scavengers, retards the polymerization. Okamura and Futami[16] reported that the radical scavengers acted as retarders for radiation-induced ionic polymerizations.

Table 1-6. Calculation of [A] at constant monomer concentration.

Dose rate $\times 10^{-4}$ (r/hr)	$R_p \times 10^7$ (mol/l·sec)	[A] $\times 10^{-3}$ (g/l)	Density of the system $\times 10^{-3}$(g/l)
0.28	1.87	0.80	0.92
0.36	3.17	1.1	0.92
0.54	4.43	0.98	0.92
0.81	7.18	1.1	0.92
1.99	17.3	1.0	0.92

Monomer concentration in THF 2.21 mol/l.

Table 1-7. Calculation of [A] at constant dose rate.

Monomer concentration (mol/l)	$R_p \times 10^7$ (mol/l·sec)	[A] $\times 10^{-3}$ (g/l)	Density of the system $\times 10^{-3}$(g/l)
0.97	1.98	1.0	0.91
1.19	2.44	1.0	0.91
1.55	3.15	0.99	0.91
2.21	4.43	0.98	0.92
3.10	6.36	1.0	0.94

Dose rate 0.54×10^4 r/hr.

A similar effect may be realized in this polymerization system.

In conclusion, it was established in the present investigation that the radiation-induced polymerization in THF solution at -78°C proceeded by an anionic mechanism. Further, the kinetic treatment led to the conclusion that all of the energy absorbed in the system contributes effectively to the initiation of the polymerization.

References

1) H. Wieland and E. Sakellarios, Ber., 52, 898 (1919).
2) G. D. Jones, J. Zomlefer, and K. Hawkins, J. Org. Chem., 9, 500 (1944).
3) A. T. Blomquist, W. J. Tapp, and J. R. Johnson, J. Am. Chem. Soc., 67, 1519 (1945).
4) G. D. Buckley and C. W. Scaife, J. Chem. Soc., 1471 (1947).
5) K. Noma, T. Okumura, and T. Sone, Kobunshi Kagaku, 5, 99 (1948).
6) L. Horner, W. Jurgeleit, and K. Klüpfel, Liebigs Ann. Chem., 591, 108 (1955).
7) D. Vofsi and A. Katchalsky, Ricerca Sci. B, 25, 165 (1955).

8) D. Vofsi and A. Katchalsky, J. Polymer Sci., 26, 127 (1957).

9) J. Grodzinsky, A. Katchalsky, and D. Vofsi, Mokromol. Chem., 44/46, 591 (1961).

10) V. N. Sokolov, I. Ya. Puddibnyi, V. V. Perekalin, and V. F. Evdokimov, Doklady Akad. Nauk. S.S.S.R., 138, 619 (1961).

11) Y. Tabata, Hoshasen Kobunshi, 2, (7), 3 (1961).

12) I. M. Gorsky and S. P. Makarov, Ber, 67B, 996 (1934).

13) C. Walling, E. R. Briggs, W. Cummings, and F. R. Mayo, J. Am. Chem. Soc., 72, 48 (1950).

14) N. S. Wooding and W. C. E. Higginson, J. Chem. Soc., 774 (1952).

15) D. C. Pepper, Quart. Rev., 8, 88 (1954).

16) S. Okamura and S. Futami, Intern. J. Appl. Rad. Isotopes, 8, 46 (1960)

C h a p t e r 2

Bulk Polymerization at Room Temperature

1. Introduction

In the preceding Chapter, the radiation-induced polymerization of nitroethylene in tetrahydrofuran solution at -78°C was shown to be strongly retarded by the addition of a small amount of hydrogen chloride to the system. Further, the radiation-induced copolymerization occurred readily with acrylonitrile.[1] Anionic propagation is thereby confirmed for the radiation-induced polymerization since it is well known[2] that this monomer is highly susceptible to catalytic polymerization induced by a wide variety of basic reagents.

The present study is concerned with the radiation-induced polymerization of bulk nitroethylene at room temperature. Nitroethylene is of particular interest because the dielectric constant for simple organic nitro-compounds (ε_{static} (nitroethane) = 28.06 at 30°C) are much higher than for hydrocarbons, so this factor might also be

expected to facilitate anionic polymerization through the formation of free ions. By the use of hydrogen bromide as a suitable polymerization retarder, an attempt has been made to determine the rate constant for anionic propagation.

2. Experimental

2.1. Materials

Nitroethylene was prepared by the procedure described in Chapter 1. Since nitroethylene is very sensitive to polymerization by traces of water, the elimination of water was carefully carried out. After drying over Drierite, the monomer was transferred onto barium oxide baked at 350°C in vacuum for 10 hours, and then stored for 24 hours at room temperature, during which time some polymerization occurred. This pre-polymerization technique may also serve to remove impurities other than water from the monomer. After this storage period, the remaining monomer was distilled in vacuum from trap to trap, and samples were finally condensed into the dilatometer bulbs. The dilatometer was equipped with a cylindrical bulb of about 5 ml capacity connected to a 10 cm length of 1 mm diameter capilary. The exact volume of dilatometer was determined by prior

calibration with mercury to a reference mark on the stem.

Hydrogen bromide (HBr) was prepared from tetrahydronaphthlene and bromine, and purified by trap-to-trap sublimation in vacuum. When HBr was added to the monomer, a precise volume of the gas was measured under standard conditions before transfer.

2.2. Polymerization

Samples were irradiated at room temperature (10°C) by gamma-rays from a 1,000 curie cobalt-60 radiation source at the Osaka Laboratory, Japan Atomic Energy Research Institute. The polymerization was followed by a dilatometric method. The volume contraction was 2.01 % per 10 % conversion to polymer at 20°C. This shrinkage factor was determined from density measurements on the polymer and monomer.

The viscosity number of the polymer was measured in dimethyl formamide solution at 20°C. The average molecular weight was determined from the same equation[3] as Chapter 1.

3. Results

The results obtained in the absence of HBr are summarized in Table 2-1. The mean value of G(-monomer) is 4.66×10^4.

Table 2-1. Radiation-induced polymerization of nitroethylene at 10°C.

Sample Code	Dose rate $\times 10^{-4}$ (r/hr)	Total dose $\times 10^{-4}$ (r)	Conversion (%)	G(-monomer) $\times 10^{-4}$
G-1	0.69	1.88	6.78	5.13
G-2	1.53	1.53	5.93	5.50
H-1	2.88	2.88	7.90	3.90
I-7	0.67	2.47	6.95	4.00
I-8	0.67	2.34	7.84	4.75

This value is slightly larger than that obtained in the radiation-induced cationic polymerization of cyclopentadiene[4] at -78°C. The common features of the large kinetic chain length and the reasonable reproducibility render these monomers particularly suitable for studies of cationic (cyclopentadiene) and anionic (nitroethylene) propagation in radiation-induced polymerization.

The effect of HBr on the rate of nitroethylene polymerization is shown in Figure 2-1. Whereas the conversion was almost proportional to the irradiation dose for the monomer alone, the addition of HBr resulted in non-linear plots showing a very low initial rate of polymerization followed by a marked increase in the rate

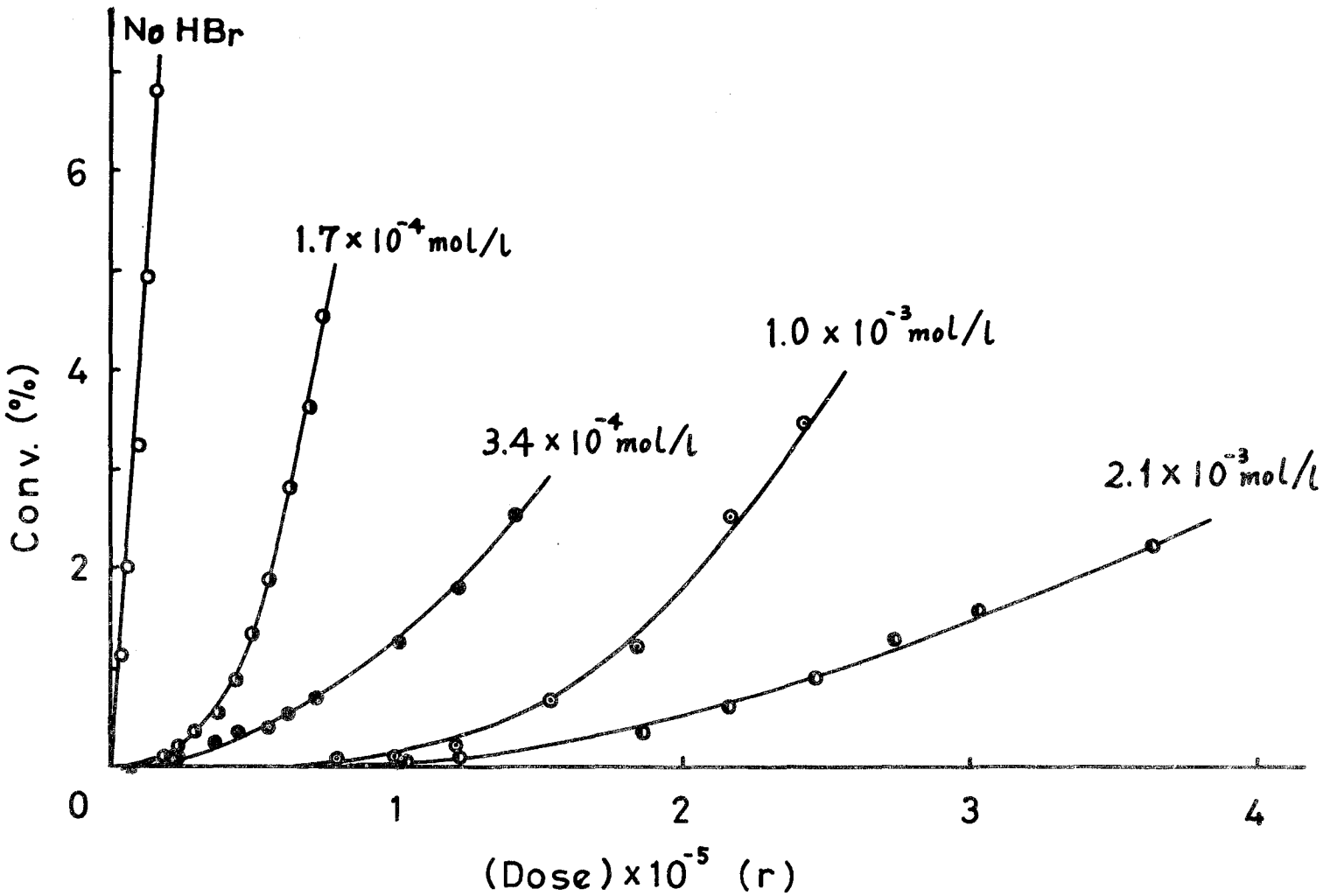

Figure 2-1. Conversion-dose curves in the absence and presence of hydrogen bromide.

of continued irradiation. As the initial HBr concentration in the monomer was raised, so the length of the "induction period" increased and higher doses were required to achieve a given level of conversion. Because of the non-linear kinetics, it is difficult to extrapolate in order to obtain the initial rates of polymerization. As an alternative approach, integral values of G_o(-monomer) were calculated for very low conversions (0.25 %) from curves such as those shown in Figure 2-1. These values give an approximate measure of the initial conversion per unit dose, which is proportional to the initial rate of polymerization because the same dose rate was used throughout.

The results for G(-monomer) and the degree of polymerization, $\overline{DP}_n$, are presented in Table 2-2. It must be emphsized that this G(-monomer) value is an integral value for the total dose in each experiment, and therefore for the HBr runs, this value will differ considerably from the "initial" G_o(-monomer) because of the non-linear kinetic plots referred to above. The initiation yield G_i is given by the quotient G(-monomer)/$\overline{DP}_n$ and in the absence of chain transfer, this quantity is unaffected by the complications due to the non-linear kinetics in the presence of HBr. These results show that within the precision of the measurements, the G_i value decreases with the amount of added HBr from a value of about 5 to 0.8. The average value of G_i for

Table 2-2. Effect of hydrogen bromide on the radiation-induced polymerization of nitroethylene at 10°C.

Sample Code	HBr (mol/l)	Total dose $\times 10^{-5}$ (r)	Conversion (%)	G(-monomer)	$\overline{DP}_n$	G_i
H-1	0	0.29	7.90	3.90×10^4	7.3×10^3	5.3
I-8*	0	0.23	7.84	4.75×10^4	1.1×10^4	4.3
H-5	3.1×10^{-5}	0.34	7.10	2.98×10^4	8.8×10^3	3.4
I-5	1.7×10^{-4}	0.57	3.32	8.32×10^3	5.8×10^3	1.4
H-4	3.2×10^{-4}	0.48	8.00	2.36×10^4	7.9×10^3	3.0
I-6	3.4×10^{-4}	1.22	2.54	2.96×10^3	2.9×10^3	1.0
I-2	1.0×10^{-3}	2.18	5.12	3.35×10^3	3.8×10^3	0.9
I-3	1.3×10^{-3}	4.26	4.24	1.41×10^3	1.7×10^3	0.8
I-1	2.1×10^{-3}	2.60	2.32	1.27×10^3	1.5×10^3	0.9
H-2	5.9×10^{-3}	9.47	0.67	1.79×10^2	——	—
H-6	2.2×10^{-2}	9.47	0	0	——	—

Dose rate 2.88×10^4 r/hr; * 0.67×10^4 r/hr.

the series is 2.3.

At HBr concentrations greater than 10^{-2}M, the rate of polymerization was extremely low for total doses not exceeding 9×10^5 r, and under these conditions the polymerization is so strongly retarded that rate measurements are no longer meaningful (Table 2-2).

4. Discussion

One of the most significant findings to emerge from this work is that the range of G_i values for the polymerization is considerably greater than the corresponding value for cyclopentadiene[4] which is about 0.1. Freeman and Fayadh[5] pointed out that the free-ion yield in the radiolysis of liquids appeared to be a function of the dielectric constant ε_{static}, in accordance with the Onsager probability exp $(-r_c/r)$ for diffusive escape in the case of an ion pair formed with an initial separation distance r, where r_c is the well-known parameter e^2/ε kT at which distance the Coulombic potential energy $-e^2/\varepsilon\, r_c$ is equal to the thermal kinetic energy kT (k is Boltzmann's constant). For nitroethylene with $\varepsilon \simeq 30$ at 300°K, the value of r_c is 19Å, and it follows that if an appreciable fraction of the ion pairs are formed with r values comparable

to r_c, a high yield of free ions is probable with a maximum value in the region of 3(ion/100eV). Unfortunately, there is no a priori distribution of r values available from theory but experimental estimates for hydrocarbons[6] indicate that the median distance r_m is about 50Å, which is somewhat lower than the de Broglic wavelength (70Å) for a thermal electron at 300°K. Despite this uncertainty, in qualitative terms, the high G_i values obtained in Table 2-2 are consistent with the dependence of G (free ions) on dielectric constant.[5] Furthermore, the chance for diffusive escape is favoured by the fact that the electron is readily captured by the nitroethylene monomer.[7]

No special significance need be attached to the apparent decrease in G_i with increasing HBr concentration. This result is expected when one considers that in the initial stages of irradiation with HBr present, the polymerization is strongly retarded and the $\overline{DP}$ of the polymer formed must be extremely low. Therefore, it is probable that some of the low molecular weight components of the polymer are not precipitated with the high molecular weight polymer, and this effect would lead to an abnormally high value of $\overline{DP}_n$ and consequently a lower G_i. In any event, it is debatable whether a very low molecular weight fraction in the total polymer would be accurately reflected in the average $\overline{DP}_n$ measured by the viscosity method. No

satisfactory method could be found for fractionating the polymer formed in the presence of HBr. This factor, as well as the limited solubility of the polymer in suitable solvents, prevented us from obtaining the molecular weight of the low polymers by techniques (cryoscopy, ebulliometry, etc.) other than viscometry.

A common source of uncertainty of G_i values measured by the polymerization technique is the possible contribution of chain-transfer processes, and this especially true for many radiation-induced cationic polymerizations. However, chain transfer is most unlikely in the present system because it would require proton transfer from the monomer, and the experimental results provide no evidence to suggest that this takes place.

The determination of the propagation rate constant by the retardation method[4] depends on the use of the equation (1),

$$\frac{G_i}{G_o(-M)} = \frac{1}{\overline{DP}_n} = \frac{k_r}{k_p}\,\frac{[HBr]}{[M]} \qquad (1)$$

where k_p and k_r are the respective rate constants for propagation and retardation. This equation is derived on the basis of homogeneous kinetics and assumes that reaction with HBr is the only effective termination step in the polymerization. In principle, either $1/\overline{DP}_n$

or $1/G_o(-M)$ may be plotted as a function of HBr concentration. However, if the retarder concentration is greatly depleted before the end of the run, a plot of $1/\overline{DP}_n$ against the initial HBr concentration is thereby invalidated. In the present case, the non-linear kinetic plots shown in Figure 2-1 strongly suggest that depletion of HBr does occur during the polymerization. The plot of $1/\overline{DP}_n$ against initial [HBr] shown in Figure 2-2 (a) reveals a large scatter and in view of the foregoing reason the data only reveals the expected qualitative trend that $1/\overline{DP}_n$ increases with [HBr]. In semi-quantitative terms, the slope of the line $0.27M^{-1}$ must be considered as a minimum value for the expression $k_r/k_p[M]$. Since the retardation reaction by HBr is of the simple acid-base form, it is reasonable to assume that k_r approaches the diffusion limit of about 10^{10} M^{-1} sec^{-1}. Therefore, these results place a maximum limit on $k_p < 2 \times 10^9 M^{-1}$ sec^{-1}.

A more realistic estimate of k_p may be obtained from the variation of $1/G_o(-M)$ against [HBr]. Figure 2-2 (b) is a plot of the data obtained by equating $G_o(-M)$ to the integral yield at very low conversion (0.25 %). The slope of the line, 3.6 M^{-1}(100eV/ion), for $k_r/G_i k_p[M]$ leads, on the basis of the previous assumptions, to a value of 1.8×10^8 M^{-1} sec^{-1} (ion/100eV) for the product $G_i k_p$. Since the G_i values of 4-5 obtained for the pure monomer are the most reliable determinations, this leads to a k_p value of

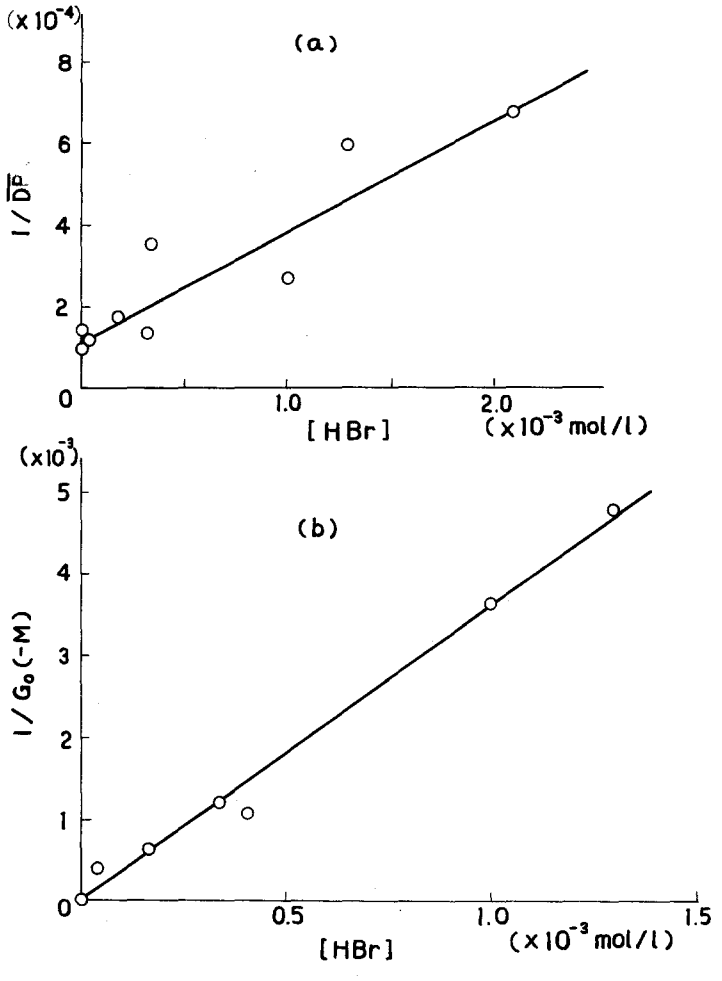

Figure 2-2. Dependence of $1/\overline{DP}_n$ and $1/G_o$(-monomer) on concentration of hydrogen bromide.

4×10^7 M^{-1} sec^{-1}. Probably, this value of k_p is still too large on account of the method used to obtain $G_o(-M)$. Some uncertainty must also be expressed concerning the effective nature and concentration of HBr in the nitroethylene. Since the monomer is expected to function as a good ionizing solvent, the actual retarder may be in the form of protonated solvent molecules. This would not effect the kinetics if complete dissociation occurred, or if both undissociated and dissociated HBr were equally effective in the retardation step. Another possible source of error would arise if HBr partially reacted with nitroethylene. Without quantitative information, it is impossible to estimate the importance of these considerations but since such effects would act to reduce the effective HBr concentration, the k_p value obtained above (4×10^7 M^{-1} sec^{-1}) must be considered an upper limit.

It is of interest to calculate the mean lifetime of the propagating ion during growth in the pure monomer according to the equation,[4)]

$$\tau_p = G_o(-M)/G_i k_p[M] \qquad (2)$$

Substituting the experimental values of $G_o(-M) = 4.66 \times 10^4$ molecules/100eV for the pure monomer, and $G_i k_p = 1.8 \times 10^8$ M^{-1} sec^{-1}. (ion/100eV), we obtain $\tau_p = 1.7 \times 10^{-5}$ sec. A value of 5×10^{-5} sec was calculated in a similar manner

for the polymerization of cyclopentadiene. These lifetimes are considerably shorter than value of 10^{-2} sec measured by the conductivity method[5] for free ions undergoing bimolecular charge neutralization at these dose rates, so the shorter propagation time is likely to be due to a termination reaction with impurities. However, undoubtedly the polymerization is caused by free ions because the lifetime of ions undergoing geminate recombination[6] would only be of the order of 10^{-9} sec.

Szwarc and his co-workers[8] recently reported that in the homopropagation of living polystyrene in tetrahydrofuran, the propagation rate constant k_p for the free anion was 6.5×10^4 M^{-1} sec^{-1} while the corresponding k_p values for the ion pairs are between 22 and 160 $M^{-1}sec^{-1}$, depending on the alkali metal cation. Although the value obtained in this work ($4 \times 10^7 M^{-1}$ sec^{-1}) is about 1000 times greater than for styrene, the comparison may not be justified in view of the different polymerization conditions. However, the present result is in accord with the concept that the reactivity of free ions in polymerization is extremely large, both for cations and anions.

Finally, it is necessary to refer to the previous report[9] by Sokolov et al. on the bulk polymerization of nitroethylene by gamma-rays. These authors reported that the degree of conversion increased with dose and the

polymerization continued after the removal of the sample from the irradiation source. To account for this effect, they suggested the presence of living radicals. No post-irradiation effects of this type were observed during the course of the present work, and the idea of "living radical" polymerization in this system seems rather improbable. The susceptibility of the monomer to polymerization by traces of impurities is well known and extreme care is necessary to prevent the occurrence of spurious effects.

References

1) H. Yamaoka, R. Uchida, K. Hayashi, and S. Okamura, Kobunshi Kagaku, 24, 79 (1967).
2) D. Vofsi and A. Katchalsky, Ricerca Sci., B 25, 165 (1955).
3) J. Grodzinsky, A. Katchalsky, and D. Vofsi, Makromol. Chem., 44/46, 591 (1961).
4) M. A. Bonin, W. R. Busler, and F. Williams, J. Am. Chem. Soc., 87, 199 (1965).
5) G. R. Freeman and J. M. Fayadh, J. Chem. Phys., 43, 86 (1965).
6) J. W. Buchanan and F. Williams, J. Chem. Phys., 44, 4377 (1966).

7) K. Tsuji, H. Yoshida, K. Hayashi, and S. Okamura, Kobunshi Kagaku, 25, 31 (1968).

8) D. N. Bhattacharya, C. L. Lee, J. Smid, and M. Szwarc, J. Phys. Chem., 69, 612 (1965).

9) V. N. Sokolov, I. Ya. Puddubnyi, V. V. Perekalin, and V. F. Evdokimov, Doklady Akad. Nauk. S. S. S. R., 138, 619 (1961).

Chapter 3

Dose Rate Dependence of Bulk Polymerization at Room Temperature

1. Introduction

The importance of the technique to dry monomers in studies of radiation-induced ionic polymerization was first reported by Williams and his coworkers in the polymerizations of α-methylstyrene[1,2] and β-pinene.[3] They found that the rate of polymerization in bulk was critically dependent on the technique of drying the monomers, and that the polymerization was remarkably retarded by the addition of even a very small amount of water into the polymerization systems. These works were followed up by detailed studies of isobutyl vinyl ether,[4] cyclopentadiene[5-7] and α-methylstyrene.[8] Further, Ueno et al.[9,10] and Metz et al[11,12] reported that the polymerization of styrene was enhanced by the use of the technique of drying the monomer extremely. Recently, Cordischi et al.[13-15] also observed the marked effect of the procedures of purifying the monomer in the polymerization of 1,2-cyclohexene oxide. However, these

investigators dealt only with the monomers susceptible to cationic polymerization.

Nitroethylene is of interest for studying the effect of the technique of drying on anionic polymerization, since it was established in the preceding Chapters that the radiation-induced polymerization of nitroethylene proceeded through an anionic mechanism. In the present study, the polymerization of extremely dried nitroethylene in bulk at 20°C has been studied as a function of dose rate.

2. Experimental

2.1. Sample preparation

Nitroethylene was synthesized by the procedure described in Chapter 1. The apparatus for preparation of samples is shown in Figure 3-1. The freshly distilled monomer was stored in A and degassed by the usual sequence of freezing, pumping and melting operations. After being pre-dried over baked Drierite in A, the monomer was transfered into the reservoir of B containing barium oxide baked at 350°C in vacuum for 10 hours. All parts connected to the vacuum line were sufficiently baked out, and then the lower part of the apparatus was isolated by sealing off at constrictions C.

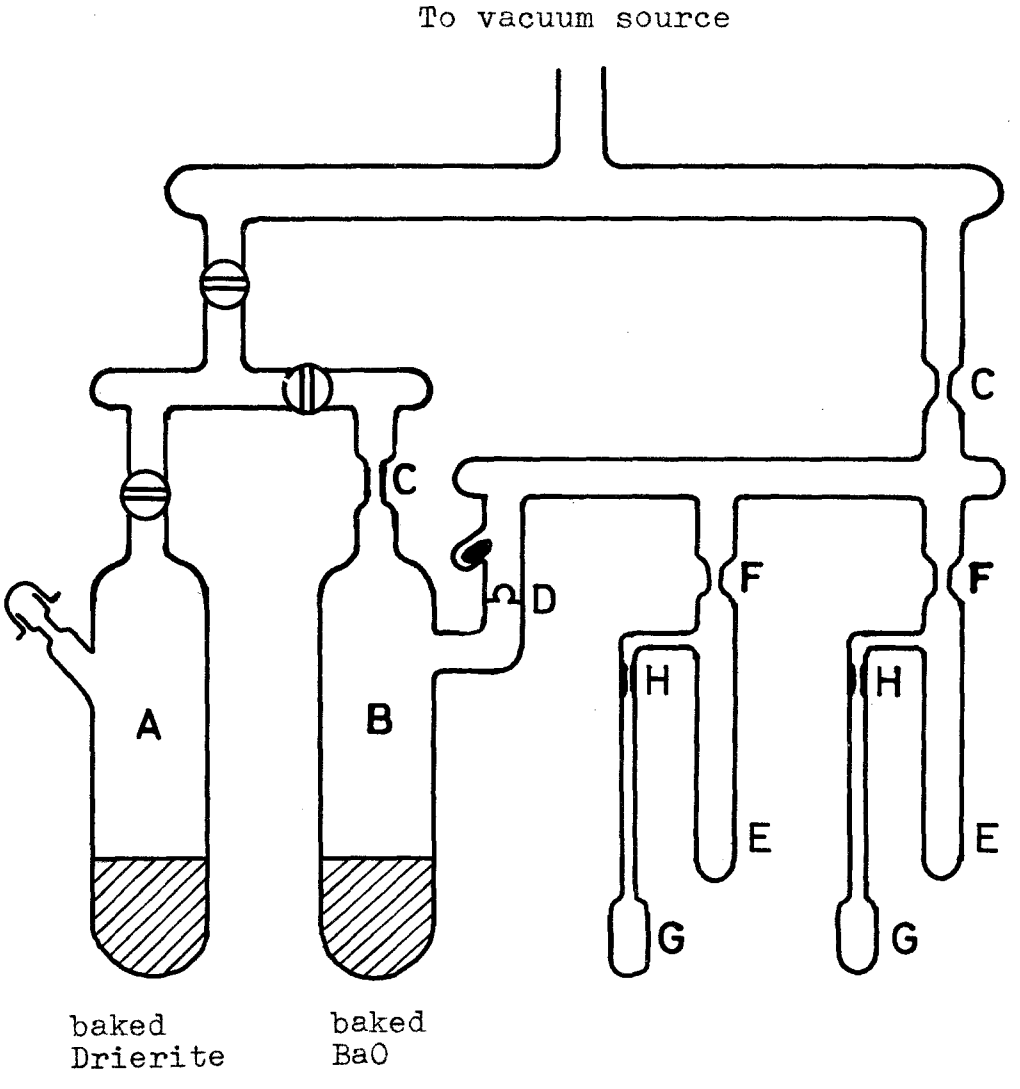

Figure 3-1. Apparatus for preparation of samples.

The monomer was stored for 24 hours at room temperature, during which time some polymerization occurred. After this storage period, the remaining monomer was distilled into an ampoule E through a break-seal at D, and sealed off at a constriction F. Finally, an appropriate amount of the monomer was condensed into a dilatometer bulb G by sealing off at a constriction H.

2.2. Polymerization

Samples were irradiated at 20°C with gamma-rays from a 1,000 curie cobalt-60 radiation source. The dose rates were changed in the range between 0.18×10^4 and 8.98×10^4 r/hr. The polymerization was followed by the dilatometric method as described in Chapter 2.

3. Results

A typical example for the difference of sample preparation is represented in Figure 3-2. The curve (a) shows the relation between the polymer conversion and the irradiation time for the extremely dried monomer. The conversion increased linearly with the increase of irradiation time without any induction period. The time-conversion curve for the monomer dried only by baked

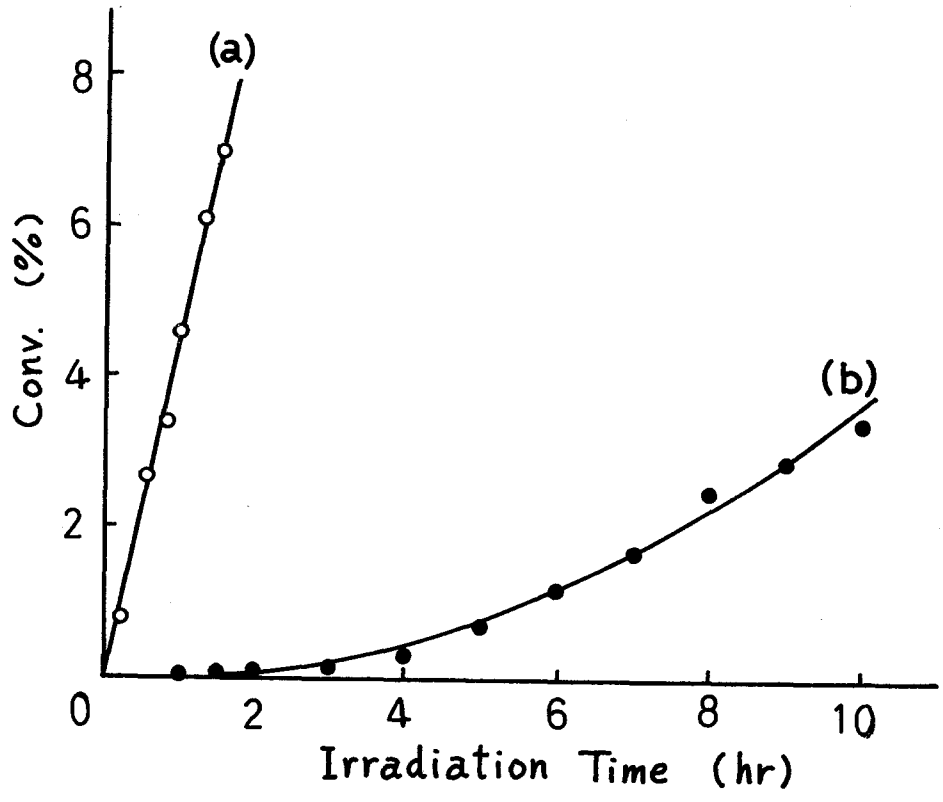

Figure 3-2. Relation between polymer conversion and irradiation time in different sample preparation methods.

o: extremely dried monomer, ●: normally dried monomer, dose rate 1.53×10^4 r/hr, polym. temp. 20°C.

Drierite (normally dried monomer) is shown in the curve (b). In this case, a certain induction period of the polymerization was observed, and the rate of polymerization was greatly depressed in comparison with that for the extremely dried monomer. The value of G(-monomer) obtained from the slope of linear part in the curve (b) was 4.86×10^3, whereas G(-monomer) in the curve (a) was as large as 4.24×10^4.

The time-conversion curves at various dose rates for the extremely dried monomer are shown in Figures 3-3 and 3-4. As the polymerization proceeded, the polymer was uniformly suspended. Beyond 10 % conversion, the polymer began to precipitate and the polymerization was slightly accelerated. Therefore, all experiments were carried out below 10 % conversion. The rates of polymerization obtained from the slopes in Figures 3-3 and 3-4 are summarized in Table 3-1. The reproducibility of the rate of polymerization in different runs was fairly good as seen from two experiments at the dose rate of 1.53×10^4 r/hr. The plots of the rate of polymerization against the dose rate are represented in Figure 3-5. The rate of polymerization is clearly proportional to the square-root of dose rate.

The values of G(-monomer), which lay in the range between 1.68×10^4 and 1.90×10^5, decreased with the increase of dose rate as shown in Table 3-1.

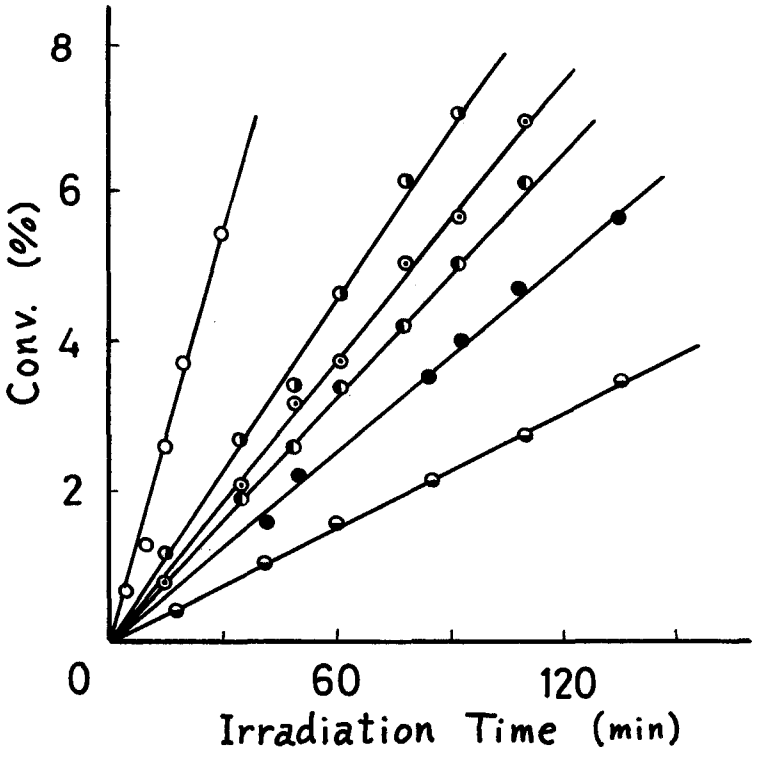

Figure 3-3. Relation between polymer conversion and irradiation time (I).

Dose rate (r/hr); ○ : 8.98×10^4, ◐ : 1.53×10^4, ◑ : 1.07×10^4, ◐ : 0.76×10^4, ● : 0.57×10^4, ◒ : 0.18×10^4, polym. temp. 20°C.

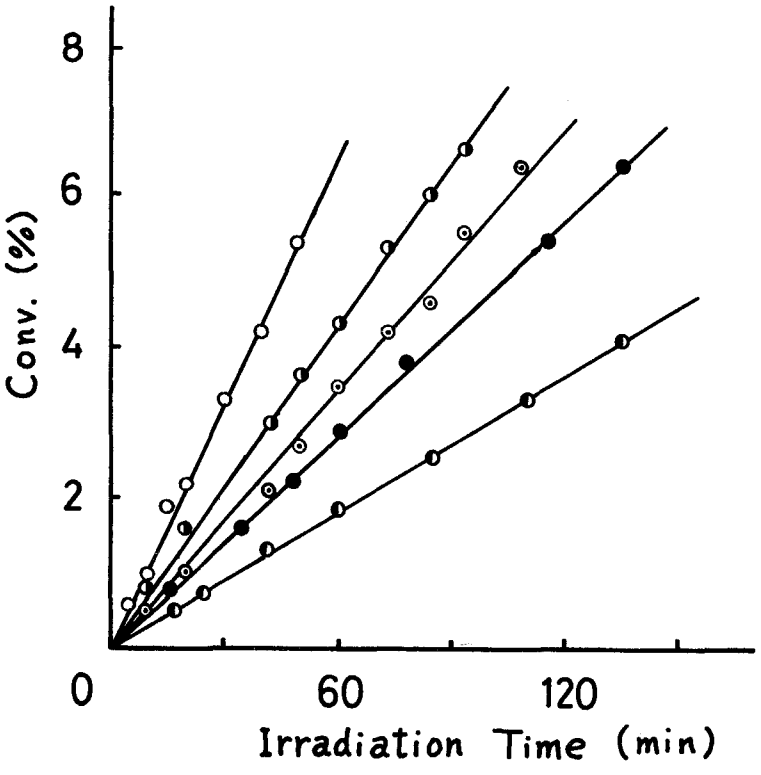

Figure 3-4. Relation between polymer conversion and irradiation time (II).

Dose rate (r/hr); ○ : 3.71×10^4, ◐ : 1.53×10^4, ◑ : 0.89×10^4, ● : 0.51×10^4, ◐ : 0.27×10^4, polym. temp. 20°C.

Table 3-1. Effect of dose rate on the radiation-induced polymerization of nitroethylene at 20°C.

Sample code	Dose rate $\times 10^{-4}$ (r/hr)	R_p (M hr^{-1})	G(-monomer) $\times 10^{-4}$
N-5	8.98	1.61	1.68
N-1	3.71	0.99	2.49
N-13	1.53	0.69	4.24
N-10	1.53	0.65	4.00
N-11	1.07	0.57	4.95
N-9	0.89	0.53	5.52
N-4	0.76	0.49	5.08
N-8	0.57	0.39	6.36
N-3	0.51	0.43	7.94
N-2	0.27	0.27	9.46
N-15	0.18	0.23	19.0

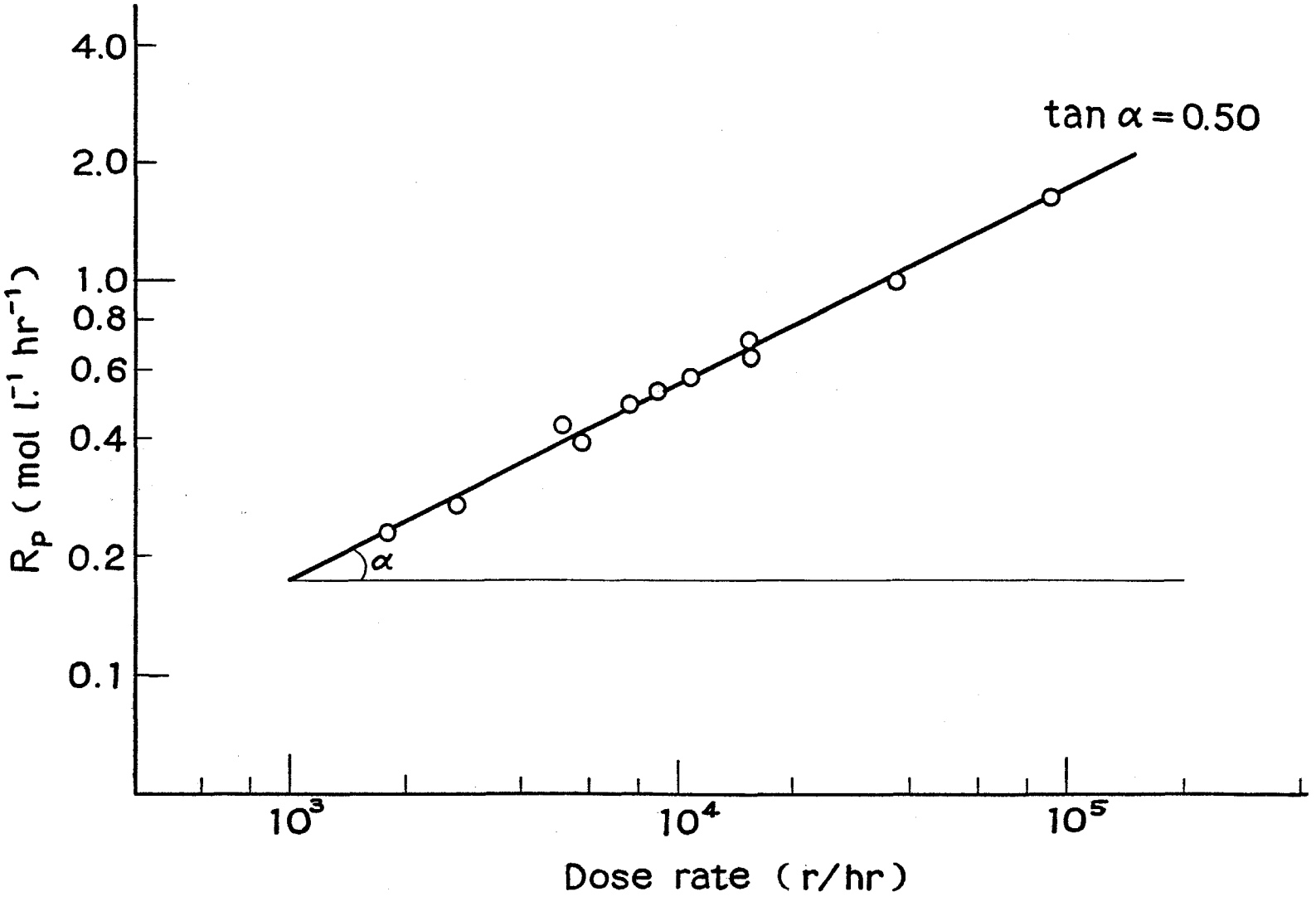

Figure 3-5. Dose rate dependence of rate of polymerization.

4. Discussion

The experimental results indicate that the technique of drying the monomer is very important in anionic polymerization as well as in cationic polymerizations.[1-15] The value of G(-monomer) in the extremely dried monomer was about 10 times as large as that in the normally dried one. The induction period observed in the normally dried monomer might be the time required for impurities to be consumed by irradiation.

In the extremely dried system, the termination reaction with impurities and the chain transfer reaction to them can be neglected, and the chain transfer to the monomer is almost improbable because of the requirement of the proton transfer from the monomer as pointed out in Chapter 2. Therefore, the elementary reactions for the present system can be simply expressed as follows:

Ionization	$M \rightsquigarrow M^{+\cdot} + e^-$	(a)
Initiation	$e^- + M \longrightarrow M^{-\cdot}$	(b)
	$M^{-\cdot} + M \longrightarrow {}^{\cdot}M\text{-}M^- \ (M_2^-)$	(c)
Propagation	$M_{n-1}^- + M \xrightarrow{k_p} M_n^-$	(d)
Termination	$M_n^- + M^{+\cdot} \xrightarrow{k_t} M_{n+1}$	(e)

where k_p and k_t are the rate constants for propagation and termination by charge recombination, respectively. Although the polymerization system became heterogeneous with the progress of polymerization, it was assumed that this heterogeneity did not affect the kinetics of polymerization in the conversion range examined. Assuming that the rate-determining step of initiation is the reaction (a) as described in Chapter 1, the rate of initiation, R_i, is given by the equation (1),

$$R_i = I\ G_i\ /\ 100 \qquad (1)$$

where I is the dose rate and G_i is the 100 eV yield of free ions capable of initiation. Since the accelerating effect in the time-conversion curves was not observed below 10 % conversion, the stationary state assumption holds in the present system. Then, the rate of polymerization, R_p, is represented by the equation (2),

$$R_p = k_p[M^-][M] = \frac{k_p}{k_t^{\frac{1}{2}}} \left(\frac{I\ G_i}{100} \right)^{\frac{1}{2}} [M]. \qquad (2)$$

The observed square-root dependence of R_p on dose rate, which is in good agreement with the equation (2), indicates that the termination of the polymerization is taken place by charge recombination between the propagating anions and positively recharged species (reaction (e)).

In order to estimate the value of k_p, the equation (2) is transformed as

$$k_p = \frac{R_p \, k_t^{\frac{1}{2}}}{R_i^{\frac{1}{2}} \, [M]} \qquad (3)$$

According to the relation between the value of G(free ion) and the dielectric constant by Freeman and Fayadh,[16] the G_i value is assumed to be about 1.2 in the present system where the dielectric constant of the monomer was estimated to be about 30 at 20°C. Unfortunately, the value of k_t was not obtained experimentally, because the electroconductivity measurements of the present system has not yet been done successfully. Here, the value of k_t is expected to be equal to or smaller than 10^{11} M^{-1} sec^{-1} which is the maximum value for diffusion-controlled reaction. In the studies of radiation-induced cationic polymerization, Williams et al.[17] estimated that the value of k_t is of the order of 10^{11} M^{-1} sec^{-1}.

The values of k_p calculated on these assumptions are summarized in Table 3-2. The average values of k_p lie between 1.7×10^4 and 5.3×10^4 $M^{-1}sec^{-1}$. These values are considerably smaller than the estimated k_p value in Chapter 2 (4×10^7 $M^{-1}sec^{-1}$). However, taking into consideration that the k_p value in Chapter 2 is an upper limit as described previously, these values obtained in the

Table 3-2. Estimation of the rate constant for propagation in the radiation-induced polymerization of nitroethylene at 20°C.

Sample code	Dose rate $\times 10^{-14}$ (eV $cm^{-3} sec^{-1}$)	$R_i \times 10^9$ (M sec^{-1})	$R_p \times 10^4$ (M sec^{-1})	$R_p/R_i^{\frac{1}{2}}[M]$ ($M^{-\frac{1}{2}} sec^{-\frac{1}{2}}$)	k_p ($M^{-1} sec^{-1}$)	
				k_t ($M^{-1} sec^{-1}$)	10^{10}	10^{11}
N-5	16.1	31.0	4.48	1.65	1.7×10^4	5.2×10^4
N-1	6.64	13.2	2.75	1.58	1.6	5.0
N-13	2.74	5.45	1.93	1.72	1.7	5.4
N-10	2.74	5.45	1.82	1.62	1.6	5.1
N-11	1.92	3.82	1.58	1.69	1.7	5.3
N-9	1.59	3.17	1.46	1.71	1.7	5.4
N-4	1.36	2.71	1.37	1.73	1.7	5.5
N-8	1.02	2.03	1.08	1.58	1.6	5.0
N-3	0.92	1.82	1.20	1.86	1.9	5.9
N-2	0.49	0.97	0.76	1.64	1.6	5.2
N-15	0.32	0.64	0.63	1.66	1.7	5.3
				Average value	1.7×10^4	5.3×10^4

present study seem to be reasonable despite the uncertainity on the value of k_t.

From the results of the present and previous investigations, it is concluded that the radiation-induced polymerization of nitroethylene at room temperature is propagated by free anionic species and terminated by charge neutralization between charged species.

References

1) T. H. Bates, J. V. F. Best, and F. Williams, Nature, 188, 469 (1960).
2) T. H. Bates, J. V. F. Best, and F. Williams, Trans. Faraday Soc., 58, 192 (1962).
3) T. H. Bates, J. V. F. Best, and F. Williams, J. Chem. Soc., 1531 (1962).
4) M. A. Bonin, M. L. Calvert, W. L. Miller, and F. Williams, J. Polymer Sci., B, 2, 143 (1964).
5) M. A. Bonin, W. R. Busler, and F. Williams, J. Am. Chem. Soc., 84, 4355 (1962).
6) W. R. Busler, D. H. Martin, and F. Williams, Disc. Faraday Soc., 36, 102 (1963).
7) M. A. Bonin, W. R. Busler, and F. Williams, J. Am. Chem. Soc., 87, 199 (1965).

8) E. Hubmann, R. B. Taylor, and F. Williams, Trans. Faraday Soc., 62, 88 (1966).

9) K. Ueno, K. Hayashi, and S. Okamura, Polymer, 7, 431 (1966).

10) K. Ueno, F. Williams, K. Hayashi, and S. Okamura, Trans. Faraday Soc., 63, 1478 (1967).

11) R. C. Potter, C. L. Johnson, D. J. Metz, and R. H. Bretton, J. Polymer Sci., A-1 4, 419 (1966).

12) R. C. Potter, R. H. Bretton, and D. J. Metz, J. Polymer Sci., A-1, 4, 2295 (1966).

13) D. Cordischi, M. Lenzi, and A. Mele, J. Polymer Sci., A, 3421 (1965).

14) D. Cordischi, A. Mele, and A. Somogyi, Proc. 2nd Tihany Symp. Radiation Chem., 451 (1967).

15) D. Cordischi, A. Mele, and R. Rufo, Trans. Faraday Soc., 64, 2794 (1968).

16) G. R. Freeman and J. M. Fayadh, J. Chem. Phys., 43, 86 (1965).

17) F. Williams, Ka. Hayashi, K. Ueno, K. Hayashi, and S. Okamura, Trans. Faraday Soc., 63, 1501 (1967).

Chapter 4

Studies on Initiating Species

1. Introduction

In order to investigate the primary processes of radiation-induced chemical reactions, the rigid glass matrix method has been proved useful by electron spin resonance (ESR)[1] and optical absorption measurements,[2] because transient active species such as ions and free radicals are stably trapped in the glass. Yoshida et al. applied this method to organic glassy systems containing styrene[3] for elucidating the mechanism of polymerization by ESR measurements. They found that cation radicals of styrene were formed in n-butylchloride glass by the transfer of positive charge and the radiation-induced polymerization proceeded in the glass where the cation radicals were present. Further, they observed no polymerization in 2-methyltetrahydrofuran (MTHF) glass where the anion radicals of styrene were formed by the capture of electrons. They suggested from these results

that the radiation-induced polymerization of styrene, especially in the glassy state, proceeded by a cationic mechanism. Bodard and Marx[4] carried out similar experiments in MTHF glass containg acrylonitrile and reported that the anion radicals observed by ESR measurements were responsible for the polymerization.

Another useful approach in investigating ionic reactions induced by radiation seems to be the application of mass spectrometry. This method is expected to provide direct information on the primary processes of radiation-induced polymerization. In the field of positive ion mass spectra, several studies on unsaturated hydrocarbons[5] have been reported and contributed to elucidate the reaction mechanism of polymerizations. However, from the viewpoint of studying the anionic polymerization, any available mass spectrometric information on negative ions has scarcely been found.

In the present investigation for the purpose of studying the initiating species of the radiation-induced polymerization of nitroethylene, the ESR measurements of irradiated MTHF glass containing nitroethylene have been carried out at -196°C, and also the negative ions from nitroethylene formed by the electron impact have been measured by the use of a mass spectrometer.

2. Experimental

2.1. ESR measurements

Nitroethylene was prepared and purified as described already. Commercial MTHF was distilled several times over metallic sodium and dried with sodium-potassium mirror. These purified materials were distilled into ESR sample tubes of pure quartz (Spectrosil, Thermal Syndicate Co.) under vacuum.

The samples were irradiated by cobalt-60 gamma-rays at -196°C in the dark. Measurements were carried out at -196°C with an X-band ESR spectrometer with the 100 kHz magnetic field modulation (Varian model V-4500) at a microwave power level of 1 mW.

2.2. Mass spectrometric measurements

The apparatus used for this study was 90° single focusing mass spectrometer (Hitachi model RMU-6) which was modified to measure negative ions. A conventional type electron gun was used without paying attention to electron energy spread. The details of measurements will be described in Chapter 7.

3. Results and Discussion

3.1. ESR measurements

A transparent glassy sample was obtained by cooling MTHF rapidly in liquid nitrogen. When the MTHF glass was irradiated at -196°C in the dark, the sample colored blue and gave an ESR signal composed of a septet spectrum and a sharp singlet one as shown in Figure 4-1 (a). The former is due to free radicals formed from MTHF molecules and the latter is due to trapped electrons in the glass as reported by Smith and Pieroni.[6] On the other hand, MTHF glass containing 1.5 mole % nitroethylene gave no spectrum due to the trapped electrons, but showed a new complex spectrum superposed on the spectrum of the MTHF radicals (Figure 4-1 (b)). On exposure of the irradiated glassy mixture to visible light, the new complex spectrum disappeared and the shape of the spectrum changed from that in Figure 4-1 (b) to that of MTHF radicals in Figure 4-1 (c). Further, upon raising the temperature of the irradiated mixture from -196°C, the new spectrum disappeared in the temperature range between -140°C and -135°C.

The new complex spectrum in Figure 4-1 (b) is thought to be due to anion radicals formed through the electron capture by added nitroethylene. The observed spectrum

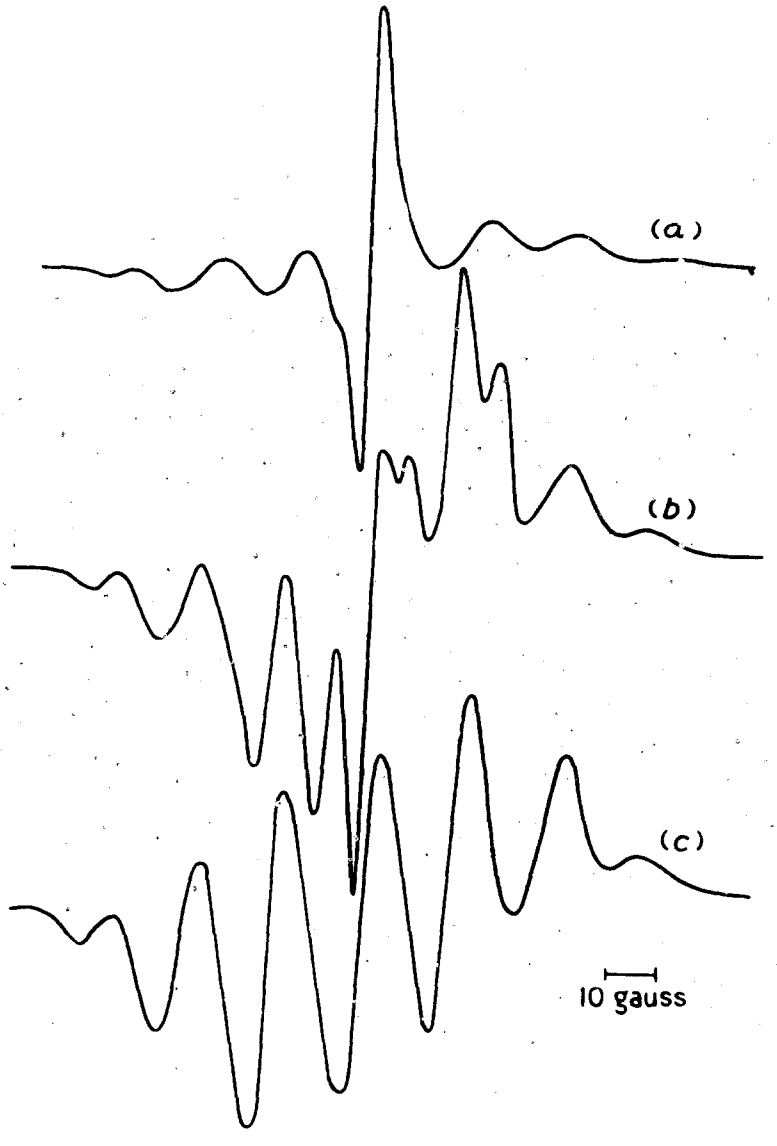

Figure 4-1. ESR spectra of irradiated 2-methyltetrahydrofuran glass irradiated up to a dose of 1.0×10^5 r at -196°C:

(a) pure 2-methyltetrahydrofuran glass (signal amplifier gain: 50),

(b) glassy mixture of 2-methyltetrahydrfuran containing 1.5 mole % nitroethylene (gain: 160),

(c) pure 2-methyltetrahydrofuran glass and glassy mixture of 2-methyltetrahydrofuran containing nitroethylene bleached with the visible light after γ-irradiation (gain: 160).

was in agreement with that expected from the Hückel LCAO-MO calculation as an anionic radical of nitroethylene.[7] The MTHF glass containing 0.15 mole % nitroethylene showed spcetra of both trapped electrons and the nitroethylene anion radicals after the irradiation. When the irradiated glassy mixture was maintained at -196°C in the dark, the signal intensity of the trapped electrons gradually decreased and that of the nitroethylene anion radicals increased with the keeping time. This fact indicates that the nitroethylene molecule has an ability as a strong electron acceptor in accordance with the results obtained from the optical[8] and the mass spectrometric investigations.[9] The new spectrum is readily bleached out with visible light. The sensitivity of the spectrum to visible light seems not to result from the nature of ordinary neutral free radicals. These results imply that the new spectrum in Figure 4-1 (b) is due to anion radicals of nitroethylene formed by the following mechanism:

$$\text{MTHF} \xrightarrow{\sim\sim\sim} (\text{MTHF})^{+\cdot} + e^-$$

$$e^- + \text{nitroethylene} \longrightarrow (\text{nitroethylene})^{-\cdot}$$

The correlation between the results of ESR measurements and the postpolymerization will be mentioned in Chapter 5.

3.2. Mass spectrometric observations

A large number of negative ions were observed from nitroethylene by electron impact with 100 eV energy. The relative abundance of main negative ions under various conditions, which were normalized to the intensity of NO_2^-, are summarized in Table 4-1.

The parent negative ion of nitroethylene, $C_2H_3NO_2^-$, was observed at a pressure of 2.6×10^{-6} mmHg. From the ionization efficiency curve of $C_2H_3NO_2^-$, the appearance potential of the parent negative ion was found to be about 0 eV, which is the same as that of SF_6^- from sulfur hexafluoride.[10] This fact indicates that nitroethylene is a strong electron acceptor, as suggested by the theoretical consideration on the anion radicals of nitroethylene.[8]

When a large quantity of inert gases such as krypton and xenon was added in the ionization chamber without changing the pressure of nitroethylene, the relative abundance of the parent negative ion increased in both cases as shown in Table 4-1. This may be due to the more frequent collisional stabilization of excited parent negative ion in the presence of inert gases.

The increasing pressure of nitroethylene which also facilitates the collisional stabilization gave the higher relative yields of the parent negative ion. Further, the

Table 4-1. Relative abundance of the main negative ions produced from nitroethylene by electron impact of 100 eV.

Samples		NE	lNE + ca.10^3 Kr	lNE + ca.10^3 Xe	NE
Total press. in ion cham.	(mmHg)	3×10^{-6}	9×10^{-3}	9×10^{-3}	9×10^{-3}
m/e	Ion				
16	O^-	7.4	5.8	6.0	6.8
17	OH^-	6.8	12	10	9.1
25	C_2H^-	19	16	17	22
30	NO^-	0.93	1.0	1.0	0.96
42	CNO^-	3.4	2.6	2.9	7.3
46	NO_2^-	100	100	100	100
55	C_2HNO^-	0.62	0.54	0.38	0.85
72	$C_2H_2NO_2^-$	0.03	0.41	0.14	5.8
73	$C_2H_3NO_2^-$	0.27	8.8	9.5	88
119	$C_2H_3N_2O_4^-$	—	0.23	—	0.64
146	$(C_2H_3NO_2)_2^-$	—	0.07	0.02	0.10
219	$(C_2H_3NO_2)_3^-$	—	—	—	2×10^{-4}

dimer and the trimer negative ions were observed at a pressure of 9×10^{-3} mmHg, although the intensities of the ions were very low. These polymerized ions are thought to be obtained by the ion-molecule reactions between the parent negative ion and neutral nitroethylene molecule. A more detailed study of these ion-molecule reactions will be described in Chapter 8.

From the results obtained in the present Chapter, it is suggested that the anion radicals of nitroethylene are readily formed by the capture of electrons and these species are responsible for the initiation process of the radiation-induced polymerization of nitroethylene.

References

1) P. B. Ayscough, R. G. Collins, and F. S. Dainton, Nature 205, 965 (1962); C. Chachaty, J. Chim. Phys., 64, 614 (1967).
2) M. R. Ronayne, J. P. Guarino, and W. H. Hamill, J. Am. Chem. Soc., 84, 4230 (1962).
3) T. Iwamoto, K. Hayashi, S. Okamura, Ka. Hayashi, and H. Yoshida, Int. J. Radiat. Phys. Chem., 1, 1 (1969).

4) M. Bodard-Gauthier and R. Marx, J. Polymer Sci., C, 16, 4241 (1968).

5) For examples, S. Wexler, A. Lifshitz, and A. Quattrochi, Advan. Chem. Series, 58, 193 (1966); P. Kebarle, R. M. Haynes, and S. Searles, ibid., 58, 210 (1966); J. H. Futrell and T. O. Tiernan, J. Phys. Chem., 72, 158, 1994, 3080 (1968).

6) D. R. Smith and J. J. Pieroni, Can. J. Chem., 43, 876 (1965).

7) K. Tsuji, H. Yoshida, K. Hayashi, and S. Okamura, Kobunshi Kagaku, 25, 31 (1968).

8) H. Kamiyama, K. Hayashi, and S. Okamura, Annual Report of Japan Assoc. Rad. Res. Polymers, 7, 145 (1965/1966).

9) H. Yamaoka, T. Shiga, K. Hayashi, S. Okamura, and T. Sugiura, J. Polymer Sci., B, 5, 329 (1967).

10) W. H. Hickam and R. E. Fox, J. Chem. Phys., 25, 642 (1956).

Chapter 5

Investigations on Postpolymerization

1. Introduction

Glassy systems containing monomers seems to be suitable for studying the initial processes of radiation-induced polymerizations, since active species involved in reactions are easily trapped in the glasses and can be observed by various spectroscopic techniques. Radiation-induced polymerizations in glasses at low temperatures have been reported in the last few years. The polymerizations of several derivatives of acrylic monomers,[1-6] vinyl acetate,[2,7] vinyl chloride,[5] styrene[2,5] and acrylonitrile[5] in oils or other glass-forming systems were found to proceed by a free radical mechanism. Bodard and Marx[8] reported that the polymerization of acrylonitrile in 2-methyltetrahydrofuran glass at low temperature proceeded by an anionic mechanism. Kamiyama et al.[9] observed the in-source polymerization of isobutene in 3-methylpentane glass at -196°C by measurements of near-inrared spectra. Recently, Chapiro et al.[10]

studied the polymerizations of acrylonitrile and styrene in various glasses, and found the remarkable post-effect of the polymerizations in both anionic and cationic propagations.

In the course of investigations of the radiation-induced polymerization of nitroethylene, anionic propagation was confirmed from the effect of additives and the copolymerization with acrylonitrile,[11] and also the propagation by free anions was assumed from the results of kinetic experiments.[12] Further, electron spin resonance (ESR)[13,14] optical[15] and mass spectrometric investigations[16] of nitroethylene suggested that the polymerization was initiated by anion radicals of nitroethylene formed by the capture of electrons.

The present study is concerned with the radiation-induced postpolymerization of nitroethylene. The glassy mixture of nitroethylene in 2-methyltetrahydrofuran (MTHF) at low temperature is chosen as a polymerization system, and the initiating species of the postpolymerization are discussed in relation to the results obtained from the ESR measurements.

2. Experimental

2.1. Materials

Nitroethylene was prepared by procedures already described. For the purification of the monomer, special attention was paid to eliminate traces of water. Commercial MTHF was distilled twice over metallic sodium and dried with a sodium mirror. The monomer and MTHF were transfered to measuring ampoules by trap-to-trap distillation in vacuum and finally condensed into quartz ampoules.

2.2. Polymerization

Preirradiations were done at -196°C in the dark by gamma-rays from a 1,000 curie cobalt-60 radiation source. The postpolymerizations were carried out in the temperature range between -150°C and -78°C. After the irradiation, the ampoules were removed to a Dewar vessel kept at the postpolymerization temperature by the following method. Nitrogen gas, which was previously cooled by passing through a spiral tube in liquid nitrogen, was blown into the Dewar vessel. The regulation of the temperature between -150°C and -78°C was performed by changing the blowing speed of cooled nitrogen gas. The precision of the temperature control was ± 2°C. The polymerization temperature of

-78°C was attained in the Dewar vessel with dry ice-methanol mixture.

Photo-bleaching of the irradiated sample was done at -196°C for 1 hour by a 150 watt tungsten lamp before warming the samples.

2.3. Polymer

In order to avoid the effect of melting technique on the polymer yield, the reaction mixture, after the polymerization, was again cooled down to -196°C and crushed to a powder. Then, the mixture was poured at room temperature into a vigourously stirred 1 : 1 water + methanol mixture, previously acidified with concentrated hydrogen chloride to prevent further polymerization. The polymer yield was determined gravimetrically. The molecular weight of the polymer was estimated from viscosity measurements as mentioned in Chapter 1.

3. Results

In order to examine the in-source polymerization of nitroethylene, the samples were irradiated at -196°C and, immediately after the irradiation, poured into the

precipitating solvent at room temperature. The results are shown in Table 5-1. No polymer was obtained in any case. It is evident that in-source polymerization does not occur at -196°C.

Table 5-1. Radiation-induced in-source polymerization of nitroethylene at -196°C.

Code	Sample			Conv. (%)
	Monomer (ml)	MTHF (ml)	Monomer Conc. (mol. %)	
10	1.0	9.0	12.7	0
75	1.5	10.5	15.6	0
76	1.9	9.9	20.0	0
2	3.5	10.5	30.3	0

Dose rate 3.12×10^4 r/hr,
Total dose 2.0×10^6 r.

The results of the postpolymerizations at various temperatures are summarized in Table 5-2. The polymer was not obtained at -150°C. In the temperature range between -135°C and -78°C, the polymer yield decreased with the rise in postpolymerization temperature.

Table 5-2. Relation between polymer conversion and postpolymerization temperature.

Code	Monomer conc. (mol. %)	Postpolym. temp. (^{o}C)	Conv. (%)
90	25.0	-78	0.6
87	25.0	-95	0.7
66	25.0	-120	1.7
64	25.0	-135	2.3
26	11.6	-150	0

Dose rate 3.12×10^{4} r/hr, total dose 2.0×10^{6} r, preirradiation temp. -196^{o}C, polym. time 150 min.

The effect of the preirradiation dose of the conversion is shown in Figure 5-1 and Table 5-3. The polymer conversion increased with the increase in preirradiation dose, and then saturated in the dose range above 0.9×10^{6} r. The mean value of G(-monomer) was calculated to be 2.73×10^{2} from the slope of the linear part in Figure 5-1. The molecular weight of the polymers was scarcely dependent on the dose even for the preirradiations above 0.9×10^{6} r as shown in Table 5-3.

The polymer yield increased linearly with the increasing monomer concentration. Consequently, the polymer conversion

Table 5-3. Effect of preirradiation dose on polymer conversion and molecular weight of polymer.

Code	Total dose ($\times 10^{-6}$ r)	Conv. (%)	G(-monomer) ($\times 10^{-2}$)	$\overline{M}_w$ ($\times 10^{-4}$)
81	0.22	0.46	2.95	—
82	0.47	0.79	2.38	2.87
83	0.68	1.37	2.84	3.28
84	0.88	1.70	2.73	3.11
85	1.43	1.71	1.36	3.24
86	2.68	1.73	0.91	3.09

Dose rate 3.12×10^4 r/hr, preirradiation temp. -196°C, postpolym. temp. -120°C, polym. time 150 min., monomer conc. 24.4 mol. %.

was independent of the monomer concentration with in the range examined, as shown in Figure 5-2. The molecular weight of the polymers obtained was almost proportional to the monomer concentration. Since the concentration of the active species responsible for chain initiation can be derived from the quotient [polymer yield]/[molecular weight], these results indicate that the concentration of the initiating species is independent of the monomer concentration.

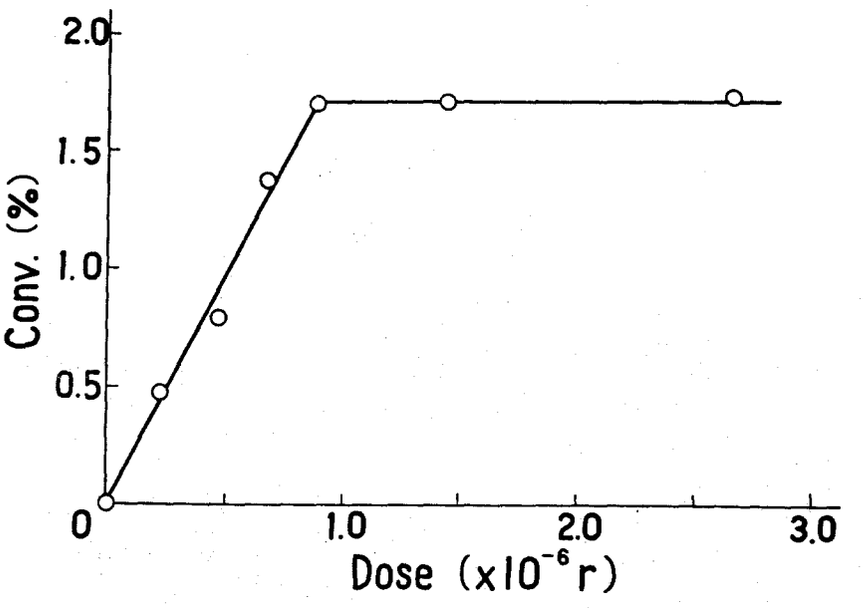

Figure 5-1. Effect of preirradiation dose on polymer conversion.

Experimental conditions are same as those of Table 5-3.

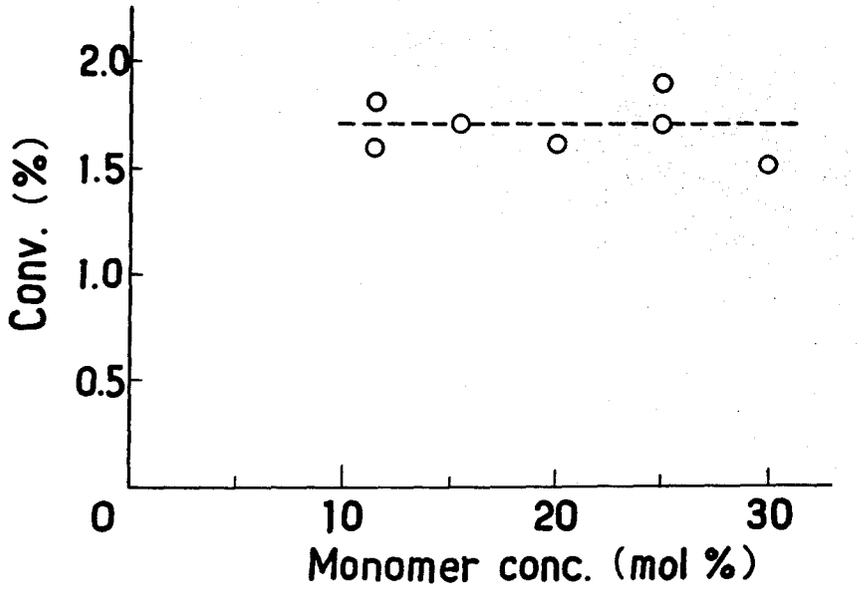

Figure 5-2. Relation between polymer conversion and monomer concentration.

Dose rate 3.12×10^4 r/hr, total dose 2.0×10^6 r, preirradiation temp. -196°C, postpolym. temp. -120°C, polym. time 150 min.

In order to compare the results of postpolymerization with those of the ESR measurements, the effect of photo-bleaching on the postpolymerization was studied. After the preirradiation at -196°C, the samples were exposed to visible light at the same temperature and then warmed up to the postpolymerization temperature. As summarized in Table 5-4, the polymer yield obviously decreased with the photo-irradiation. Similar results were reported for acrylonitrile by Bodard and Marx.[8)]

4. Discussion

From the viewpoint of studying the initiation process of the radiation-induced polymerization, it is worthwhile to compare the results of the postpolymerization with those of the ESR measurements described in Chapter 4: (i) The postpolymerization does not occur at temperatures below -150°C. Under the same conditions, the anion radicals of nitroethylene formed by the capture of electrons are stably trapped in the glassy mixture. Further, the postpolymerization starts in the temperature range between -140°C and -135°C where the ESR spectrum due to the anion radicals disappears. (ii) The polymer yield of the postpolymerization decreases with the photo-irradiation at -196°C. This fact

Table 5-4. Effect of photo-irradiation on the postpolymerization of nitroethylene.

Code	Monomer conc. (mol. %)	Postpolym. temp. (°C)	Photo-irradiation [a]	Conv. (%)
18	11.6	-120	○	0.7
16	11.6	-120	×	1.6
65	25.0	-120	○	0.5
66	25.0	-120	×	1.7
69	25.0	-120	×	1.9
63	25.0	-135	○	1.0
64	25.0	-135	×	2.3
24	11.6	-150	○	0
26	11.6	-150	×	0

a) ○ : Photo-irradiation by a tungsten lamp for 1 hour,
× : Non-irradiation.

Temp. of preirradiation and photo-irradiation -196°C, dose rate 3.12×10^4 r/hr, total dose 2.0×10^6 r, polym. time 150 min.

suggests that the initiating species of the polymerization are deactivated by exposure to visible light. Also the anion radicals in the glassy mixture are bleached out by photo-irradiation. These correlations indicate that the polymerization is initiated by the anion radicals of nitroethylene as predicted by the optical[15] and the mass spectrometric investigations.[16] In the photo-bleaching experiments, the absence of the polymer on the postpolymerization could be expected from the results of ESR measurements. However, the results of Table 5-4 indicate that the photo-irradiation in the conditions used is insufficient for the polymerization system. The reason for this may be that the ampoules for the polymerization are much bigger than those for the ESR measurements.

Figure 5-2 shows that the concentration of the initiating species is independent of the monomer concentration. Further, the ESR study shows that the electrons trapped in MTHF matrix are easily captured by a small quantity of nitroethylene in the system. These facts indicate that the G value for the production of the anion radicals of nitroethylene is about 2.6, which is the same as that for trapped electrons.[17] In order to deduce the initiating efficiency of the anion radicals for the postpolymerization, it is necessary to estimate the

initiation yield G_i. In the present study, G_i is obtained from the quotient G(-monomer)/$\overline{DP}_n$ in the preirradiation dose range below 0.9×10^6 r. Since the average degree of polymerization was obtained as 2.1×10^2 from the results of Table 5-3, the G_i value was estimated to be about 1.3. From these results, it is concluded that the anion radicals formed in the glassy mixture can effectively initiate the postpolymerization of nitroethylene.

The dependence of the preirradiation dose on the polymer conversion (see Figure 5-1) indicates that the population of trapped ions reaches a certain limit at about 0.9×10^6 r, beyond which the average distance between ion pairs probably interrupts further trapping. This argument is also supported by the fact that the molecular weights of the polymers obtained in the saturation range are almost the same as those at the dose below 0.9×10^6 r as shown in Table 5-3.

It is not yet clear as to why the polymer yield decreases with the rise in postpolymerization temperature in the range between -135°C and -78°C. Recently, Chapiro et al.[10] reported that a very fast polymerization occurred in a narrow temperature range, a few degrees above the glass transition point. Although the glass transition point in the present system is unknown, it may lie in the temperature range between -140°C and 135°C, where the ESR

spectrum dur to the anion radicals disappears. If the postpolymerization takes place in a limited temperature range around -140°C, the polymerization time, which means the remaining time in this temperature range, is considered to be inversely proportional to the raising speed of the temperature. Consequently, the polymer yield at lower temperatures is relatively higher than that at higher temperatures. An alternative explanation for these results may be that charge recombination between charged species, which leads to prevent further propagation, occurs rapidly at higher temperature range. From the results of Chapiro et al. and our experimental results (that the postpolymerization starts at the same temperature at which the ESR spectrum, due to the anion radicals, disappears), the former explanation seems to be more likely for this polymerization system.

In conclusion, the results obtained in the present study support the concept that the radiation-induced polymerization of nitroethylene is initiated by the anion radicals and proceeds by a free anionic mechanism.

References

1) Y. Amagi and A. Chapiro, J. Chim. Phys., 59, 537 (1962).

2) A. Chapiro and M. Pertessis, J. Chim. Phys., 61, 991 (1964).

3) A. Chapiro and L. Perec, J. Chim. Phys., 63, 842 (1966).

4) A. Chapiro and S. Nakashio, J. Chim. Phys., 63, 1031 (1966).

5) A. Chapiro and D. Roussel, J. Polymer Sci., C, 16, 3011 (1967).

6) I. Kaetsu, K. Tsuji, K. Hayashi, and S. Okamura, J. Polymer Sci., A, 5, 1899 (1967).

7) I. M. Balkalov, V. I. Goldanskii, N. S. Enikolopyan, S. F. Terekhova, and G. M. Trofimova, Vysokomol. Soed., 6, 98 (1964); J. Polymer Sci., C, 4, 909 (1964).

8) M. Bodard-Gauthier and R. Marx, J. Polymer Sci., C, 16, 4241 (1968).

9) H. Kamiyama, K. Hayashi, and S. Okamura, Annual Report of Japan Assoc. Rad. Res. Polymers, 8, 139 (1966/1967).

10) A. Chapiro, A. M. Jendrychowska-Bonamour, and L. Perec, "Radiation Chemistry," Adv. Chem. Ser., 82, 513 (1968).

11) H. Yamaoka, R. Uchida, K. Hayashi, and S. Okamura, Kobunshi Kagaku, 24, 79 (1967).

12) H. Yamaoka, F. Williams, and K. Hayashi, Trans. Faraday Soc., 63, 376 (1967).

13) K. Tsuji, H. Yamaoka, K. Hayashi, H. Kamiyama, and H. Yoshida, J. Polymer Sci., B. 4, 629 (1966).

14) K. Tsuji, H. Yoshida, K. Hayashi, and S. Okamura, Kobunshi Kagaku, 25, 31 (1968).

15) H. Kamiyama, K. Hayashi, and S. Okamura, Annual Report of Japan Assoc. Rad. Res. Polymers, 7, 145 (1965/1966).

16) H. Yamaoka, T. Shiga, K. Hayashi, S. Okamura, and T. Sugiura, J. Polymer Sci., B, 5, 329 (1967).

17) D. R. Smith, and J. J. Pieroni, Can. J. Chem., 43, 876 (1965).

Chapter 6

Reaction Mechanism in Polymerization

1. Introduction

Under the action of ionizing radiation on monomers several kinds of active species are formed. Radical, cationic or anionic polymerization reactions are thought to be possibly initiated by the active species as radicals, ions, ion radicals and excited molecules. Which mechanism takes place deponds on the polymerization conditions, such as the state of the system, the nature of the monomer, the polymerization temperature and the effect of additives.

Compared with catalytic polymerizations, the characteristics of radiation-induced polymerizations appear to be as follows: (1) coexistence of radical and ionic polymerizations, and contribution of ion radicals to the initiation process, and (2) propagation by free ions.

In the present Chapter, for the purpose of clarifying these characteristic points, the reaction mechanisms of the radiation-induced polymerization of nitroethylene reported in

the preceding Chapters are summarized and discussed in comparison with the results of other monomers obtained by several workers.

2. Results and Discussion

2.1. Coexistence of ionic and free radical polymerizations, and contribution of ion radicals to the initiation reaction

Possible formation processes of active species in the irradiated system are shown schematically in Figure 6-1.

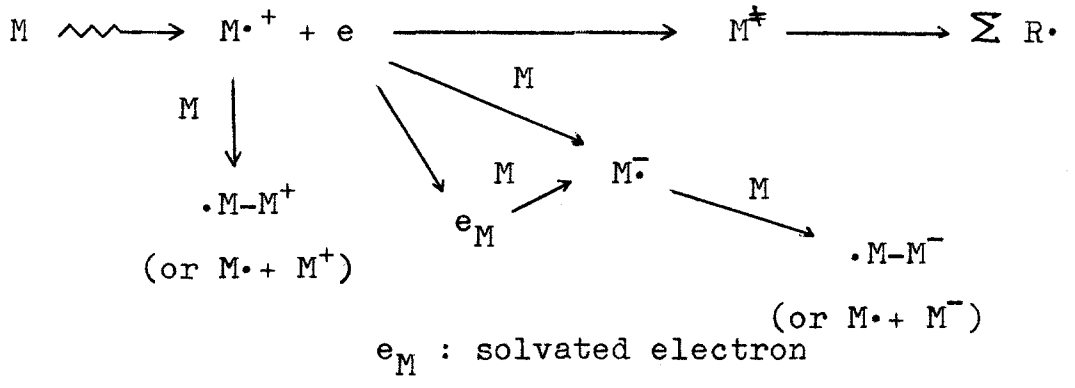

The great majority of ions and electrons, which are primarily produced by the irradiation of M, seems to undergo geminate recombination in liquid state, and this process will yield excited molecules (M^*) which should decompose to give several kinds of free radicals ($\Sigma R\cdot$). Cation radicals which

escape from geminate recombination may give rise to dimer cation radicals or both cations and free radicals by an ion-molecule reaction. Anion radicals may be formed by either the direct electron capture of M or the reaction between M and solvated electrons. The anion radicals can produce dimer anion radicals or both anions and free radicals as the cation radicals do. All of these active species are in principle able to contribute to the initiation process in radiation-induced polymerization.

The copolymerization study is one of the most useful method to make clear which polymerization, ionic or radical, really occurs. A typical example to indicate the coexistence of ionic and free radical polymerizations has be shown in the radiation-induced copolymerization of p-chlorostyrene (Cl-St) with styrene (St).[1] The monomer reactivity ratios (MRR) in various conditions are summarized in Table 6-1. The MRR at 9°C were almost same as those obtained by conventional free radical initiator and the MRR at -78°C coincided with those by cationic catalyst. When the copolymerization was carried out at -40°C, the intermediate values of the MRR between 9°C and -78°C were obtained. Further, the copolymer composition curve at -40°C approached the cationic one by the addition of a small amount of DPPH which is a typical radical scavenger, and it was almost consistent with the free radical one by the addition of triethylamine as a cation

Table 6-1. Monomer reactivity ratios in the copolymerization of Cl-St with St under various conditions.

Polymerization conditions			r_1(Cl-St)	r_2 (St)
Initiator	Temp. (°C)	Additive		
γ-rays	9	Non	1.36 ± 0.16	0.61 ± 0.08
	-78	Non	0.48 ± 0.10	1.52 ± 0.28
	-40	Non	0.88 ± 0.40	0.84 ± 0.30
	-40	DEA	1.46 ± 0.30	0.51 ± 0.18
	-40	DPPH	0.45 ± 0.20	1.51 ± 0.35
BPO[2]	60	Non	1.32 ± 0.03	0.742± 0.030
$AlBr_3$[3]	0	Non	0.40 ± 0.02	1.51 ± 0.03

scavenger as shown in Figure 6-2. These results suggested that the cationic and free radical species coexisted in the system and that the contribution of both species in the initiation process was almost equal at -40°C.

Similar results showing the coexistence of anionic and free radical species were reported by Tsuda.[4] In the radiation-induced copolymerization of acrylonitrile with styrene or methylmethacrylate at -78°C, the copolymer composition curves were changed by the variation of solvents

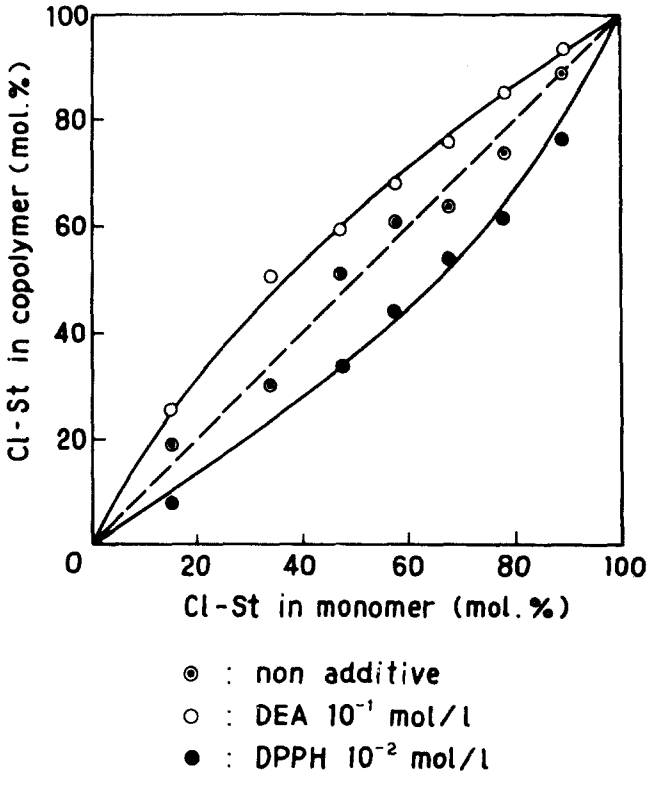

Figure 6-1. Copolymerization of p-chloro-styrene with styrene.

Temp. -40°C, monomer concentration 25 vol % solvent CH_2Cl_2, dose rate 3.6×10^4 r/hr.

and the resultant copolymer was proved to consist of a block of anion copolymer attached to a block of free radical copolymer. He concluded from these results that the anion radicals formed by the irradiation initiated simultaneously both anionic and free radical copolymerizations.

In the radiation-induced polymerization of nitroethylene, combining the kinetics of the postpolymerization and the ESR measurements in irradiated 2-methyltetrahydrofuran (MTHF) glass containing the monomer, it was suggested that the initiating species of the polymerization might be the anion radicals resulting from electron transfer from the matrix to the solute monomer.[5] A similar suggestion was also made in the study of electronic spectra by Kamiyama et al.[6] When MTHF glass containing a small amount of the monomer was irradiated at -196°C, three absorption bands were observed : an absorption maximum at 440 mμ with satelite at 460 mμ, a weak absorption band at 560 mμ, and a broad band with maximum at about 1200 mμ. Among them, the 1200 mμ band is due to the trapped electrons in the MTHF matrix.[7] The absorption band at 440 mμ was estimated, from a semi-empirical molecular orbital calculation, to be due to the anion radicals of nitroethylene.[6] By the photo-irradiation with lights of wave length longer than 660 mμ, the absorption due to the trapped electrons disappeared completely and the intensity

pf absorption at 440 mμ increased. When the irradiated glass, where both 440 and 1200 mμ bands were present, was maintained at -196°C in the dark, the intensity of the latter band decreased gradually, whereas that of the former increased with the keeping time. This behavior of the anion radicals and the trapped electrons is similar to that observed by the ESR measurements as described in Chapter 4.

From these results, the initiation process of the polymerization could be considered as follows. The free electrons are formed primarily from solvent molecules by irradiation:

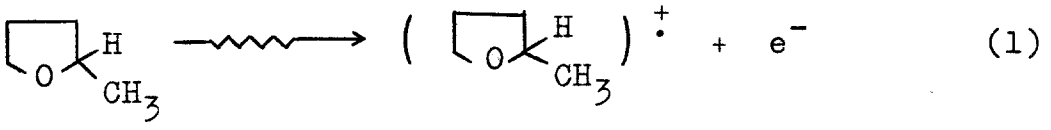

(1)

They are readily captured by nitroethylene molecules because the electron affinity of nitroethylene is considerably large.[6] This process produces the anion radicals of nitroethylene as the primary anionic intermediates involving the monomer:

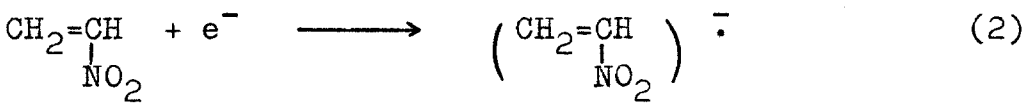

(2)

The stable carbanion seems to be formed by an ion-molecule reaction between the anion radicals and neutral nitroethylene molecules as reaction (3).

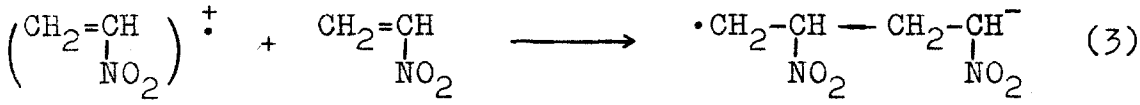

(3)

The polymerization can take place by the successive addition of the monomer to the anionic ends because of high susceptibility of the monomer to anionic polymerization.

The occurrence of this ion-molecule reaction was confirmed by mass spectrometric observations. The parent negative ions, which are identical with the anion radicals observed by the ESR measurements, were formed by the capture of thermarized electrons, and the dimer negative ions were observed at higher ion source pressure as mentioned in Chapter 4. The intensity of the dimer negative ions was found to be proportional to the square of the pressure in the ionization chamber, as presented in Chapter 8, while that of the parent negative ions was linearly proportional to the pressure. These results suggest that the dimer negative ions were formed by the ion-molecule reaction between the parent negative ions and neutral nitroethylene molecules.

The results mentioned above indicate that ionic and free radical species which are capable of initiating the polymerizations coexist in the irradiated system, and the contribution of ion radicals for the initiation process is very important in radiation-induced ionic polymerizations.

2.2. Propagation by free ions

It is probable that in all cases of radiation-induced anionic polymerization of vinyl monomers the initiation reaction involves the addition of an electron to a monomer molecule forming an anion radical, and the stable carbanion is formed by an ion-molecule reaction between the anion radical and the monomer molecule as described in the preceding section.

The propagation reaction then follows by successive addition of the monomer,

$$\cdot M\text{-}M^- + M \longrightarrow \cdot M\text{-}M\text{-}M^- \quad (M_3^-) \qquad (4)$$

$$M_n^- + M \longrightarrow M_{n+1}^-$$

and the termination reaction which competes with the propagation reaction involves the addition of positively recharged species to the growing polymer end.

$$M_n^- + A^+ \longrightarrow M_n - A \qquad (5)$$

In addition to the above mechanism, the termination reaction can occur by the reaction with impurities in the system.

$$M_n^- + X \longrightarrow M_n \qquad (6)$$

The chain transfer reaction could also take place by proton transfer from the monomer or the solvent molecule to the growing end. A kinetic scheme based on the assumption that the termination reaction takes place by the bimolecular recombination between charged species leads to a square-root dependence of the rate of polymerization on the dose rate as discussed in Chapter 3.

In the radiation-induced polymerization of nitroethylene in bulk, the fact that the rate of polymerization is proportional to the square-root of the dose rate[8] seems to indicate that the termination reaction with impurities is absent and the propagation reaction proceeds through free ions.

The possibility of the propagation by free ions in radiation-induced polymerization was suggested about ten years ago by both Magat[9] and Szwarc.[10] Recently, the studies in the radiation-induced cationic polymerizations have been concentrated to elucidate the reaction mechanism of polymerizations and provided the experimental evidence of free cationic propagation.[11] Measurements of radiation-induced electroconductivity in the polymerization system have also been established the presence of free ions.[12] In comparison with cationic studies, however, much less information is available on the polymerization by free anions.

As is well known, ionic polymerization by conventional catalysts is characterized by the fact that the active

propagating ends are, for the most part, closely associated with counter ions. In the studies of cationic polymerization of styrene by catalysts, Kanoh et al.[13] reported that the pre-exponential factor (A_p) of the propagation rate constant (k_p) was much smaller than that of the radical polymerization. They also suggested, from the statistical consideration, that the presence of counter ions restricted the mobility of the monomer unit in the transition state of the propagation reaction.

These discussions lead to the suggestion that the k_p values for ionic polymerizations are sensitive to the presence and the nature of counter ions, and that the k_p values for free ions, which are considered to depend mainly on the A_p values, would be very large, because the propagation reaction in ionic polymerization requires almost no activation energy. In the anionic polymerization of styrene in tetrahydrofuran at 25°C by catalysts, Szwarc and his coworkes[14] reported that the k_p for ion pairs was affected by the variation of counter ions and the k_p for free anions was about 10^5 $M^{-1}sec^{-1}$ which was 1000 times greater than the corresponding values for propagating ion pairs with alkali metal cations.

In order to compare the results obtained in the present works with those of cationic propagations, the maximum value of G(-monomer), the dose rate dependence, and the propagation rate constant in various polymerization systems are summarized

Table 6-2. Maximum G(-monomer), dose rate dependence and propagation rate constant in extremely dried polymerization systems.

Monomer	Temp. (°C)	Dore rate (r/hr)	Maximum G(-monomer)	n (I^n)	k_p ($M^{-1}sec^{-1}$)	Ref.
α-methylstyrene	30	2.6×10^5	7.9×10^3	0.80	—	15
	30	3.7×10^5	6.9×10^3	—	3×10^6	16
	0	—	—	—	4×10^6	17
	0	1.9×10^3	3.4×10^4	0.48	—	18
isobutyl vinyl ether	30	3.1×10^4	1.4×10^4	0.65	—	19
	30	—	—	—	3×10^5	17
cyclopentadiene	-78	2.8×10^5	2.5×10^4	1.0	6×10^8	20
styrene	15	1.0×10^4	4.0×10^5	0.62	3.5×10^6	17, 21
	0	2.2×10^3	6.0×10^5	0.70	—	22
1,2-cyclohexene oxide	25	6.4×10^4	7.6×10^4	1.0	—	23
nitroethylene	10	1.5×10^4	5.5×10^4	—	4×10^7	this thesis Chapter 2
	20	1.8×10^3	1.9×10^5	0.50	5×10^4	Chapter 3

in Table 6-2.

Although the quantitative comparison of these k_p values may be improbable because of the different polymerization conditions and estimation methods, the concept seems to be established that the propagation rate constant for free ions is very large for both cationic and anionic propagations.

Unfortunately, the value of A_p for the propagation of nitroethylene can not be obtained, but Williams et al.[17] estimated that the A_p value for styrene should be about 10^8 $M^{-1}sec^{-1}$ for free carbonium ion propagation which was similar with that for free radical propagation. This estimation is in accord with the prediction by Kanoh.[13]

To conclude, it is shown from the results mentioned in Part 2 that the radiation-induced polymerization of nitroethylene is initiated by the anion radicals of nitroethylene, propagated by free anionic species, and terminated by charge recombination between the propagating anions and the positively recharged species.

References

1) H. Yamaoka, K. Nishiyama, K. Hayashi, and S. Okamura, Kobunshi Kagaku, 24, 649 (1967).

2) F. M. Lewis, C. Walling, W. Cummings, E. R. Briggs, and F. R. Mayo, J. Am. Chem. Soc., 70, 1519 (1948).

3) C. G. Overberger, R. J. Ehrig, and D. Tanner, J. Am. Chem. Soc., 76, 772 (1954).

4) Y. Tsuda, J. Polymer Sci., 58, 289 (1962).

5) H. Yamaoka, I. Obama, K. Hayashi, and S. Okamura, J. Polymer Sci. A-1, in press.

6) H. Kamiyama, K. Hayashi, and S. Okamura, Annual Report of Japan Assoc. Rad. Res. Polymers, 7, 145 (1965/1966).

7) M. R. Ronayne, J. P. Guarino, and W. H. Hamill, J. Am. Chem. Soc., 84, 4230 (1962).

8) H. Yamaoka, H. Mori, K. Hayashi, and S. Okamura, J. Polymer Sci. B, 7, 371 (1969).

9) M. Magat, Makromol. Chem., 35, 159 (1960).

10) M. Szwarc, Makromol. Chem., 35, 123 (1960).

11) F. Williams, "Fundamental Processes in Radiation Chemistry" (P. Ausloos ed.), p.515, Interscience, New York, 1968; and references cited therein.

12) Ka. Hayashi, Y. Yamazawa, T. Takagaki, F. Williams, K. Hayashi, and S. Okamura, Trans. Faraday Soc., 63 1489 (1967).

13) N. Kanoh, T. Higashimura, and S. Okamura, Makromol. Chem., 56, 65 (1962).

14) D. N. Bhatthacharyya, C. L. Lee, J. Smid, and M. Szwarc, J. Phys. Chem., 69, 612 (1965).

15) J. V. F. Best, T. H. Bates, and F. Williams, Trans. Faraday Soc., 58, 192 (1962).

16) E. Hubmann, R. B. Taylor, and F. Williams, Trans. Faraday Soc., 62, 88 (1966).

17) F. Williams, Ka. Hayashi, K. Ueno, K. Hayashi, and S. Okamura, Trans. Faraday Soc., 63, 1501 (1967).

18) D. J. Metz, "Irradiation of Polymers", Adv. Chem. Ser., 60, 170 (1967).

19) M. A. Bonin, M. L. Calvert, W. L. Miller, and F. Williams, J. Polymer Sci., B, 2, 143 (1964).

20) M. A. Bonin, W. R. Busler, and F. Williams, J. Am. Chem. Soc., 87, 199 (1965).

21) K. Ueno, F. Williams, K. Hayashi, and S. Okamura, Trans. Faraday Soc., 63, 1478 (1967).

22) R. C. Potter, R. H. Bretton, and D. J. Metz, J. Polymer Sci., A-1, 4, 2295 (1966).

23) D. Cordischi, A. Mele, and R. Rufo, Trans. Faraday Soc., 64, 2794 (1968).

P A R T 3

MASS SPECTROMETRIC STUDY ON NEGATIVE ION-MOLECULE REACTIONS OF NITROETHYLENE

C h a p t e r 7

Formation of Negative Ions

1. Introduction

The use of mass spectrometry to detect and indentify transient intermediates formed by the action of ionizing radiation has provided new insight into the mechanism of radiation chemistry. From the viewpoint of the radiation-induced reactions, one of the most interesting problems in mass spectrometry is to investigate the mechanism of ion-molecule reactions in gas phase.

The present Chapter forms part of a series of studies on negative ion-molecule reaction in nitroethylene. It was established in Part 2 of this thesis that the radiation-induced polymerization of nitroethylene was initiated by negative intermediates. Therefore, it seems to be particular interest to study the formation of negative ions and the negative ion-molecule reaction in nitroethylene. and compare the reaction mechanism in gas phase with that in condensed phase.

Although the existence of negative ions in mass spectrometry was known as early as 1933,[1] the information on negative ions was far less than that on positive ions, because of their low relative abundances. In recent years, however, several studies on negative ions[2] have been reported as a result of the development of new techniques which increase the detection sensitivity of the mass spectrometer.

In general, negative ions can be formed in gas phase by three different processes:

(a) electron capture (resonance capture)

$$AB + e^- \longrightarrow AB^-$$

(b) dissociative resonance capture

$$AB + e^- \longrightarrow A + B^-$$

(c) ion pair formation

$$AB + e^- \longrightarrow A^+ + B^- + e$$

The negative ion formation by the process (c) is usually found at higher electron energies than that by resonance capture processes, since the ionization potential of A is comparatively large. In the processes (a) and (b), an excited negative species AB^{-*} is firstly formed by the electron capture. If AB^{-*} has enough excess energy, it will decompose into a fragment negative ion B^- and a radical A, both having excess kinetic energy (process (b)).

On the other hand, if AB^{-*} has not sufficient energy for decomposition, it will give a vibrationally excited ion AB^{-}. The AB^{-} thus formed may be stabilized by collisions with neutral molecules or by radiation (process (a)).

In the present study, the formation of negative ions from nitroethylene by the processes (a) and (b) has been studied by use of a mass spectrometer.

2. Experimental

The apparatus used for this study was a 90° single-focusing Hitachi RMU-6 mass spectrometer which was modified to measure the negative ions.[3] A conventional-type electron gun was used without paying attention to the energy spread of impact electrons. A 10 stage Ag-Mg electron multiplier combined D.C. amplifier was used for ion detector, and out put current was recorded by Rikadenki B-34 three pen recorder, consequently the minimum detectable ion current is 5×10^{-19}A. During the experiments, except for studying the effect of ion accelerating potential, the ion acceleration voltage and the supplied voltage to conversion dynode of the electron multiplier were kept at -3.5 and -1.5 kV, respectively. The repeller and the electron trap voltage were maintained at the same potential as the ionization

chamber. A source magnet, which has 150 gausses flux intensity, was also used for the collimation of the electron beam. The total emission was maintained 100 μA in all energy range of the electron impact, and then 40 % trap currents were obtained above 10 eV electron energies. Electron accelerating potentials were read in each 1/50 volts by the 10 turn precision Helipot variable resister in the range from 0 to 20 volts, previously well calibrated by Yokokawa D.C. Voltage Standard GOS-11.

Sulfur hexafluoride and oxygen were used to calibrate the electron energy scale. The appearance potentials of the SF_6^- ion from sulfur hexafluoride and O^- ion from oxygen were taken as 0.03 eV[4] and 4.53,[5] respectively. The appearance potentials of negative ions formed by the resonance capture process were determined by the linear extraporation method.

Nitroethylene was prepared and purified as described previously. Sulfur hexafluoride (Allied Chemical Co.) was purified by trap-to-trap distillation in vacuum. Oxygen and methane (Takachiho Chemical Ind.) were used without further purification.

3. Results

A large number of negative ions were observed from nitroethylene by electron impact of 100 eV as mentioned in Chapter 4. The relative abundance of main negative ions, which were normalized to the intensity of NO_2^-, are reproduced in Table 7-1.

The ionization efficiency curves of the main negative ions from nitroethylene, such as O^-, C_2H^-, NO_2^-, and $C_2H_3NO_2^-$, and that of SF_6^- from sulfur hexafluoride are shown in Figure 7-1 as a function of the electron energy. The intensity of these negative ions in the electron energy region less than 10 eV was proportional to the pressure of nitroethylene in the ionization chamber. From these curves, the appearance potentials and the apparent energy widths of the resonance electron capture processes for the parent and the fragment ions were obtained. The main results are summarized in Table 7-2. The appearance potential of NO_2^- in this study is much higher than that of NO_2^- from nitrobenzene (0.42 eV[6] or 1.0 eV[7]).

From the ionization efficiency curve of $C_2H_3NO_2^-$ shown in Figure 7-1, it is clear that the appearance potential is about 0 eV and the width of the resonance capture is very narrow, both of which properties are also exhibited in the parent negative ion of sulfur

Table 7-1. Relative abundance of the main negative ions produced from nitroethylene by electron impact of 100 eV.

m/e	Ion	Source Pressure (mmHg) 2.6×10^{-6}	9×10^{-3}
16	O^-	7.4	6.8
17	OH^-	6.8	9.1
25	C_2H^-	19	22
30	NO^-	0.93	0.96
42	CNO^-	3.4	7.3
46	NO_2^-	100	100
55	C_2HNO^-	0.62	0.85
72	$C_2H_2NO_2^-$	0.03	5.8
73	$C_2H_3NO_2^-$	0.27	88
98	$C_2H_3NO_2C_2H^-$	—	0.2
99	$C_2H_3NO_2C_2H_2^-$	—	0.6
146	$(C_2H_3NO_2)_2^-$	—	0.1
219	$(C_2H_3NO_2)_3^-$	—	2×10^{-4}

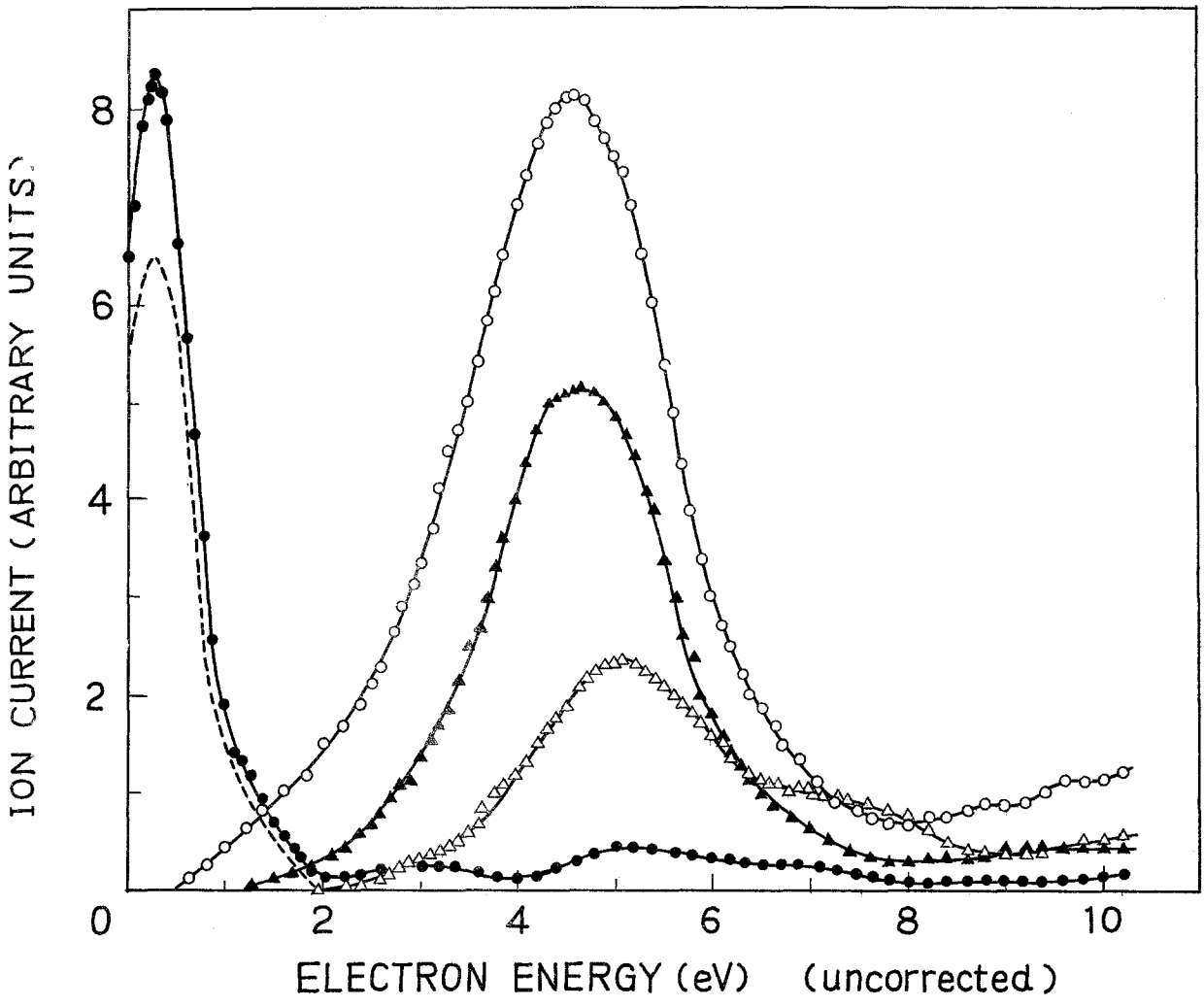

Figure 7-1. Ionization efficiency curves of the main negative ions from nitroethylene.

△ : O^- (x10), ▲ : C_2H^- (x2), o : NO_2^- (x1)

● : $C_2H_3NO_2^-$ (x4), ----: SF_6^-.

Table 7-2. Appearence potentials and apparent energy widths of the main negative ions formed by the resonance electron capture processes from nitroethylene.

m/e	Ion	1st Appearance potential (eV)	Half width (eV)
16	O^-	2.5 ± 0.2	1.5
17	OH^-	2.8 ± 0.2	1.6
25	C_2H^-	2.2 ± 0.2	1.4
26	$C_2H_2^-$	2.8 ± 0.2	1.5
30	NO^-	2.8 ± 0.2	1.4
46	NO_2^-	1.5 ± 0.2	1.8
55	C_2HNO^-	2.5 ± 0.2	1.3
72	$C_2H_2NO_2^-$	2.1 ± 0.2	1.5
73	$C_2H_3NO_2^-$	0	0.7

hexafluoride. These facts indicate that the nitroethylene molecule has an ability to capture easily thermal electrons by nondissociative process. Similar results in the cases of nitrocompounds of benzene derivatives were reported by Christophorou et al.[6] and Henglein et al.[7] The width of nondissociative resonance capture of nitroethylene seems to be the energy spread of impact

electrons used, since the energy spread of the resonance electron capture process of SF_6 has been considered to be narrower than 0.05 eV.[4)]

Compton et al.[8)] measured the lifetimes of the parent negative ions for SF_6, $C_6H_5NO_2$ and $(CH_3CO)_2$ by means of time-of-flight mass spectrometer. For the parent negative ion of nitroethylene, an attempt to estimate the mean lifetime was made by following procedures. The ion intensity of $C_2H_3NO_2^-$ was remarkably dependent upon the ion accelerating potential. As shown in Figure 7-2, the dependences of the ion accelerating potential on the ion intensity were measured for $C_2H_3NO_2^-$ and SF_6^- by using a Faraday cage as the ion detector. The dotted lines in Figure 7-2 are the first differential curves obtained from the relations between the ion intensity and the ion accelerating potential. Neglecting the change of the ion collection efficiency with the variation of the accelerating potential, the sum of the residence time of the ions in the ionization chamber and the flight time of the ions at the peak of the first differential curve may be considered as the mean lifetime of the ions. From the results of Figure 7-2 and the estimated residence times in the ionization chamber described in the next Chapter, the mean lifetimes for $C_2H_3NO_2^-$ and SF_6^- were calculated to be 14 μ sec and 28 μ sec, respectively. The value for SF_6^-

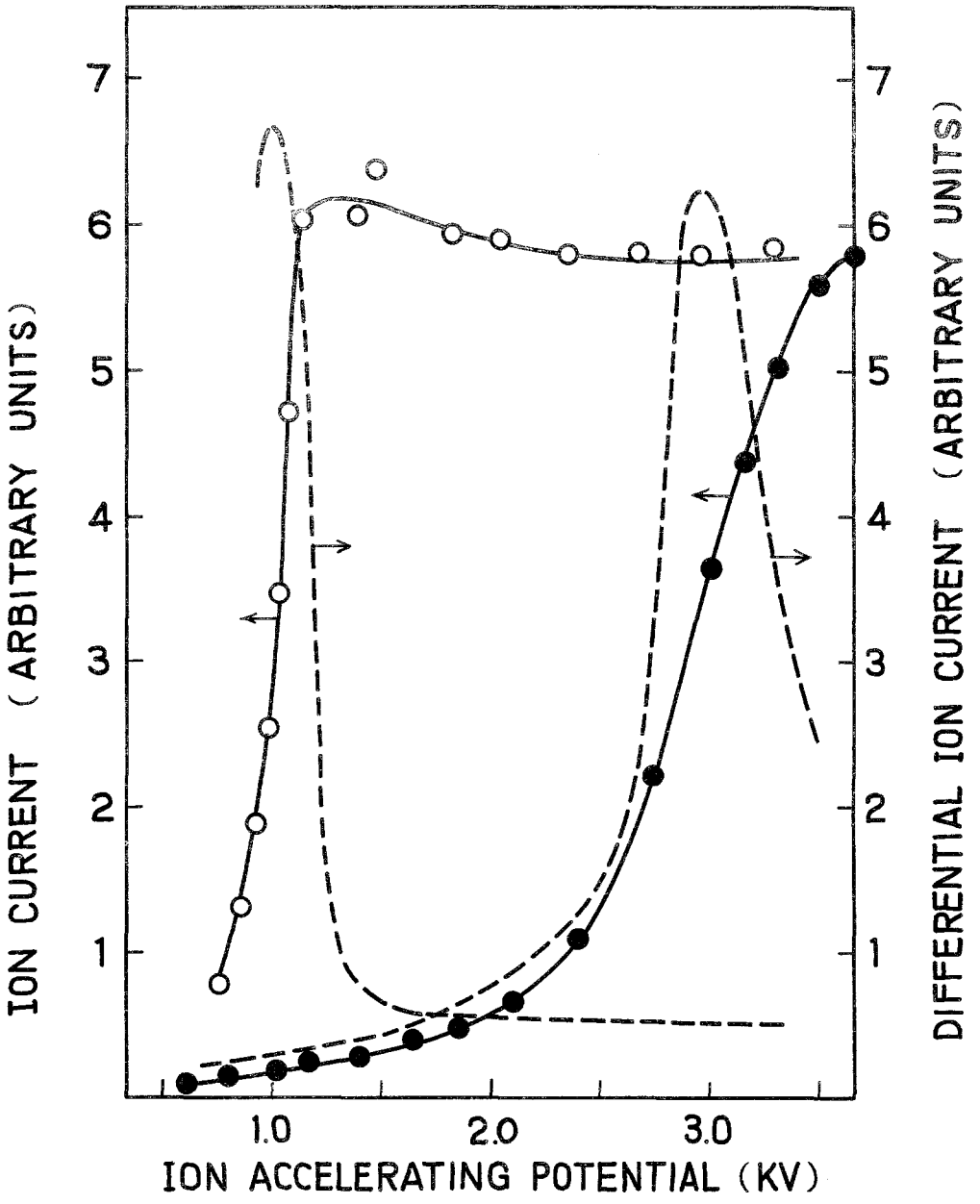

Figure 7-2. Dependences of the ion accelerating potential on the ion intensity for $C_2H_3NO_2^-$ and SF_6^-.

● : $C_2H_3NO_2^-$, ○ : SF_6^-.

shows a close agreement with the result obtained by Compton (25 μ sec[8]).

4. Discussion

The results presented in Table 7-2 clearly show that many of the fragment negative ions from nitroethylene have appearance potentials which are almost identical. It might be expected that some of them result from ion-molecule reactions. However, the experimental evidence that the intensities of the ions increase linearly with the increase of pressure in the ionization chamber indicates that these fragment ions are not produced by ion-molecule reactions, but formed by the dissociative resonance capture processes.

It is interesting that the parent negative ion of nitroethylene is observed at lower pressure in the ionization chamber. The formation of parent negative ions is generally classified in two different processes as pointed out by Compton et al.[8]: (i) temporary parent negative ion formation, and (ii) parent negative ion formation in which the ion is stabilized by collision or radiation.

In the present study, the intensity of the parent

negative ion of nitroethylene is also proportional to the pressure by the electron impact less than 1 eV. This fact indicates that the parent negative ion is predominantly formed by the precess (i), in which the molecule is able to capture thermal electrons while maintaining the interatomic distances. The exact cross section of the electron capture can not be determined by the apparatus used. However, the relative intensity of the parent ion of nitroethylene in the energy range of the resonance capture was about 1/200 of that for SF_6^- at normalized pressure. Several values for the cross section of SF_6^- formation by nondissociative electron attachment have been reported.[4,8-13] Among them, the value of 2.6×10^{-14} cm^2 determined by Mahan and Young[13] was chosen as the most reliable one. Consequently the cross section of nondissociative resonance capture of nitroethylene was estimated to be approximately 1.3×10^{-16} cm^2.

Now the technique used in the present study for determining the ion lifetime should be discussed, since it has not been clearly established. As is well known, there is a strong tendency toward defocusing as the ion accelerating potential is reduced and, of cource, the beam will tend to spread as the retention time in the analyzer tube is increased. It would therefore be necessary to obtain some information of the effect of

ion accelerating voltage upon the collected current of several stable positive ions. As an attempt to correct some uncertain effects, the dependence of accelerating voltage on the ion intensities of Ar^+ and SF_6^- was measured by changing the sign of the supplied voltage. The ion intensity ratio of SF_6^-/Ar^+ changed in almost same manner as represented in Figure 7-2 with the variation of accelerating voltage. This fact and the close agreement of the lifetime for SF_6^- between the value obtained by Compton[8] and ours seem to imply that the method in the present study may still be valid despite the limitations imposed by the obvious oversimplification.

The lifetime of the parent negative ion thus formed is closely related to the electron affinity of the molecule.[8] Kamiyama et al.[14] calculated the electronic configurations, matrix elements and the energy levels for the parent negative ion of nitroethylene by semi-empirical MO method, and also gave the value of 1.53 eV as the electron affinity of nitroethylene. The observed long lifetime of the parent negative ion of nitroethylene may be given by this positive electron affinity and the stable molecular configuration in the electron attachment.[14] The nature of nitroethylene molecule as a strong electron acceptor in this study is in reasonable agreement with those obtained from the ESR[15,16] and the optical investi-

gations.[14] On the other hand, in the case of the electron impact with 100 eV, the remarkable increase of the parent negative ion at higher pressure shown in Table 7-1 seems to be caused by the process (ii) or other processes. The formation processes of the parent negative ion at higher pressure will be discussed in Chapter 9.

References

1) F. W. Aston, "Mass Spectra and Isotopes", p. 27, Edward Arnold, London, 1933.

2) For examples, C. E. Melton, "Mass Spectrometry of Organic Ions" (F. W. McLafferty ed.), p. 163, Academic Press, New York, 1963; E. W. McDaniel, "Collision Phenomena in Ionized Gases", p. 368, John Wiley & Sons, New York, 1964; F. Fiquet-Fayard," Actions Chimiques et Biologiques des Radiations", Vol. 8, p.29, Masson et Cie, Paris, 1965; and references cited therein.

3) T. Sugiura, K. Arakawa, and A. Matsumoto, Mass Spectroscopy, 14, 187 (1966).

4) W. M. Hickam and R. E. Fox, J. Chem. Phys., 25, 642 (1956).

5) D. C. Frost and C. A. McDowell, J. Am. Chem. Soc., 80, 6183 (1958).

6) L. G. Christophorou, R. N. Compton, G. S. Hurst, and P. W. Reinhardt, J. Chem. Phys., 45, 536 (1966).

7) K. Jäger and A. Henglein, Z. Naturforschg., 22a, 70((1967).

8) R. N. Compton, L. G. Christophorou, G. S. Hurst, and P. W. Reinhardt, J. Chem. Phys., 45, 4634 (1966).

9) I. S. Buchel'nikova, Zh. Eksperim. i Teor. Fiz., 35, 1119 (1958); Soviet Phys. JETP., 8, 783 (1959).

10) R. K. Asundi and J. D. Craggs, Proc. Phys. Soc. (London), 83, 611 (1964).

11) D. Rapp and D. D. Briglia, J. Chem. Phys., 43, 1480 (1965).

12) J. B. Hasted and S. Beg, Brit. J. Appl. Phys., 16, 1779 (1965).

13) B. H. Mahan and C. E. Young, J. Chem. Phys., 44, 2192 (1966).

14) H. Kamiyama, K. Hayashi, and S. Okamura, Annual Report of Japan Assoc. Rad. Res. Polymers, 7, 145 (1965/1966).

15) K. Tsuji, H. Yamaoka, K. Hayashi, H. Kamiyama, and H. Yoshida, J. Polymer Sci., B, 4, 629 (1966).

16) K. Tsuji, H. Yoshida, K. Hayashi, and S. Okamura, Kobunshi Kagaku, 25, 31 (1968).

Chapter 8

Dimer Negative Ion Formation by Ion-molecule Reaction

1. Introduction

A number of studies of ion-molecule reactions for positive ions at pressures up to a few torr[1-9] and even near atomospheric pressures[10] by use of a mass spectrometer have been reported in recent years. Such investigations have provided available information on the radiation-induced chemical reactions where more than one half of the product formation usually results from reactions of intermediate ions. For negative ion-molecule reactions, however, detailed studies have been limited to reactions which occur in oxygen and other gases of innopheric interest,[11-15] although negative ions have also been considered to play an important role as active species in radiation-induced reactions.

In the preceding Chapter, the formation of negative ions from nitroethylene was studied and the parent

negative ion of nitroethylene was observed to be abundant at near thermal electron energies. For the second part of this series, the present study is mainly concerned with the dimer negative ion formation of nitroethylene by the ion-molecule reaction in order to obtain the information on the initial process of the radiation-induced polymerization of nitroethylene.

2. Experimental

The apparatus and techniques used in the present study were the same as those described in the preceding Chapter.

The pressure in the ionization chamber was determined indirectly from the pressure in the sample reservoir, which was measured by the manometer, McLeod gauge and CEC 23-105 Micro-Manometer. The ratio of the sample pressure of steady state in the ionization chamber to that in the reservoir was determined by the static operation of the inert gases (He, Ne and Ar[16]), in the energy range where the ion intensity of the resonance electron capture was linearly proportional to the pressure. The pressure thus determined was confirmed by the positive ion-molecule reaction of methane.[17]

3. Results

In the case of electron impact of 100 eV, many secondary products by ion-molecule reactions were observed. However, at electron energy of less than 1 eV, the secondary ions were the only products obtained by the reaction with $C_2H_3NO_2^-$, and the mass numbers of main secondary ions were 99, 119 and 146.

From the viewpoint of studying the initial process of the polymerization, special attention was paid to the formation process of the dimer negative ion. The ionization effeciency curves of $C_2H_3NO_2^-$ and $(C_2H_3NO_2)_2^-$ are shown in Figure 8-1. The close agreement of the shape of the two peaks indicates that the precursor of $(C_2H_3NO_2)_2^-$ is $C_2H_3NO_2^-$. The intensity of $(C_2H_3NO_2)_2^-$ at the peak in Figure 8-1 was proportional to the square of the pressure of nitroethylene, whereas that of $C_2H_3NO_2^-$ was linear to the pressure as shown in Figure 8-2. The plots of the ratic $(C_2H_3NO_2)_2^-/C_2H_3NO_2^-$ vs. the pressure of nitroethylene give a linear relation as presented in Figure 8-3. From these results, it is evident that $(C_2H_3NO_2)_2^-$ is produced by the ion-molecule reaction of the parent ion with neutral nitroethylene molecule, demonstrated as follows:

$$C_2H_3NO_2^- + C_2H_3NO_2 \xrightarrow{k} (C_2H_3NO_2)_2^- \quad (a)$$

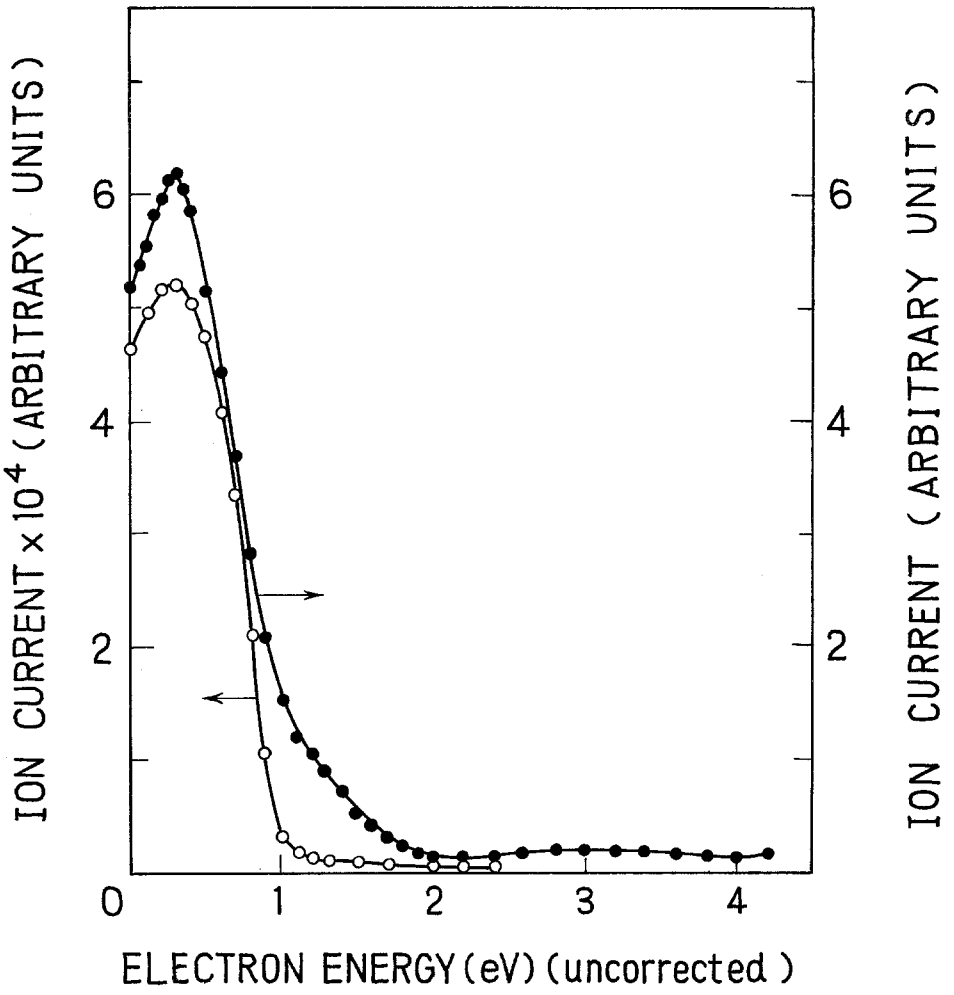

Figure 8-1. Ionization efficiency curves of $C_2H_3NO_2^-$ and $(C_2H_3NO_2)_2^-$.
Source pressure: 4.4×10^{-4} mmHg.
● : $C_2H_3NO_2^-$, o : $(C_2H_3NO_2)_2^-$.

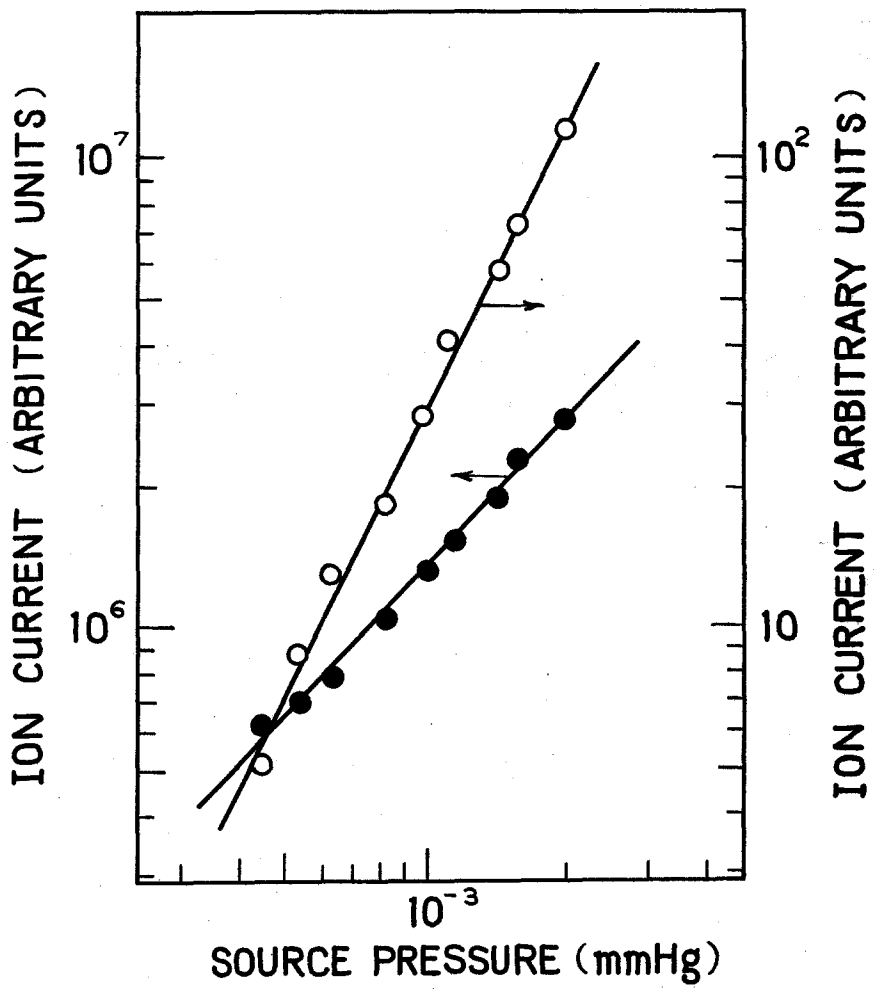

Figure 8-2. Dependences of the pressure in the ionization chamber on the ion intensity for $C_2H_3NO_2^-$ and $(C_2H_3NO_2)_2^-$.

● : $C_2H_3NO_2^-$, o : $(C_2H_3NO_2)_2^-$.

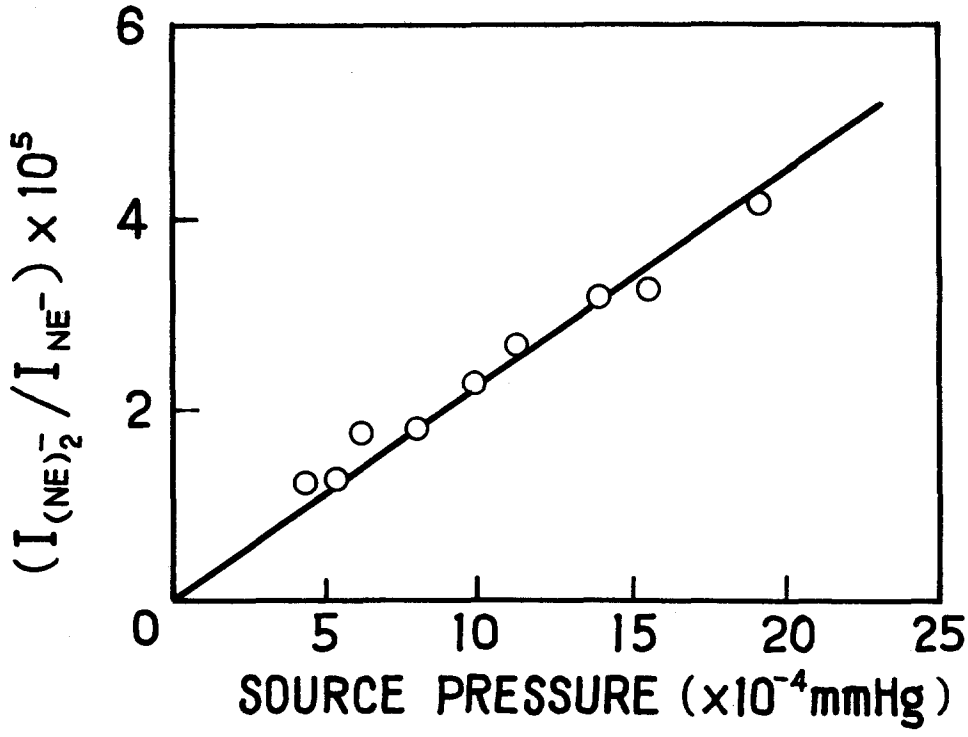

Figure 8-3. Relation between the intensity ratio $(C_2H_3NO_2)_2^-$ / $C_2H_3NO_2^-$ and the pressure in the ionization chamber.

The rate constant of the reaction (a) was estimated by the following procedures. Assuming that the source pressure is low and the fraction of the parent ion which reacts is very small, the equation (1) is obtained by introducing a similar treatment to that developed by Koyano et al.[18] for reaction cross section.

$$g\left(\frac{I_D}{I_P}\right) = k\,[C_2H_3NO_2]\,\tau_N \qquad (1)$$

where I_D/I_P is the ratio of the intensities of the dimer ion and the parent ion, $[C_2H_3NO_2]$ is the concentration of nitroethylene, τ_N is the residence time of the parent ion in the ionization chamber, and g is the ratio of the electron multiplier gain of I_D to that of I_P. g was experimentally obtained as $1/\sqrt{2}$. For the estimation of τ_N, the ion-molecule reaction of methane positive ion represented by the formula (b) was taken as a standard.

$$CH_4^+ + CH_4 \longrightarrow CH_5^+ + CH_3 \qquad (b)$$

Using the published value of the rate constant for this reaction (1.1×10^{-9} cm^3 molecule^{-1}sec^{-1} [19,20]), the residence time of CH_4^+ in this apparatus ($\tau_{CH_4^+}$) was determined to be 2.1 μsec from the slope of the linear relation between $I_{CH_5^+}/I_{CH_4^+}$ and the pressure of methane

in the ionization chamber. It is generally known that the residence time of ions in the ionization chamber is a function of the mass of ions, the field strength in the chamber, and the distance from the electron beam to the exit slit of the chamber. In the reactions (a) and (b), the distance from the electron beam to the exit slit is the same, and the field strength is considered to be equal for positive and negative ions, although the sign of the gradient is opposite. Consequently, the residence time of ions in this study is only a function of the mass of ions. With multiplying $\tau_{CH_4^+}$ by the square root of the mass ratio of $C_2H_3NO_2^-$ and CH_4^+, τ_N was estimated as 4.6 μsec.

Since $k\tau_N$ in the equation (1) was obtained from the slope of Figure 8-3, the rate constant of the reaction (a) was determined to be 3.2×10^{-13} $cm^3 molecule^{-1} sec^{-1}$.

4. Discussion

It is clear from the results of Figures 8-1 and 8-2 that the precursor of the dimer negative ion is the parent negative ion of nitroethylene, and that the dimer negative ion is formed by the ion-molecule reaction of the parent ion with neutral nitroethylene molecule.

The theoretical kinetic equation of ion-molecule reactions was first derived by Gioumousis and Stevenson[21] based on an ion-induced-dipole model. The rate constant of ion-molecule reactions was given by the following equation which is independent of the relative velocity of the colliding pair:

$$k = 2\pi e \left(\frac{\alpha}{\mu}\right)^{\frac{1}{2}} \qquad (2)$$

where e is the electron charge, α is the polarizability of the neutral molecule, and μ is the reduced mass of the colliding pair. Moran and Hamill[22] have considered the interaction of an ion with a molecule possessing a permanent dipole. Using a similar model, Harrison et al.[23] have proposed the modified collision theory including the effect of ion-dipole interaction. They have shown that the mean rate constant for collisions where both an ion and a neutral molecule have thermal velocities is given by

$$\bar{k}_{\text{therm}} = 2\pi e \left(\frac{\alpha}{\mu}\right)^{\frac{1}{2}} + \frac{2\pi e \mu_D}{\mu} \left(\frac{2\mu}{\pi kT}\right)^{\frac{1}{2}} \qquad (3)$$

where μ_D is the dipole moment of the molecule and kT is the thermal kinetic energy.

According to this theory, the rate constant for the

dimerization reaction of nitroethylene was calculated. Although the polarizability and the dipole moment of nitroethylene molecule are unknown, it can be assumed that they are in the same orders as those of nitroethane. The calculated values are 6.2×10^{-9} and 5.9×10^{-9} cm^3 $molecule^{-1}sec^{-1}$ at $323^{\circ}K$ and $373^{\circ}K$, respectively. The rate constant measured experimentally (3.2×10^{-13} cm^3 $molecule^{-1}sec^{-1}$) is several orders of magnitude smaller than that predicted by the theory. This may indicate that a great portion of collisions do not give rise to the dimerization reaction. The reasons for the apparent low rate constant of the dimerization reaction are not clear. One possible explanation is that the collisions lead to other ion-molecule reactions. However, the secondary ions observed at the electron energy of less than 1 eV are not abundant as already mentioned. It therefore would appear that the contribution of other ion-molecule reactions is not so large. Alternatively the apparent low rate constant could be explained by the occurrence of charge transfer of collision-induced electron detachment from the parent negative ion which was not detected in the present study. A more likely explanation is that the model used does not adequately describe the ion-molecule collision since it contains no consideration of the electronic structure of interacting species. Recently, Schaefer and Henis[24] have

presented a qualitative description of low-energy ion-molecule reactions which is based on the assumption that the probability of reaction can be described by the change in electron density around the nuclear centers involved. For the dimerization reaction of nitroethylene, however, this discription is unable to apply because of the difficulty for calculating the detailed electron density distributions in complicated reaction systems.

No experiment of the polymerization in gas phase has yet been carried out, since the vapor pressure of nitroethylene is extremely low at room temperature. The rate constant of the polymerization in liquid phase was determined from the kinetical experiments to be 6.7×10^{-4} cm^3 $molecule^{-1} sec^{-1}$ at $20^{\circ}C$.[25)]

For the trimer negative ion, the measurements of the ionization effeciency curve and the dependence of the pressure in the ionization chamber are difficult because of low intensity of the trimer ion. In positive ion mass spectra, however, neither dimer nor trimer positive ions are observed in the pressure range examined. This fact also indicates that neither the dimer nor the trimer negative ion are produced by a direct electron capture process of neutral nitroethylene dimer or trimer, but both are formed as secondary products. Concequently, the formation process of the trimer negative ion can only involve a concecutive reaction as follows:

$$(C_2H_3NO_2)_2^- + C_2H_3NO_2 \longrightarrow (C_2H_3NO_2)_3^- \quad (c)$$

Although only a limited range of the pressure was examined, the mass spectrometric observation mentioned above supports the concept that the precursor of the radiation-induced polymerization of nitroethylene is the parent negative ion.

References

1) C. E. Melton and P. S. Rudolph, J. Chem. Phys., 32, 1128 (1960).
2) F. H. Field, J. Am. Chem. Soc., 83, 1523 (1961).
3) S. Wexler and N. Jesse, J. Am. Chem. Soc., 84, 3425 (1962).
4) F. H. Field, J. L. Franklin, and M.S. B. Munson, J. Am. Chem. Soc., 85, 3575 (1963).
5) G. A. W. Derwish, A. Galli, A. Giardini-Guidoni,and G. G. Volpi, J. Chem. Phys., 39, 1599 (1963).
6) S. Wexler and R. Marshall, J. Am. Chem. Soc., 86, 781 (1964).
7) M. S. B. Munson, J. Am. Chem. Soc., 87, 5313 (1965).
8) D. J. Hyatt, E. A. Dodman, and M. J. Henchman, "Ion-molecule Reactions in Gas Phase", Adv. Chem. Ser., 58, 131 (1966).

9) J. H. Futrell and T. O. Tiernan, J. Phys. Chem., 72, 153, 1994, 3080 (1968); ibid., 73, 829 (1969).

10) D. A. Durden, P. Kebarle, and A. Good, J. Chem. Phys., 50, 805 (1969); and their earlier papers.

11) B. P. Burtt and J. Henis, J. Chem. Phys., 41, 1510 (1964).

12) J. F. Paulson, "Ion-molecule Reactions in Gas Phase", Adv. Chem. Ser., 58, 28 (1966).

13) J. M. Warman and R. W. Fessenden, J. Chem. Phys., 49, 4718 (1968).

14) J. L. Moruzzi and J. T. Dakin, J. Chem. Phys., 49, 5000 (1968).

15) E. E. Ferguson, Can. J. Chem., 47, 1815 (1969); and references cited therein.

16) T. Sugiura, Y. Inoue, O. Toyama, T. Hayakawa, J. Okamoto, and T. Noda, Mass Spectroscopy, 11, 141 (1964).

17) F. H. Field, J. L. Franklin, and F. W. Lampe, J. Am. Chem. Soc., 79, 2419 (1957).

18) I. Koyano, I. Omura, and I. Tanaka, J. Chem. Phys., 44, 3850 (1966).

19) V. I. Tal'roze and E. L. Frankevich, Izv. Akad.Nauk SSSR, Otd. Khim, Nauk, 1351 (1959); Chem. Abstr., 53, 21184e (1959).

20) C. W. Hand and H. von Weyssenhoff, Can. J. Chem., 42, 195 (1964).

21) G. Gioumousis and D. P. Stevenson, J. Chem. Phys., 29, 294 (1958).

22) T. F. Moran and W. H. Hamill, J. Chem. Phys., 39, 1413 (1963).

23) S. K. Gupta, E. G. Jones, A. G. Harrison, and J. J. Myher, Can. J. Chem., 45, 3107 (1967).

24) J. Schaefer and J. M. S. Henis, J. Chem. Phys., 49, 5377 (1968).

25) H. Yamaoka, F. Williams, and K. Hayashi, Trans. Faraday Soc., 63, 376 (1967).

Chapter 9

Formation of the Parent and the Dimer Nagative Ions at Higher Electron Energies

1. Introduction

For the formation process of parent negative ions, several investigators[1)] have conducted studies mainly at low electron energies where a nondissociative resonance capture process dominates. In the field of radiation chemistry, however, the parent negative ion formation at higher electron energies is of considerable interest because chemical reactions are usually induced by ionizing radiation having nigh energies.

In the experiments of Chapter 7, it was found that the intensities of the parent and the dimer negative ions of nitroethylene increased remarkably with the increase of source pressure at higher electron energies. In order to elucitate this phenomenon, the experiments at higher electron energies under higher source pressures have been carried out in the present study.

2. Results and Discussion

The intensities of main negative ions from nitroethylene as a function of electron energy above 20 eV are shown in Figure 9-1. Among them, special attention was paid to the formation of the parent and the dimer negative ions in connection with the results of the preceding Chapters.

Figure 9-2 shows the source pressure dependence on the parent negative ion formation produced with electron energies of 25, 50, and 100 eV. At pressures less than 10^{-4} torr, the intensity of the parent negative ion appeared to be of second order with respect to the pressure in all the electron energies. A three-body process obviously occurred under the present conditions, indicating that the parent negative ion is stabilized by collision as classified in Chapter 7.

At source pressures above 10^{-4} torr, the intensity of the parent negative ions was revealed to be higher than second order dependence with respect to the pressure. In order to obtain further information on the parent negative ion formation at higher pressure, experiments of adding rare gases in the ionization chamber were carried out at electron energy of 100 eV. At the constant pressure of nitroethylene (10^{-5} torr), the intensities of the parent

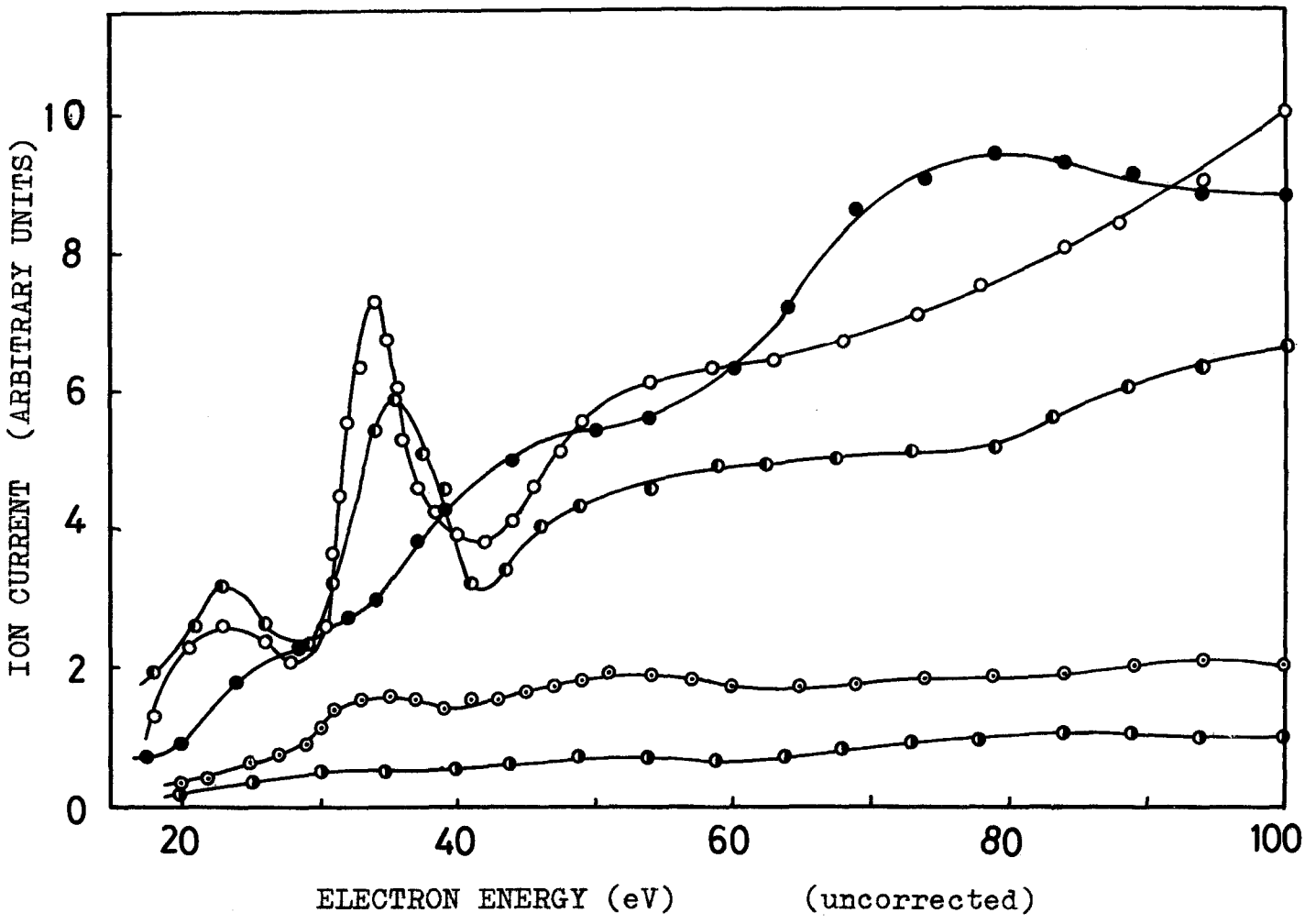

Figure 9-1. Ionization efficiency curves of the main negative ions from nitroethylene.

● : O^- (x 3), ● : C_2H^- (x 3), ● : NO_2^- (x 1)
● : $C_2H_3NO_2^-$ (x 1), ● : $(C_2H_3NO_2)_2^-$ (x 100).

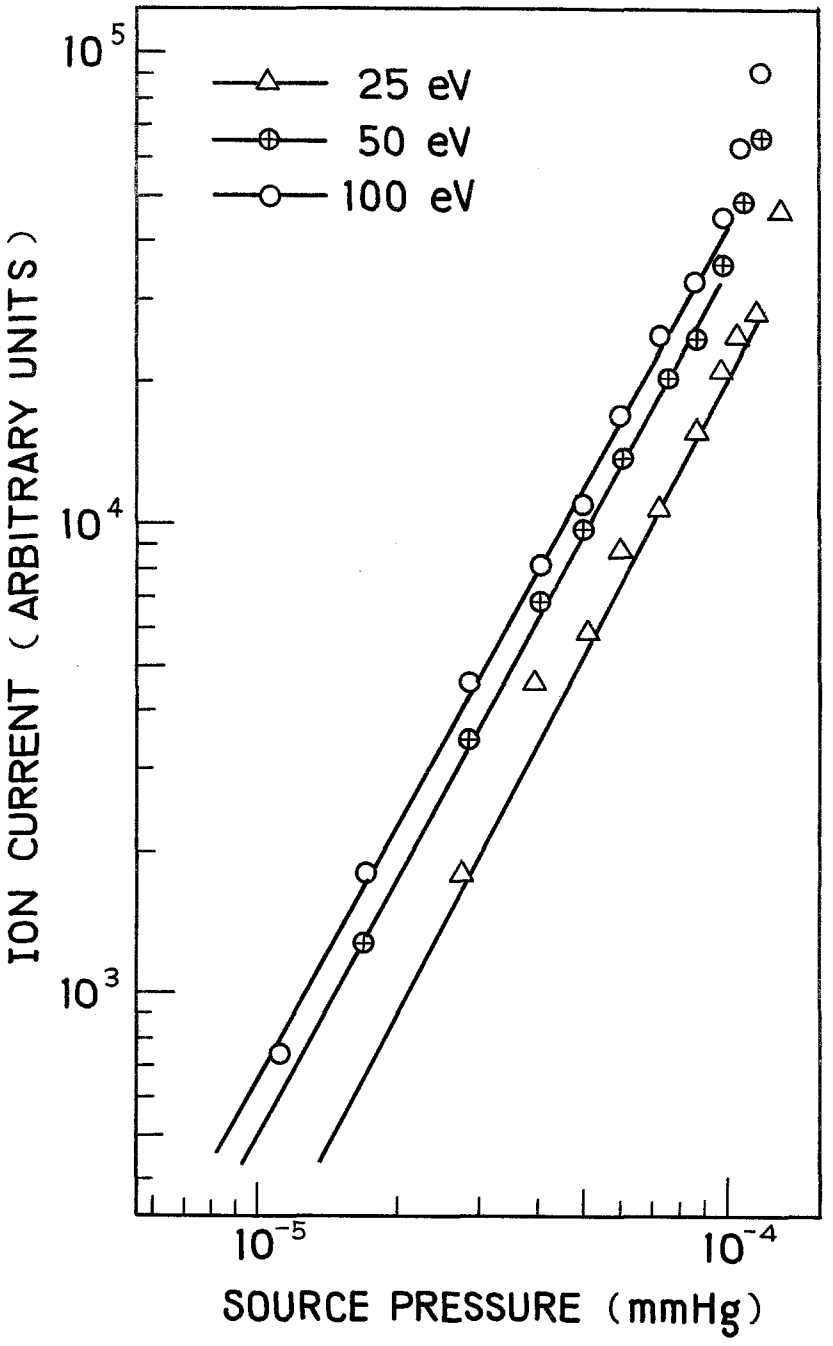

Figure 9-2. Source pressure dependence on the parent negative ion formation produced with higher electron energies.

negative ions as a function of added rare gas pressure are shown in Figure 9-3, using neon, argon, krypton, and xenon. In all cases, second order dependence of added gas pressure on the ion intensity was observed, and the relative intensities were found to increase in the order;Ne, Ar, Kr, and Xe. At the constant pressure of rare gases (10^{-3} torr), the intensity of the parent negative ion was linearly proportional to the pressure of nitroethylene in the pressure range examined, as seen in Figure 9-4. The results thus obtained may be explained as follows: The parent negative ion is formed by the capture of secondary electrons having some kinetic energies which are released predominantly from rare gas atoms, and then it is stabilized by collision with rare gas atoms. In such cases, the efficiency of collisional stabilization by heavy gas atoms may be expected to be larger than that stabilized by light gas atoms. Thus, the relative intensities of the parent negative ion formation shown in Figure 9-3 seem to be qualitatively correlated with the order of mass number of rare gas atoms. Another possible explanation is to consider the existence of long-lived highly excited states of rare gas atoms. The importance of collisions of electronically excited particles with other neutral particles leading to the ionization of particles has been well recognized since the discovery of

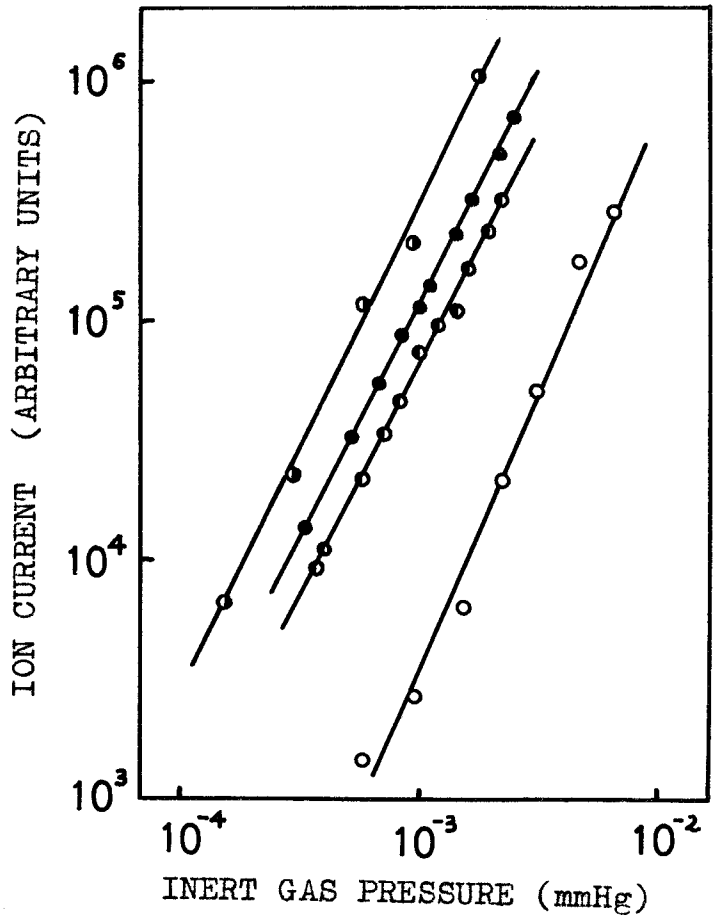

Figure 9-3. Dependence of rare gas pressure on the parent negative ion intensity.
Electron energy: 100 eV, nitroethylene pressure: 10^{-5} mmHg.
Rare gas; o : neon, ◐ : argon, ● : krypton, ◑ : xenon.

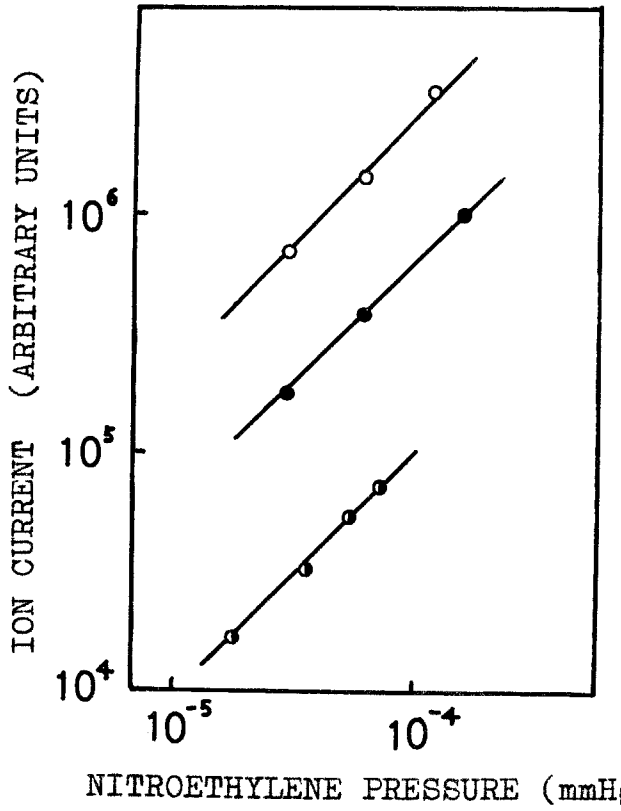

Figure 9-4. Dependence of nitroethylene pressure on the parent negative ion intensity;
Electron energy: 100 eV,
rare gas pressure: 10^{-3} mmHg.
Rare gas; ◐ : neon, ● : argon, o : xenon.

Penning ionization.[2] For the negative ion formation, Hotop and Niehaus[3] found that the parent negative ion of sulfur hexafluoride was produced in collisions of highly excited atoms (X**) with certain ground-state molecules of sulfur hexafluoride where X means rare gas atoms. In a recent study of parent negative ion formation of deuterized acetonitrile (CD_3CN), Sugiura and Arakawa[4] reported that the parent negative ion from a binary mixture of CD_3CN and rare gases appeared at electron energies which were close to the ionization potentials of corresponding rare gas atoms, and that the contribution of long-lived highly excited rare gas atoms was very important. Similar effects of rare gas atoms may also be anticipated in the present system. However, more exact measurements of the effects of ionizing electron energy and of rare gas pressure would be necessary to discuss the contribution of highly excited atoms.

Although there remains uncertainty about many factors in formation process of parent negative ions at higher electron energies, it can be tentatively concluded that the vibrationally excited parent negative ion of nitroethylene is first produced by the capture of secondary electrons or by the interaction with highly excited molecules and then it is stabilized by collision with other neutral molecules.

For the dimer negative ion at electron energy of 100 eV, the ion intensity was found to be of fourth order with respect to the nitroethylene pressure in the ionization chamber at pressures less than 10^{-4} torr and to be higher than fourth order at pressures above 10^{-4} torr. As seen in Figure 9-5, however, the intensity ratio of the dimer ion to the parent ion showed second order dependence with respect to the nitroethylene pressure in the whole pressure range examined, whereas the linear dependence was observed in the case of 0 eV energy, as mentioned in Chapter 8. In the experiments using a binary mixture of nitroethylene and rare gases, the intensity of the dimer negative ion appeared to be of third order with reference to the pressure of rare gases added in the ionization chamber, as shown in Figure 9-6.

Although the reaction mechanism leading to the dimer negative ion at higher electron energies is not yet clear, it can be reasonably assumed that the precursor of the dimer negative ion at higher electron energies is the parent negative ion of nitroethylene as it is in the case of 0 eV energy, and that the dimer ion is therefore formed by the ion-molecule reaction between the parent ion and the neutral molecule. The experimental evidence that the intensity ratio of the dimer ion to the parent ion is proportional to the square of nitroethylene pressure may indicate that such a process

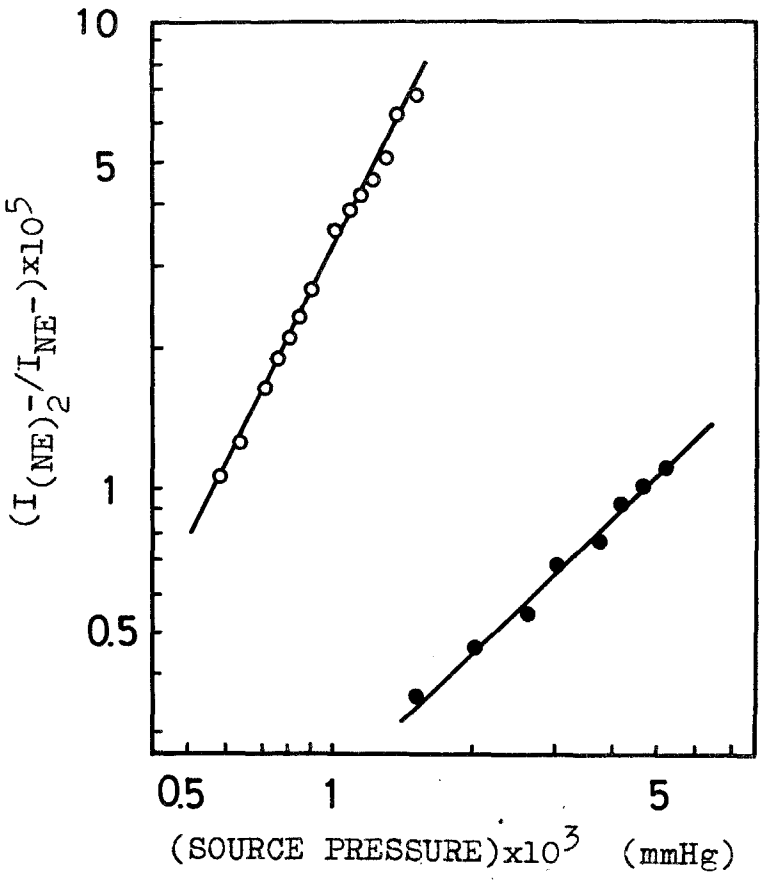

Figure 9-5. Relation between the intensity ratio $(C_2H_3NO_2)_2^-/C_2H_3NO_2^-$ and the source pressure.
o : electron energy 100 eV,
● : electron energy 0 eV.

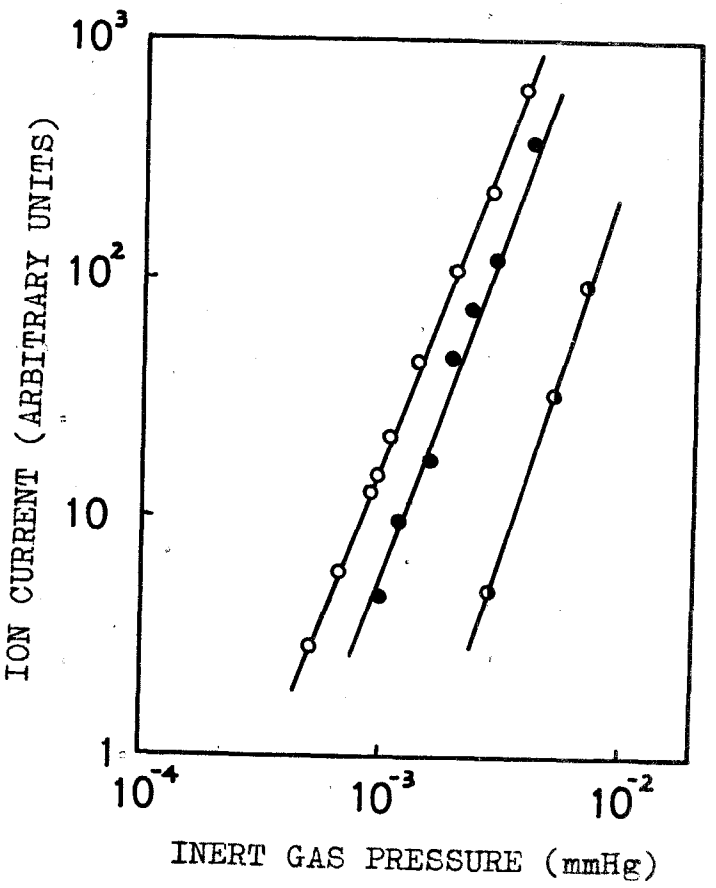

Figure 9-6. Dependence of rare gas pressure on the dimer negative ion intensity.
Electron energy: 100 eV,
nitroethylene pressure: 10^{-5} mmHg.
Rare gas; ◐ : neon, ● : argon,
o : krypton.

requires collisional stabilization of the initially formed, vibrationally excited, dimer negative ion. The effect of added rare gases might be similarly explained by the supposition that rare gas atoms act as colliding particles to stabilize the excited dimer ion produced by the ion-molecule reaction.

It is concluded from the results mentioned in Part 3 that the precursor of the dimer negative ion of nitroethylene is the parent negative ion formed by the capture of thermal or near-thermal energy electrons and that the dimer ion, which leads to the trimer ion through a consecutive reaction, is produced by the ion-molecule reaction between the parent ion and the neutral molecule. Further, it seems probable that the process of collisional stabilization of the product ions is very important at higher electron energies. These findings give rise to the suggestion that the precursor of the radiation-induced polymerization of nitroethylene is the parent negative ion.

References

1) W. E. Wentworth and J. C. Steelhammer, "Radiation Chemistry", Adv. Chem. Ser., 82 (II), 75 (1968); L. G. Christophorou and R. P. Blaunstein, Radiation Res., 37, 229 (1969); and references cited therein.

2) A. A. Kruithof and F. M. Penning, Physica, 4, 430 (1937).

3) H. Hotop and A. Niehaus, J. Chem. Phys., 47, 2506 (1967).

4) T. Sugiura and K. Arakawa, Preprints of 1969 Intern. Conference on Mass Spectrom., p. 137, Kyoto, 1969.

P A R T 4

MASS SPECTROMETRIC STUDY ON PRIMARY PROCESSES OF RADIATION-INDUCED REACTION

Chapter 10

Collision-induced Dissociation of Acetylene Ions.

Part I. Process $C_2H_2^+ \longrightarrow C_2H^+ + H$

1. Introduction

One of the easiest ways of studying the dissociative states of molecular ions is to excite fast ground-state or metastable-state ions into such states by collision with atomic or molecular targets, according to the following scheme:

$$AB^+ \xrightarrow{M} AB^{+*} \longrightarrow A^+ + B \qquad (1)$$

If the AB^{+*} excited state has some excess internal energy over its dissociated threshold, a part $\underline{W}$ of it (for polyatomic species) will appear as translational energy of products A^+ and B in the centre-of-mass system. The energy $\underline{E^*}$ required for excitation to the AB^{+*} state, and possibly for excitation of the target itself, will be taken from the translational energy $\underline{V_o}$ of the incident AB^+

ions. Thus the final translational energy of the fragment A^+ will have a component along the initial flight direction $\underline{V}$ equal to

$$V = \frac{m_A}{m_A + m_B}(V_o - E^*) + 2\frac{(m_A\, m_B)^{1/2}}{m_A + m_B}[(V_o - E^*)W]^{1/2}\cos\theta + \frac{m_B}{m_A + m_B} W \cos^2\theta \qquad (2)$$

where m_A and m_B are the masses of A and B, and θ is the angle between the direction of separation of the fragments in the centre-of-mass system and the incident flight direction. The measurement of $\underline{V}$ distributions thus allows the determination of $\underline{W}$ and $\underline{E^*}$.

Such analyses were made by various authors in the well-known case of the collision-induced dissociation of hydrogen molecule ions.[1-6] It turned out that two types of phenomena were observed:

(i) "vertical" excitation of the incident ions to a dissociative electronic state, and

(ii) momentum transfer leading to the adiabatic dissociation of ground-state ions.

A third possible type of process, not observed in the case of H_2^+, is

(iii) collision-induced predissociation of ions in a metastable state.

For any new study of this kind, it is interesting to be able to distinguish between these three kinds of processes. This information may be obtained by a study of the dissociation induced by collision with various targets at varying incident ion energies.

Indeed, process (i) was shown to be favoured by the use of small targets (e.g. helium atoms), process (ii) by the use of large targets (e.g. xenon atoms, nitrogen molecules, etc.).[1),4),6)]

On the other hand, the cross section for process (i) is expected to increase along with the incident energy and to reach a maximum for a velocity $\underline{v_o}$ comparable to that given by the "adiabatic criterion",

$$v_o \approx aE^*/h$$

For $C_2H_2^+$ incident ions, assuming the "adiabatic parameter" $\underline{a}$ to be equal to 7 Å [7)], this $\underline{v_o}$ corresponds to incident translational energies $\underline{V_o}$ = 4 to 100 keV for excitation energies $\underline{E^*}$ ranging from 1 to 5 eV.

In contrast to this behaviour, the cross section for process (ii) is expected to reach a maximum for incident translational energies (with respect to the centre-of-mass of the ion + targent system) equal to a few times the

dissociation energy of the incident ions. This corresponds to laboratory energies in the range of 40 to 200 eV for $C_2H_2^+$-on-He collisions and 6 to 30 eV for $C_2H_2^+$-on-Xe collisions if the whole kinetic energy of relative motion may be used, and in the range of 50 to 250 eV for $C_2H_2^+$-on-He collisions and 30 to 150 eV for $C_2H_2^+$-on-Xe collisions if only the relative kinetic energy of the couple H atom-target may be used (for dissociation into $H + C_2H^+$ or $H^+ + C_2H$).

The behaviour of process (iii) with respect to variations of the incident translational energy, and of the kind of target used, is so far unknown. It may be tentatively expected that the cross section will be maximum for a velocity given by the "adiabatic criterion" used with an E^* equal to the separation, perturbation-induced, between the two adiabatic states involved. Thus a maximum at a comparably low velocity would be expected.

Other information required for disentangling the various processes which may occur is the knowledge of the initial vibronic state of the incident ions. As regards the vibrational energy of ions in the ground electronic state, this information is obtained by studying the effect of varying the energy of the ionizing electrons used to produce these ions.

As regards electronically excited states, they usually decay before the ions are accelerated and have experienced a

collision; possible collision-induced dissociations of metastable ions may be characterized through the effect of varying the residence time of the ions in the ion source, since the radiative lifetime for some allowed electronic transitions is of the same order of magnitude as the time between ion formation and collision.

For a first study along these lines, we chose the dissociation of $C_2H_2^+$ ions induced by collision with helium or xenon stoms in the incident energy range V_o = 1 to 5 keV. The scope of the present study will be limited to the dissociation of $C_2H_2^+$ into $C_2H^+ + H$.

Collision-induced dissociation of acetylene molecule ions was studied previously by Henglein,[8] by Melton et al.,[9] and by Kuprijanov and Perov.[10] These authors observed the dissociation of $C_2D_2^+$ into $D^+ + (C_2D)$[8] and of $C_2H_2^+$ into $C_2H^+ + H$,[8),10] $C_2^+ + (2H)$, $CH^+ + (CH)$, $C^+ + (CH_2)$;[9),10] and $CH_2^+ + C$.[9]

In order to study the dissociation processes of acetylene ions, it is necessary to discuss the available evidence concerning the relevant states of $C_2H_2^+$ and its fragments. The electronic states of $C_2H_2^+$ resulting solely from the ejection of an electron without additional excitation and which lie lower than 21.21 eV above the

C_2H_2 ground state are known from photoelectron spectroscopy.[11] These are the $^2\Pi_u$ (11.36 eV), $^2\Sigma_g^+$ (16.27 eV) and $^2\Sigma_u^+$ (18.23 eV) states, the electronic configuration of ground-state C_2H_2 being:

$$(1\sigma_g)^2\ (1\sigma_u)^2\ (2\sigma_g)^2\ (2\sigma_u)^2\ (3\sigma_g)^2\ (1\pi_u)^4.$$

From the pattern of the vibrational levels which are significantly excited in each of these states[11] it was shown that the equilibrium distance of the $^2\Pi_u$ state is close to that of the neutral molecule, whereas in the $^2\Sigma_g^+$ and $^2\Sigma_u^+$ states the excitation of C - H and C - C stretching vibrations indicates an increase in the internuclear equilibrium distances.

Photoionization experiments by Botter et al.[12] yielded similar information on the $^2\Pi_u$ state; these authors also calculated theoretical Franck-Condon factors in close agreement with the experimental ones.

Other electronic states of $C_2H_2^+$ in the range of 16 to 20 eV which are not significantly excited in direct ionization are those resulting from the ejection of a $1\pi_u$ electron with simultaneous excitation of another $1\pi_u$ electron to one of the first unoccupied orbitals, viz. $1\pi_g$ or 3s $4\sigma_g$. The $1\pi_g$ orbital, from spectroscopic data, lies 6 eV above the $1\pi_u$ orbital; the position of the $4\sigma_g$ orbital was estimated as lying about 8 eV above $1\pi_u$.[13]

Configuration

$$(1\sigma_g)^2(1\sigma_u)^2(2\sigma_g)^2(2\sigma_u)^2(3\sigma_g)^2(1\pi_u)^2(4\sigma_g)^1,$$

$$^4\Sigma_g^-,\ ^2\Delta_g,\ ^2\Sigma_g^+,\ ^2\Sigma_g^-$$

therefore leads to states in the range of about 17 to 23 eV above ground-state C_2H_2. Among these states, the $^4\Sigma_g^-$, $^2\Delta_g$ and $^2\Sigma_g^-$ are adiabatically correlated with the first electronic states of the fragments $C_2H^+ + H$, as shown by Fiquet-Fayard[13] (see later, Figure 10-8).

Configuration

$$(1\sigma_g)^2(1\sigma_u)^2(2\sigma_g)^2(2\sigma_u)^2(3\sigma_g)^2(1\pi_u)^2(1\pi_g)^1,$$

$$^4\Pi_g,\ ^2\Phi_g,\ ^2\Pi_g$$

leads to states in the range of about 15 to 21 eV. These states are adiabatically correlated with high-energy states of the fragments in so far as the linear geometry of the molecule is conserved. However the properties of the $1\pi_g$ orbital may be used to show, using arguments similar to Mulliken's in his study of the excited states of neutral C_2H_2,[14] that most substates of the configuration under consideration are less stable in the linear geometry than in the <u>cis</u>-bent or the <u>trans</u>-bent geometry. Thus the lowest Φ_g or Π_g

states are very probably correlated with low-energy states of the fragments through non linear geometrical configurations with C_{2v} or C_{2h} symmetry.

A number of autoionized states are apparent on the photoionization curves of Botter et al.[12] The corresponding absorption is particularly important in the regions of 12.5 to 14 eV and 14.5 to 16.5 eV.

C_2H^+ ions are the first fragment ions appearing in acetylene on impact of electrons or photons of increasing energy. The appearance potential of C_2H^+ was determined by electron impact as 17.8±0.2 eV[15] or 17.9±0.1 eV[16]; a value in the same range was obtained from the charge transfer experiments of Lindholm et al.[17] A somewhat lower value of 17.22 eV was measured accurately by photoionization.[12]

From these data it appears that for the processes occurring through vertical transitions the first step in the production of C_2H^+ ions near threshold is very probably the $3\sigma_g$ ionization leading to the $^2\Sigma_g^+$ state of $C_2H_2^+$. Similar conclusions were derived by Čermak from Penning ionization experiments.[18]

Adiabatic correlations between electronic states of $C_2H_2^+$ and of its fragments were proposed by Fiquet-Fayard[13]. Her theoretical[13] and experimental[19] results however left unresolved the question of whether the appearance threshold of C_2H^+ ions is related to predissociation or to direct

(but delayed by vibrational relaxation) dissociation of the $^2\Sigma_g^+$ state. The new photoelectron spectra of Baker and Turner[11 b)] show that a possible dissociation of this state at 17.22 eV would need a time much longer than a vibrational period, which observation is in agreement with the isotopic effects observed by Guyon and Fiquet-Fayard.[19)]

From the variation with incident ion energy of the cross section for C_2H^+ production by charge transfer of Ar^+ ions on C_2H_2 at low energies, Maier[20)] found an energy of formation of $C_2H^+ + H$ from C_2H_2 lower than 16.97 eV and probably equal to 16.72 ± 0.12 eV. This type of experiment is likely to yield an adiabatic threshold, which may be relevant to either of the two lowest states of $C_2H^+ + H$ (cf. Figure 10-8).

2. Experimental

The apparatus used for the present work is represented in Figure 10-1 and resembles essentially a magnet sector mass spectrometer. The ion source S is an electron impact source of the Nier type (Atlas AN4). After leaving the source, the ions enter a collision chamber C, which consists of an inconel cylinder 50 mm in length with an entrance slit 0.5×2 mm^2 and an exit slit 1×0.5 mm^2 (in directions $\underline{y} \times \underline{z}$, see Figure 10-1).

Acetylene was admitted into the ionization chamber of the ion source, and the target gas into the collision chamber. No monochromatization of the electron beam was achieved. The half-width of the energy distribution was about 0.5 eV. A strong differential pumping insured that no more than 1 % of the collisions experienced by the primary ions took place after they had left the collision chamber.

Ions leaving the collision chamber were analyzed by one of their transverse velocity components with a parallel-plate condenser P_1, P_2. Then they were collimated in the y direction by a slit D (2.4×8 mm^2) at the entrance of the magnetic analyzer. This analyzer, of radius 21 cm, was used both for mass analysis, with resolving power up to 2000, and for the scanning of the velocity component of the ions in the direction of flight of the incident ions. The magnetic field was measured with a differential gaussmeter. The ions were detected by an electron multiplier.

In all the experiments carried out in the present study, the parallel-plate condenser was set in order that only the ions scattered to essentially zero angle were collected. The collimation of the beam leaving the collision chamber defined it to a solid angle 2.5×10^{-5} steradian.

The acetylene used was manufactured by Société Air Liquide and further purified by trap-to-trap distillation

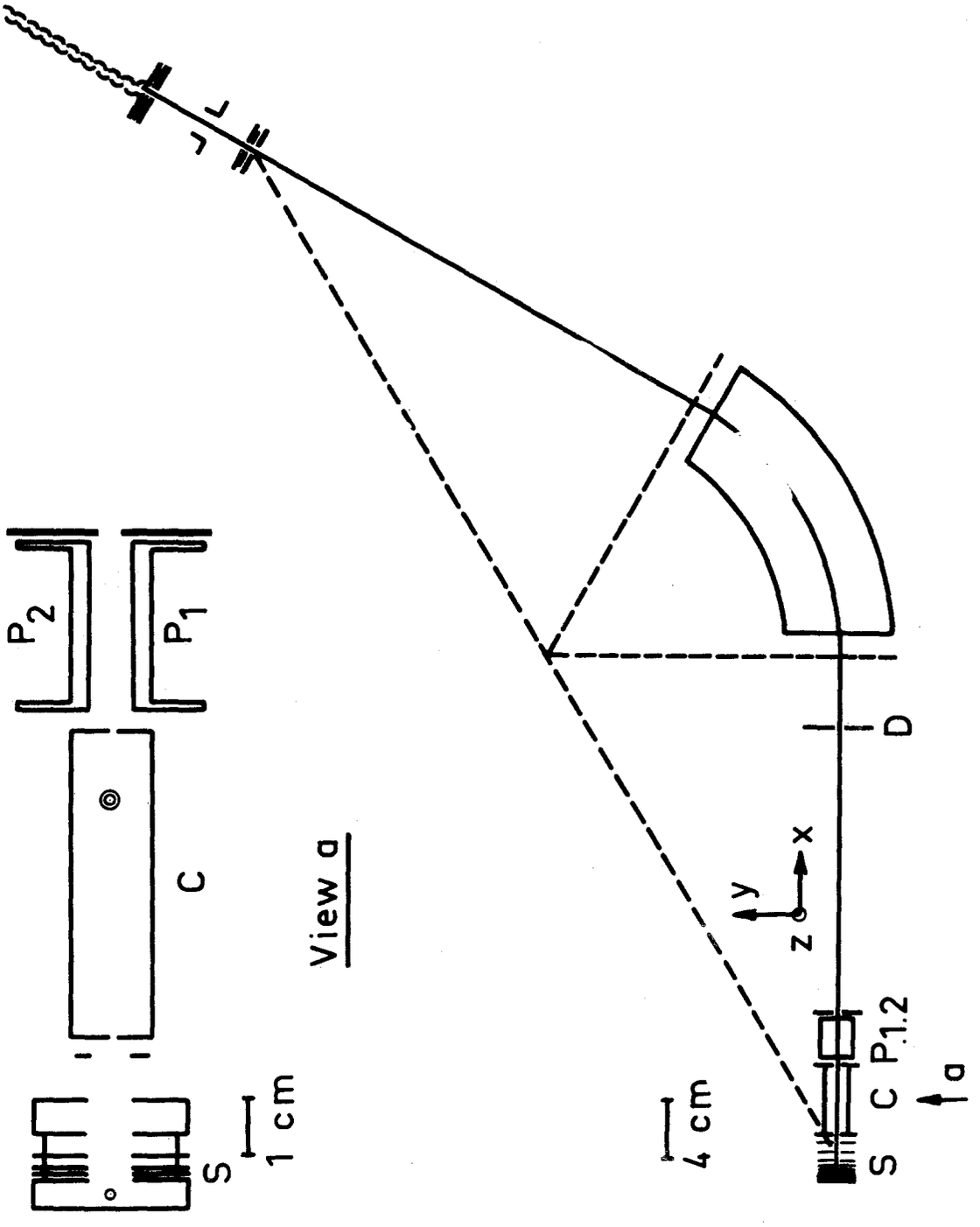

Figure 10-1. Scheme of the apparatus.

in vacuum. Helium and xenon from the same manufacturer, of purity $\geq$ 99.998 % and 99.995 % respectively, were used without further purification.

3. Results and Discussion

3.1. Main features

As is well known, any single-charged ion appears on the apparent mass scale of a magnetic sector mass spectrometer at a position

$$m^* = (V/V_o) \cdot m \qquad (3)$$

where $\underline{V}$ is the translational energy component of the ion parallel to main flight direction, $\underline{m}$ its mass, $\underline{V_o}$ the translational energy of a reference ion.

From equations (2) and (3), it appears that C_2H^+ ions produced in the collision chamber will be collected, if $\underline{E^*}$ and $\underline{W}$ are equal to zero, at the apparent mass $m^* = 24.04$, where is very close to the mass of C_2^+ ions, 24.00.

Thus, if the electron energy is higher than the appearance potential of C_2^+ ions from C_2H_2, collision-produced C_2H^+ and primary C_2^+ ions will give rise to two peaks very close to one another.

If the electron energy is lower than this appearance potential, the collision-induced peak will appear alone.

In the case of helium as a target gas, such behaviour is apparent in Figure 10-2, where the magnetic field was scanned in the vicinity of mass 24, at ionizing electron energies 16 and 23 eV. The narrower peak is of course that of C_2^+ primaries. The appearance potential of these ions was determined by Pham as 18.85 ± 0.15 eV.[16)]

The width of the collision-induced peak at half-maximum corresponds to a mean total translational energy of the fragments in the centre-of-mass system

$$W_{av} = 0.15 \text{ eV}$$

The collisional origin of this peak was ascertained by studying the dependence of its intensity with respect to the pressure in the gas inlet line leading to the collision chamber, as shown in Figure 10-3. It may be seen that the intensity of the peak is of the first order with respect to the pressure in the whole range used; thus, any contribution of unimolecular dissociation (so-called "pure metastable" transitions) would be negligible.

Since the study of the collision-induced dissociation of H_2^+ ions showed that helium and xenon were representative of two kinds of targets which favour the processes of types (i) and (ii) respectively, these two gases were chosen as

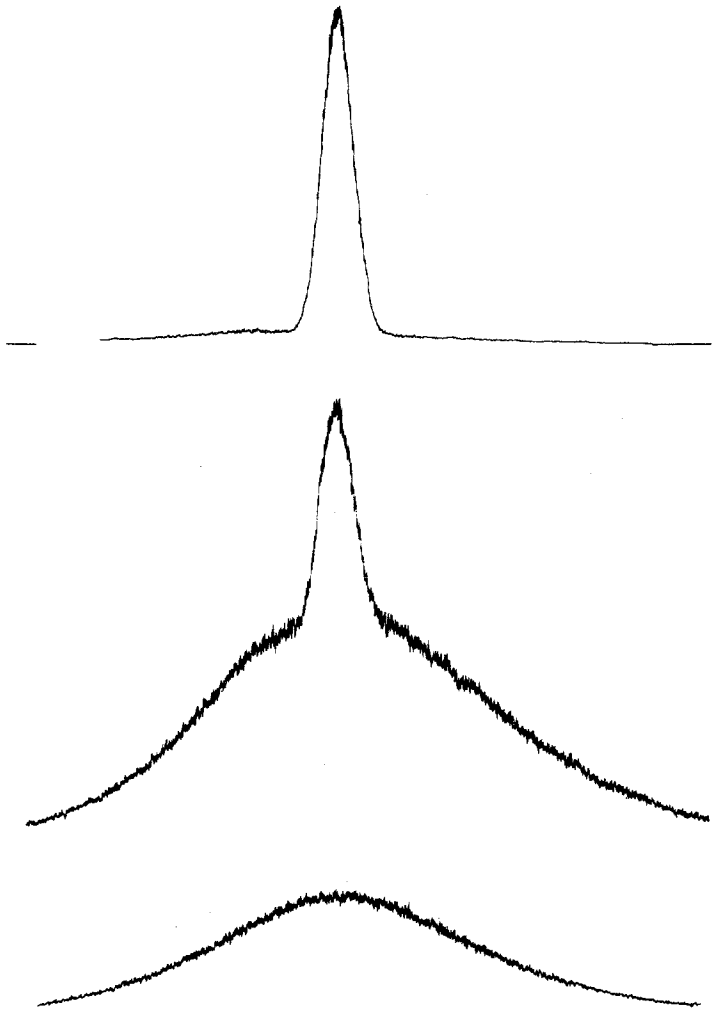

Figure 10-2. Registration of the $C_2H_2^+ \longrightarrow C_2H^+$ peak.

Ion incident energy: 3000 eV.

Upper curve: the peak of primary C_2^+ ions.
Electron energy: 23 eV, target gas: absent.

Middle curve: coexistence of the peaks of primary C_2^+ and secondary C_2H^+ ions.
Electron energy: 23 eV, target gas: helium.

Lower curve: the peak of secondary C_2H^+ ions.
Electron energy: 16 eV, target gas: helium.

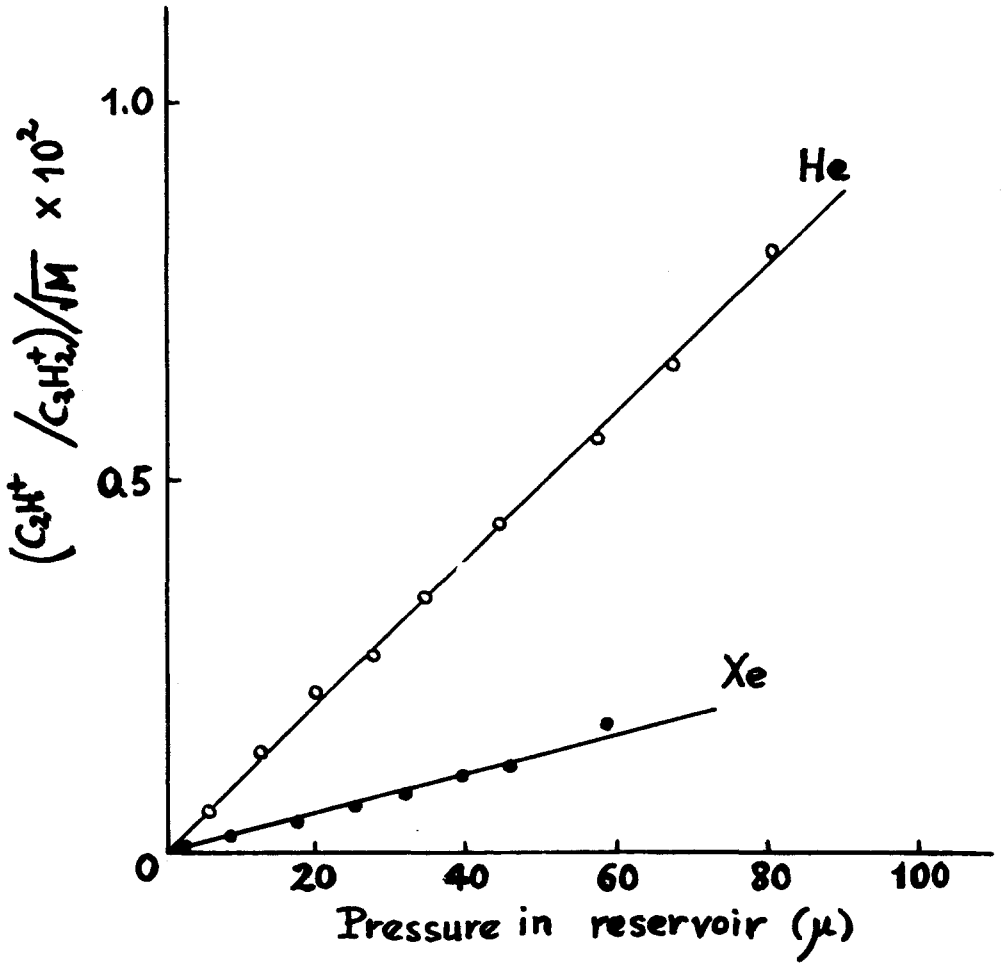

Figure 10-3. Ratio of peak heights for $C_2H_2^+ \longrightarrow C_2H^+$ and for $C_2H_2^+$ for varying pressure in the collision chamber.

Incident ion energy: 3000 eV, electron energy: 16 eV, target: helium or xenon.

targets for the present study.

The results obtained with xenon were similar to those obtained with helium. However, the efficiency of the collision-induced dissociation was much lower for xenon than for helium, as can be seen in Figure 10-3. Relative cross sections may be calculated from the pressure measured in the gas inlet line leading to the collision chamber, by considering that the flow from inlet line to chamber is a viscous flow, thus roughly mass-independent, whereas the flow from collision chamber to the pumps is molecular, thus proportional to the reciprocal square root of the atomic mass. Under these assumptions, the following ratio of collision-induced dissociation cross sections was obtained:

$$\sigma_{Xe}/\sigma_{He} = 0.26 \qquad \text{at electron energy 16 eV.}$$

From the observations made in the case of H_2^+ dissociation, this result is indicative of an electronic rather than vibrational transition.

3.2. Influence of ionizing electron energy

The influence of ionizing electron energy on the cross section for collision-induced dissociation reflects the variation of this cross section with the vibronic energy of incident ions.

The electron energy scale was calibrated using the ionization efficiency curve of helium, which was found to be linear from a few tenths of an eV above threshold. The intercept of this linear part was identified with the ionization potential of helium.

Appearance curves of the collision-induced dissociation peak (Figures 10-4 and 10-5) show that it appears between 11.5 and 12 eV, close to the ionization potential of acetylene (11.40 eV[21]). Ground-state $C_2H_2^+$ ions are thus able to undergo a collision-induced dissociation into $C_2H^+ + H$.

As regards the variation of the cross section with ionizing electron energy, two types of results are presented.

Firstly, relative cross sections for production of fragments with a given translational energy in the centre-of-mass system, W, are obtained from the ratio of the ion current corresponding to this particular W (i.e., to a particular abscissa on the curve of Figure 10-2) to the ion current at the top of the parent ion peak. This method is justified since: (i) the angular aperture and the velocity distribution of the parent ion beam are independent of ionizing electron energy; and (ii) any variation of the angular aperture of the fragment ion beam with the energy of the electrons, which could arise from the variation of the kinetic energy of the fragments in the centre-of-mass system,

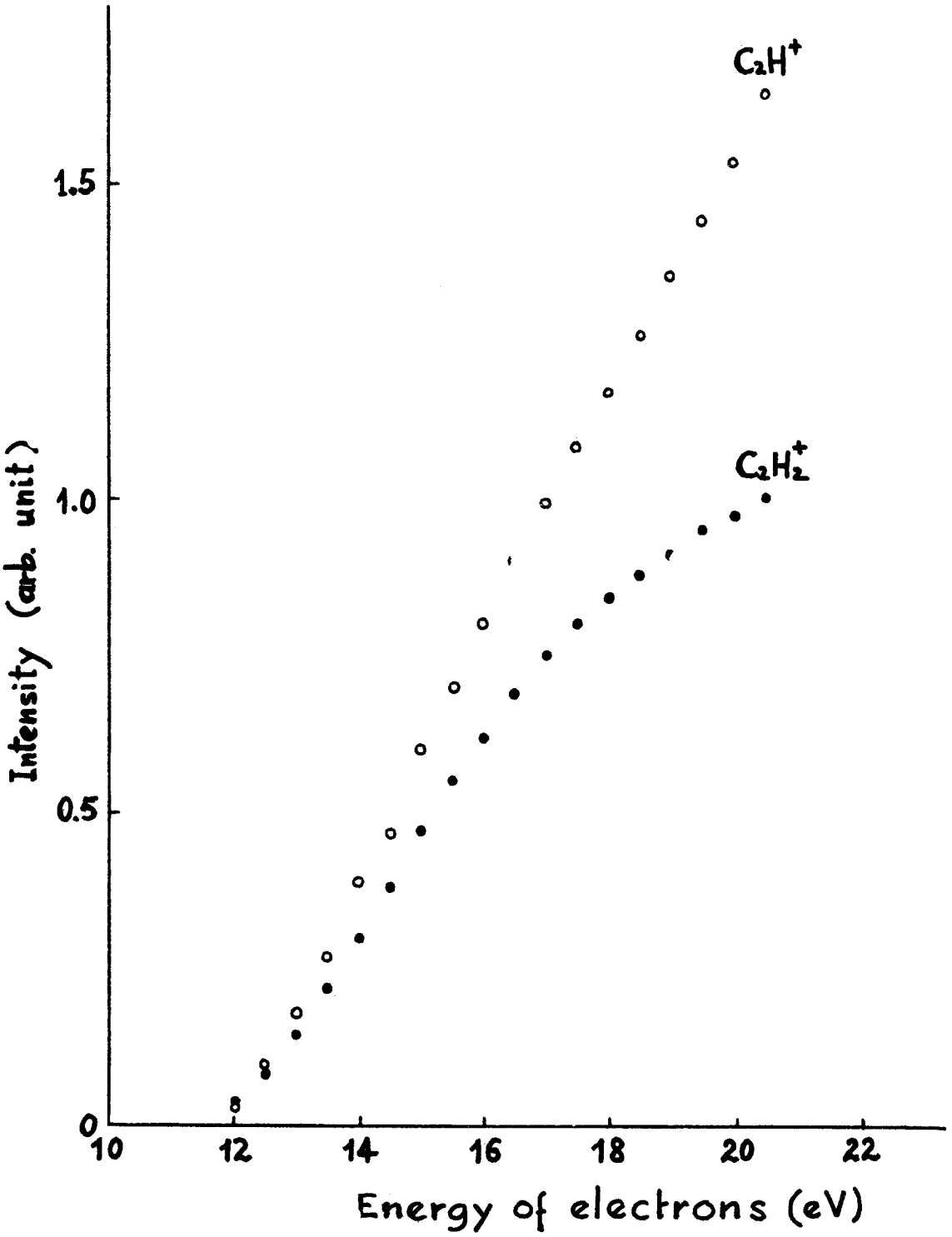

Figure 10-4. Apparance curves of the $C_2H_2^+$ peak and the $C_2H_2^+ \longrightarrow C_2H^+$ peak.

Ion incident energy: 3000 eV, target: helium.

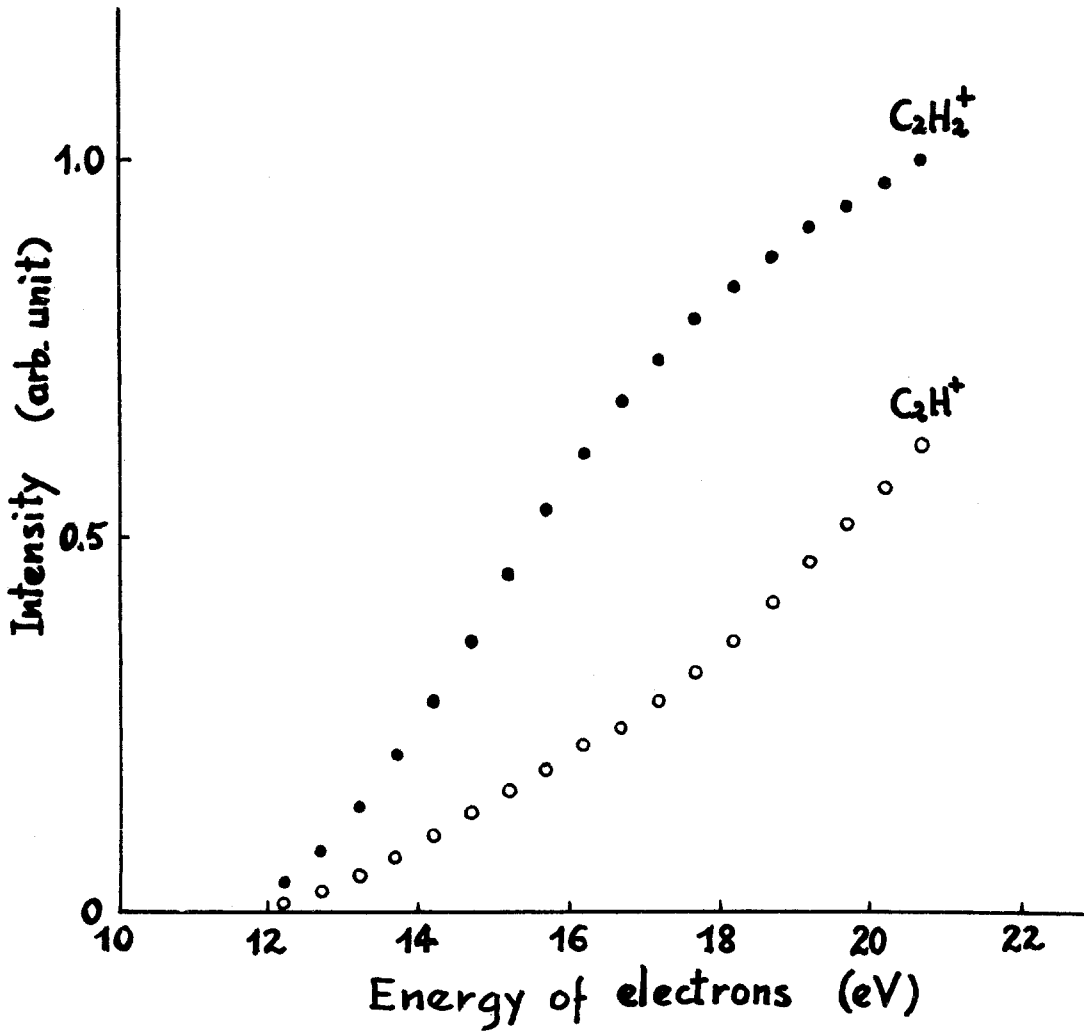

Figure 10-5. Appearance curves of the $C_2H_2^+$ peak and the $C_2H_2^+ \longrightarrow C_2H^+$ peak.

Ion incident energy: 3000 eV, target: xenon.

would be small compared to the collection solid angle since the C_2H^+ ions receive only a $1/26^{th}$ of the total kinetic energy of both fragments.

Relative cross sections thus obtained are plotted in Figures 10-6 and 10-7 against electron energy for three different values of $\underline{W}$ (0, 0.03, and 0.12 eV). It appears that the cross sections increase with increasing electron energy in the whole range studied; further, the rate of increase of the cross section with electron energy suddenly rises at 17.2 ± 0.2 eV (for $\underline{W} = 0$), at 17.4 ± 0.2 eV (for $\underline{W} = 0.03$ eV) and at 17.8 ± 0.3 eV (for $\underline{W} = 0.12$ eV).

Secondly, relative total cross sections are given by the ratio of the peak areas of collision-produced C_2H^+ ions and of parent $C_2H_2^+$ ions, thus integrating the distribution of the kinetic energy component parallel to flight direction. The occurrence of a sudden increase in the rate of variation of cross section with ionizing electron energy at about 17.2 eV was confirmed (see Figure 10-9).

Discussion of the significance of these results, as well as of those presented in the following sections, requires some knowledge of the potential surfaces of $C_2H_2^+$ states, and especially of the section of these surfaces along the C_2H-H coordinate. A semi-quantitative plot of these potential curves was given by Fiquet-Fayard based on theoretical considerations;[13] this plot, with the kind

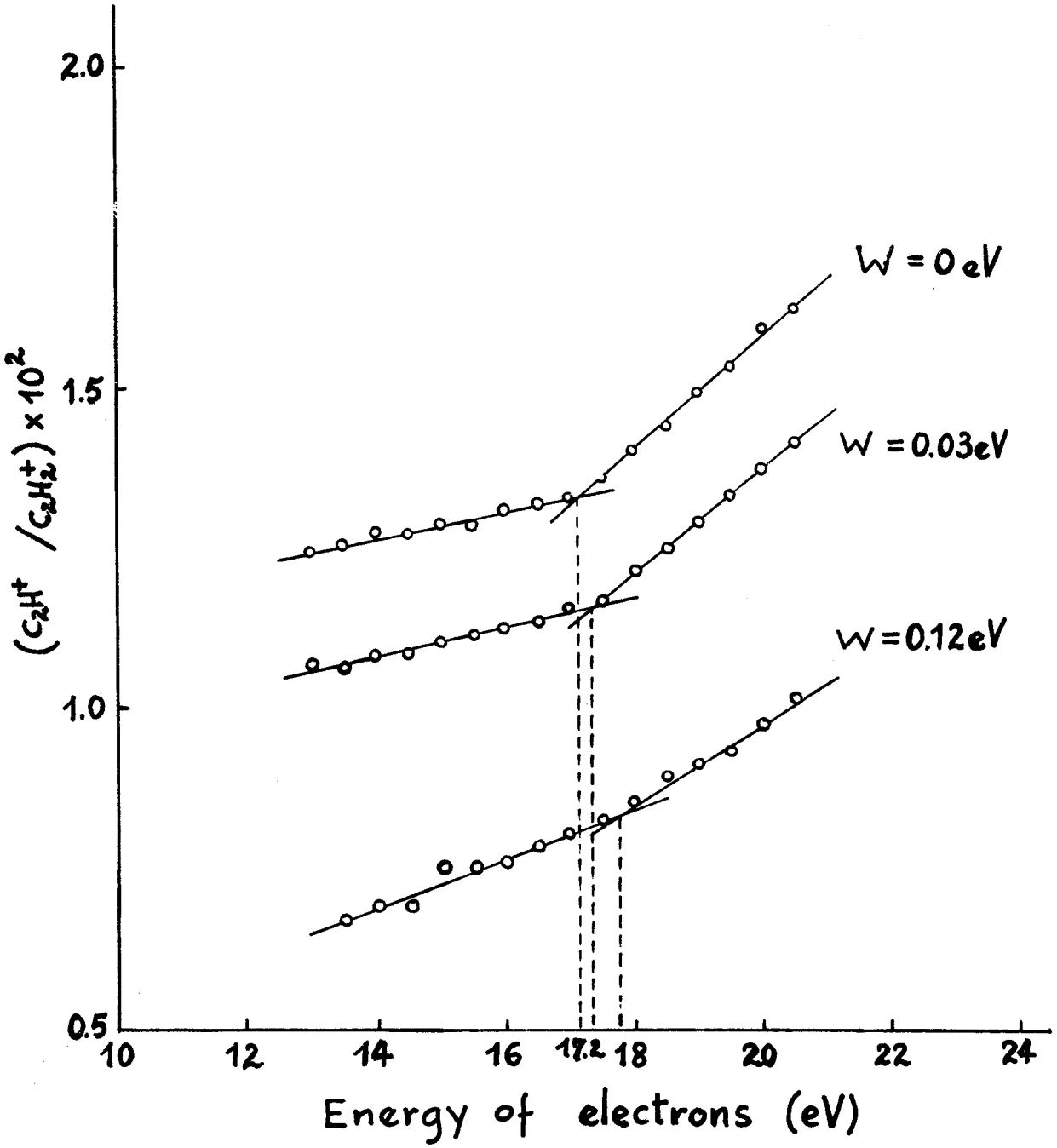

Figure 10-6. Ratio of peak heights for $C_2H_2^+ \longrightarrow C_2H^+$ and for $C_2H_2^+$ as a function of electron energy. Incident ion energy: 3000 eV, target: helium.

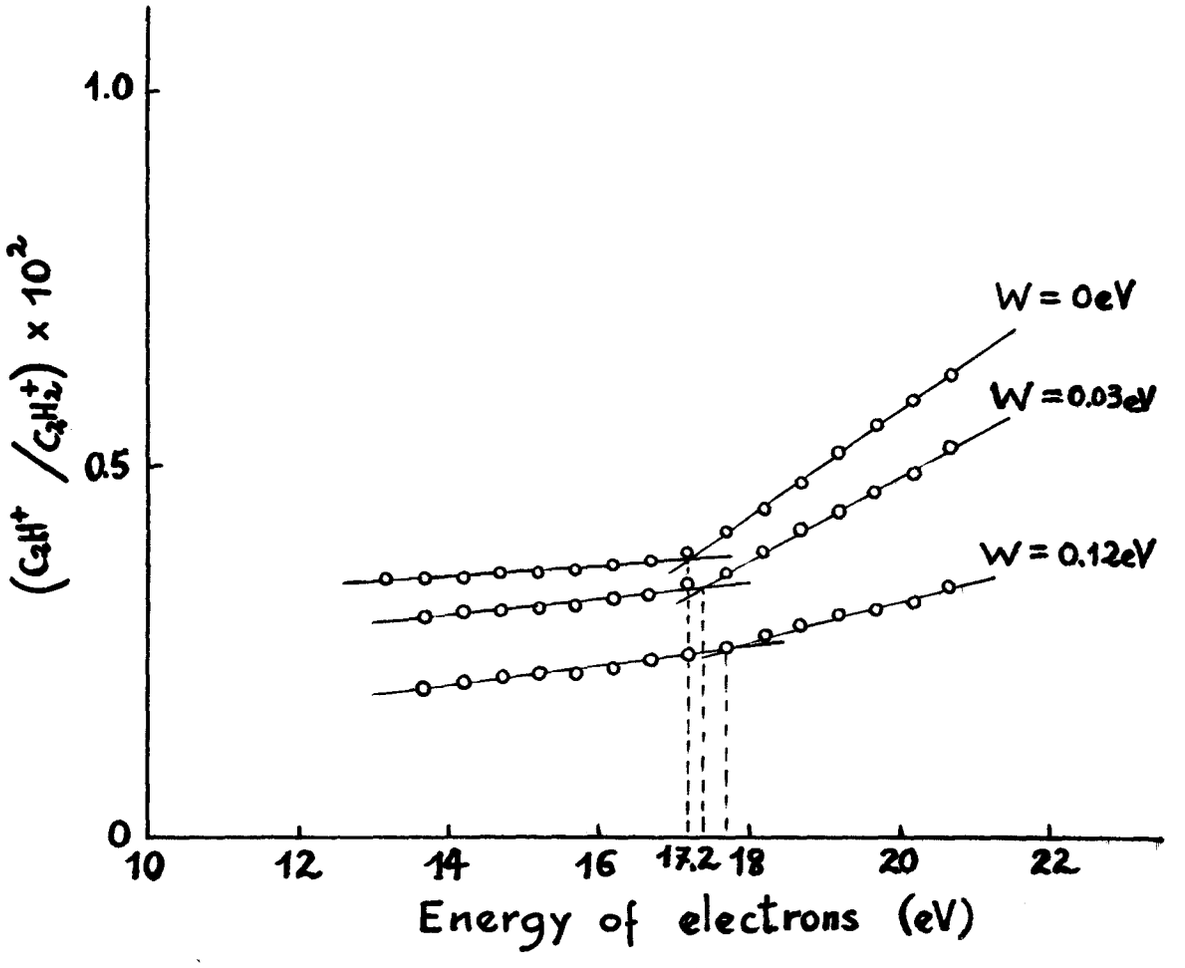

Figure 10-7. Ratio of peak heights for $C_2H_2^+ \longrightarrow C_2H^+$ and for $C_2H_2^+$ as a function of electron energy. Incident ion energy: 3000 eV, target: xenon.

permission of the author, is reproduced with slight modifications in Figure 10-8. Solid curves are those of the $C_2H_2^+$ states the energies of which in the $D_{\infty h}$ configuration are exactly known from photoelectron spectroscopy.[11] The energy levels of $C_2H^+ + H$ fragments as estimated by Fiquet-Fayard are probably correct to within 0.5 eV. The striated areas indicate the occurrence of strong autoionization.

The state dissociating into fragments(*) $C_2H\ (X\ ^2\Pi_u) + H^+$, for the sake of clarity, was not drawn in Figure 10-8; its asymptotic energy was estimated by Fiquet-Fayard as being about 0.3 eV above that of $C_2H^+(^3\Pi_u) + H(^2S)$.

However, in view of the uncertainty on the energies of the various states involved, it is not unlikely that $C_2H(X^2\Pi_u) + H^+$ would be slightly lower than $C_2H^+(^3\Pi_u) + H(^2S)$, in which case the ground state of $C_2H_2^+$ would be adiabatically correlated with $C_2H + H^+$ instead of $C_2H^+ + H$. One of the aims of the present work was to test this possibility.

In the Figures 10-6 and 10-7, the slow increase of the cross section from threshold to 17.2 eV shows that successive vibrational levels of the ground $X^2\Pi_u$ state are populated, and that the collision-induced dissociation cross section,

---

(*) Following Fiquet-Fayard,[13] we call g or u the states of C_2H and C_2H^+, in analogy with corresponding C_2 states.

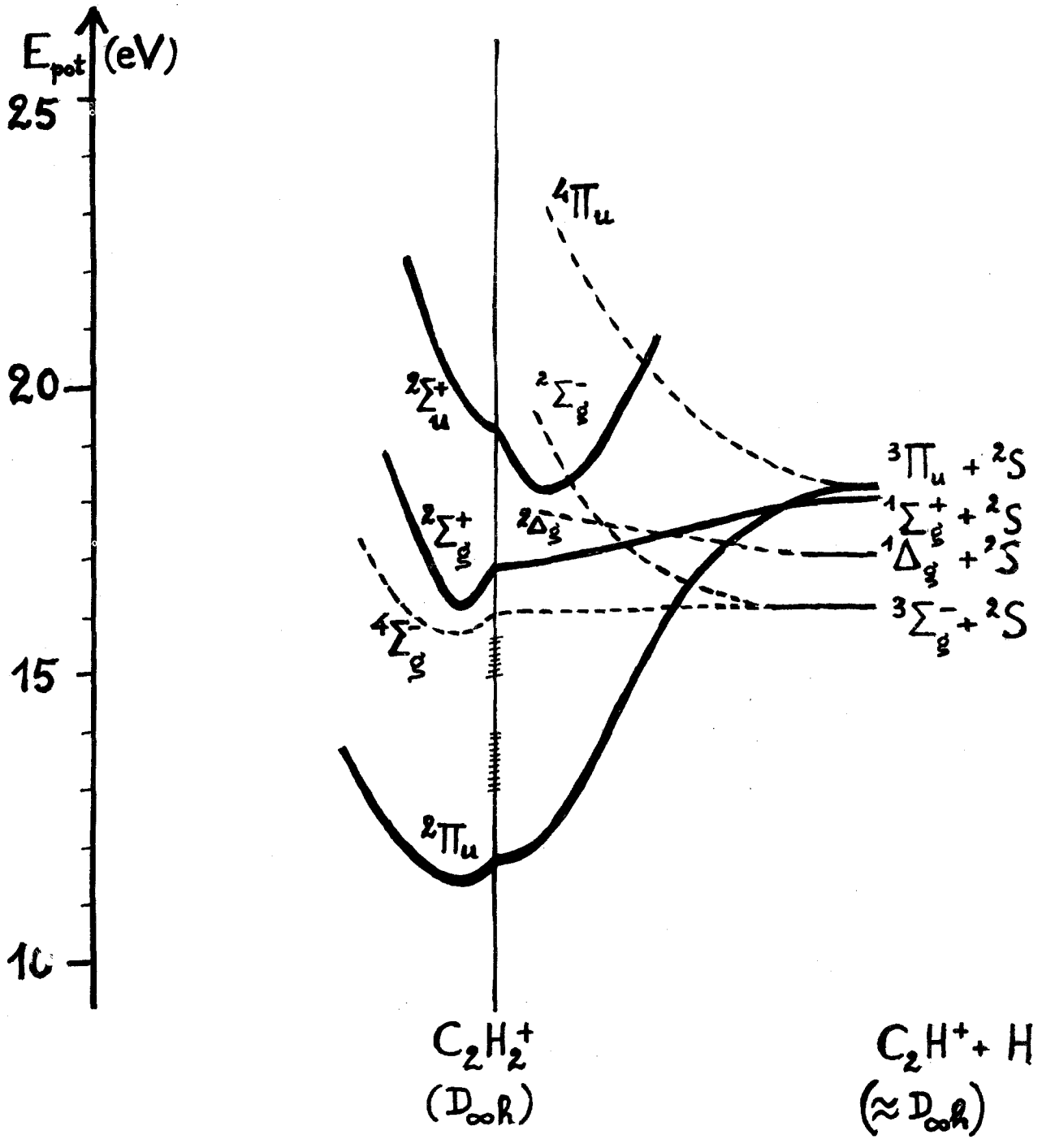

Figure 10-8. Schematic sections of the potential hypersurfaces of $C_2H_2^+$ states (slightly modified from Fiquent-Fayard[13]). The right side of the Figure refers to the C_2H-H coordinate, the left side to the C-C coordinate. The potential energy is defined from C_2H_2 ground state as zero.

as expected, increases along with the vibrational energy of the initial state.

Further, the fact that our collion-induced dissociation cross section increases more rapidly with the electron energy above 17.2 eV (or a value slightly higher if the fragments are to be formed with some excess kinetic energy) means that $C_2H_2^+$ ions in a particular state formed at this energy will more readily dissociate on collision than other $C_2H_2^+$ ions formed at lower energy; the latter ions are, for example, the vibrationally excited ions in the electronic ground state, which are likely to be formed through autoionization in the range 12.5 - 14 eV or 14.5 - 16.5 eV.

Several possible hypotheses have to be examined as regards this particular state formed at 17.2 eV. This state may be:

a) a highly vibrationally excited level of the $^2\Pi_u$ ground state, close to the C_2H^+ ($^3\Pi_u$) + H(^{2}S) level, the dissociation taking place by an electronic transition to the repulsive $^4\Pi_u$ state (process (i), see the introduction);

b) the same state (possibly less highly vibrationally excited), dissociating by an adiabatic transition (process (ii));

c) the same state, dissociating through collision-induced predissociation into the $^2\Sigma_g^+$ or $^2\Sigma_g^-$ or $^2\Delta_g$ or $^4\Sigma_g^-$ state (process (iii));

d) the $^4\Sigma_g^-$ state, dissociating either by process (i) or by process (ii);

e) the $^2\Sigma_g^+$ state, dissociating either by process (i), by process (ii) or by process (iii);

f) the $^2\Sigma_u^+$ state, dissociating either by process (i) or by process (iii).

Before discussing these various hypotheses, it should be called to mind that the appearance potential of C_2H^+ ions from C_2H_2, as determined by photoionization,[12] is also equal to 17.2 eV. If this is not a coincidence, it means that the state of $C_2H_2^+$ formed at 17.2 eV, which we are considering, probably needs a very small amount of energy for dissociating. This would be in agreement with all hypotheses stated here.

Among them, however, hypotheses (d) and (f) are unlikely on following grounds: The $^4\Sigma_g^-$ state, which would be formed according to hypothesis (d), cannot have an energy as high as 17.2 eV without being rapidly dissociated into the fragments with which it is correlated, <u>viz.</u> $C_2H^+(^3\Sigma_g^-) + H(^2S)$, the energy of which is known as

$$D(C_2H - H) + I.P.(C_2H) = 4.9 \pm 0.4 \text{ eV}^{22)} + 11.25 \pm 0.15^{16)}$$
$$= 16.15 \pm 0.55 \text{ eV},$$

which is significantly lower than 17.2 eV.

Hypothesis (f) may be rejected on opposite grounds: the adiabatic ionization potential corresponding to the $^2\Sigma_u^+$ state is 18.38 eV,[11] which is significantly higher than 17.2 eV.

As regards hypothesis (e), the point is whether the ions in the excited $^2\Sigma_g^+$ state may live long enough to be still in significant amounts when arriving in the collision chamber. The time of flight from ionization chamber to collision chamber is several 10^{-7}s under standard conditions of operation. The lifetime of the $^2\Sigma_g^+$ state with respect to optical transition to the ground $X^2\Pi_u$ state may be estimated, as regards its order of magnitude, by comparison with the lifetime of the $A^2\Pi$ state of the isoelectronic CO^+ molecule ion with respect to optical transition to its ground $X^2\Sigma^+$ state. The lifetime with respect to a given optical transition is

$$\tau = \frac{mc}{8\pi^2 \nu^2 f}$$

where m is the electron mass, c the velocity of light, ν the frequency of the transition, f its oscillator strength, and the energies of the transitions are 3.27 eV[23] for the (4 - 0) line of CO^+ ($A^2\Pi - X^2\Sigma^+$) and 4.96 eV[11] for $C_2H_2^+$($^2\Sigma_g^+ - x^2\Pi_u$). Then, assuming that the oscillator strengths of these two transitions are of an equal order

of magnitude, the ratio of the corresponding lifetimes would be

$$\frac{(C_2H_2^+ \ , \ ^2\Sigma_g^+)}{(CO^+ \ , \ A^2\Pi)} \approx \left[\frac{3.27}{4.96}\right]^2 = 0.4$$

where the lifetime of the ($A^2\Pi$, v = 4) state of CO^+ is known to be 2.6×10^{-6} s.[23] Thus, $\tau(C_2H_2^+, {}^2\Sigma_g^+) \approx 10^{-6}$s.

It must be stressed that the lifetime of the $^2\Sigma_g^+$ state may be shorter than the radiative lifetime if a predissociation (by spin-orbit coupling) through the $^4\Sigma_g^-$ state occurs.[13] Such a process would be responsible for the first appearance potential of C_2H^+ in the mass spectrum of acetylene as obtained by electron or photon impact, as discussed in the introduction; it could also be responsible for the occurrence of a "true metastable" transition, some evidence of which was given[24] although the importance of this process under usual conditions is negligible with respect to the collision-induced dissociation.

From the preceding discussion it appears possible that $C_2H_2^+$ ions formed in the $^2\Sigma_g$ state are responsible for the strong increase in the dissociation cross section at ionizing electron energies higher than 17.2 eV. This possibility will be further tested by studying the effect of the residence time of the ions in the ionization chamber on the dissociation cross section (see later, section 3.4).

Now, hypotheses (a), (b) and (c) will be discussed. Hypothesis (a) is unlikely since an electronic excitation of the ion, which would be mainly the effect of the electronic field of the induced dipole,[25] should be an optically allowed transition, whereas neither the $^2\Pi_u \longrightarrow {}^4\Pi_u$ transition, nor the transitions to the dissociative $^2\Pi_u$ states lying just above the $^4\Pi_u$ state (see Figure 1 of ref.[13]) are optically allowed.

In addition, the fact that the break on the curves of cross section vs electron energy appears somewhat higher from fragment ions produced with excess kinetic energy in the centre-of-mass system contradicts hypothesis (a) and supports hypothesis (c).

Indeed, for an electronic excitation from an attractive to a repulsive state (hypothesis (a)), the higher the excess energy above the dissociation threshold of the upper state, the lower the vibrational level of the initial state, according to Franck-Condon principle. This effect was actually observed in the case of H_2^+ dissociation by process (i).[6]

In contrast, for a predissociation (hypothesis (c)), the excess energy above the dissociation threshold must increase linearly (with a slope equal to 1) with the energy of the crossing point and, consequently, with the energy of the initial state; the possible values of this energy can

extend over a significant range in the case of polyatomic species, since their potential hypersurfaces cross along multidimensional curves.

It may be noticed that the ionizing electron energy corresponding to the break in our curves of cross section vs electron energy increases with the translational energy of the fragments in the centre-of-mass system, with a slope of about 6. This is not surprising on account of the preceding discussion, if we keep it in mind that in the dissociation of a tetraatomic molecule the translational energy of separation is the energy evolved on one degree of freedom out of the existing six for sharing the excess energy.

In the case of hypothesis (b), the kinetic energy of the fragments would probably be uncorrelated with the vibrational energy of the initial state.

The preceding discussion also applies to the three possible processes included in hypothesis (e), thus favouring process (iii).

Thus, to summarize the present section, it is concluded that the state at 17.2 eV, which is infered from our cross section vs electron energy curves, is a vibrationally excited level either of the $^2\Sigma_g^+$ state or of the ground $X^2\Pi_u$ state, and that the collision most probably gives rise to a predissociation of this state, or possibly to its adiabatic dissociation, but not to its electronic excitation to an

upper state.

The choice between the two possible states: $^2\Sigma_g^+$ or $X^2\Pi_u$ (vibrationally excited), will be deduced from the study of the effect of the delay between ionization and collision (Section 3.4). It was estimated that the lifetime of the $^2\Sigma_g^+$ state lay in the microsecond range, whereas the vibrational lifetimes are known to be much larger, at least in the millisecond range.

On the other hand, as regards the collision-induced dissociation of $C_2H_2^+$ ($X^2\Pi_u$) ions formed with energy between the threshold (11.4 eV) and 17.2 eV, it is not yet possible to decide whether the process involved is of type (i) or (ii); the observations of Section 3.1 only gave indications favouring a process of type (i).

3.3. Dependence on the translational energy of the incident ions

Figure 10-9 shows the ratio of the areas under the peaks registered at apparent mass 24 (process $C_2H_2^+ \longrightarrow C_2H^+ + H$) and mass 26 (parent $C_2H_2^+$) as a function of ionizing electron energy, for various initial translational energies V_o of $C_2H_2^+$ primaries. The target used was helium.

As already mentioned, the broadening of the C_2H^+ beam, which could result from the excess kinetic energy of

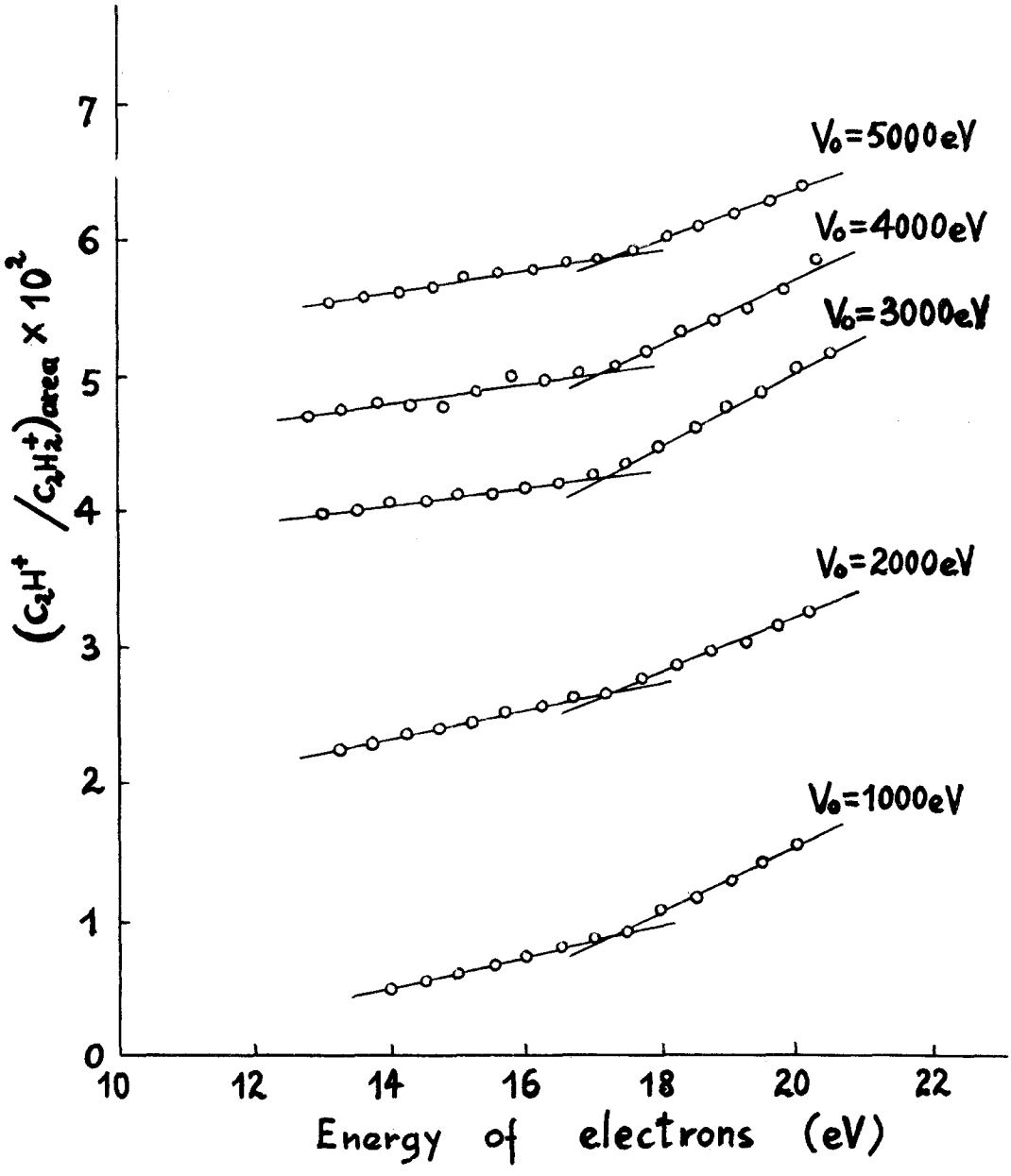

Figure 10-9. Ratio of the peak areas for $C_2H_2^+ \longrightarrow C_2H^+$ and for $C_2H_2^+$, as a function of electron energy, for various incident ion energies.

Target: helium.

fragments $C_2H^+ + H$, is small compared to the allowed angular aperture of the ion beam. On the other hand, the variation with ion energy of the apparatus bandwidth, and of the electron multiplier efficiency, are very similar for $C_2H_2^+$ ions and for collision-produced C_2H^+ fragments. Thus the ordinate of Figure 10-9 may be considered as a scale of relative cross sections.

It appears that the cross section strongly increases with increasing incident translational energy in the whole range studied, in agreement with the results of Kuprijanov and Perov.[10] From the discussion in the introduction, it may be concluded that the main process, which concerns $C_2H_2^+$ ions in the low vibrational levels of the electronic ground state, is an <u>electronic excitation</u>.

As regards the dissociation of the ions formed with an energy of about 17.2 eV above ground-state neutral C_2H_2, no definite conclusion can be drawn from Figure 10-9, since the way the cross section for the first process should be extrapolated over 17.2 eV is unknown. We could tentatively state that there is no strong variation of the cross section for the second process. However, since the technique used in the present study introduces a connection between the incident energy of the ions and their time of flight between formation and collision, the present discussion has to be delayed until the next Section, which is devoted to the study

of the effect of this time.

3.4. Dependence on the residence time of the primary ions in the ionization chamber

The residence time of the primary ions in the ionization chamber may be estimated from the ratio of the ion currents for secondary ions arising from ion-molecule reactions and for parent ions. At the same pressure in the ionization chamber (about 10^{-4} torr), the ratio of the ion currents at mass 51 ($C_4H_3^+$ ions) and mass 26 ($C_2H_2^+$ ions) was varied by a factor 2.5 to 4.0 by changing the operating conditions of the ion source: in the first case, we used a relatively high extraction field (16 V/cm); in the second case, a small negative field (-3 V/cm), favouring ion trapping by the space charge of the electron beam; the ionizing electron current was 20 μA. From the rate constant of the reaction

$$C_2H_2^+ + C_2H_2 \longrightarrow C_4H_3^+ + H \ ,$$

$k = 3.9 \times 10^{-10}$ cm^3 s^{-1},[26] the residence times of the primary ions in the ionization chamber under both operating conditions could be estimated.

Under each of these conditions, the ionization efficiency curve of helium was determined for calibration of the electron energy scale, which is affected by space charge effects.

The ion currents at each mass were measured for the same actual electron energy under both conditions.

Then the ion currents of collision-produced C_2H^+ ions and of parent $C_2H_2^+$ ions were both measured under the above mentioned conditions and at electron energies 16 and 20 eV in each case. The kinetic energy of the incident ions was V_o = 1000 volts; this low value was chosen since it appears from Figure 10-9 that the highest relative importance of the process with threshold at 17.2 eV is attained under such conditions. At higher ion energies, little effect of the residence time of the ions in the ionization chamber is to be expected; indeed, no measureable variation of the apparent cross section as a function of residence time was observed at incident ion energies of 4000 eV.

The results at incident energy of 1000 eV are given in Table 10-1 along with the estimated residence times of the ions in the ionization chamber.

It appears that the cross section for the first process observed at ionizing electron energies lower than 17 eV does not depend on the residence time, as expected, since this process concerns $C_2H_2^+$ ions in the ground electronic state and since the lifetime of these ions with respect to radiative vibrational deexcitation is comparatively very large.

On the contrary, the cross section at 20 eV is

Table 10-1. Effect of the residence time of the ions in the ionization chamber on the collision-induced dissociation cross section.
Incident translational energy V_o = 1000 eV. Target: helium.

Ionizing electron energy, eV	Estimated residence time, s	Ion current ratio C_2H^+ (coll.)/ $C_2H_2^+$
16	1.5×10^{-7}	$(3.0 \pm 0.7)\ 10^{-4}$
	6×10^{-7}	$(2.5 \pm 0.5)\ 10^{-4}$
20	4×10^{-7}	$(2.5 \pm 0.3)\ 10^{-3}$
	1×10^{-6}	$(2.0 \pm 0.6)\ 10^{-4}$

markedly reduced for the larger residence time. This result shows that the lifetime of the ions responsible for the second process (appearing at 17.2 eV) is of the order of magnitude of 10^{-7} s. From the discussion in the introduction and in Section 3.2 of the present part, this is a strong evidence for the identification of the metastable state to the $^2\Sigma_g^+$ state of $C_2H_2^+$.

The predissociation of this state can be induced by collision if a selection rule is broken; in particular, the

transition one $^2\Sigma_g^-$ state (see Figure 10-8) will be possible since the symmetry with respect to a plane is broken by the relative motion of the ion + target system.

Another possibility, as stated earlier, is the dissociation of the $^2\Sigma_g^+$ state by an adiabatic transition produced by the collision.

Now, it is clear that the amount of $^2\Sigma_g^+$ ions which enter the collision chamber before deexcitation is strongly reduced when their time of flight is increased, which occurs in particular when the acceleration high tension is reduced, everything else being constant. Inspection of Figure 10-9 and Table 10-1 then shows that the cross section for the collision-induced dissociation process occurring above 17.2 eV actually decreases when the ion energy increases. This dependence of the cross section on the incident ion energy is in agreement with either hypotheses: collision-induced predissociation (needing no excitation) or collision-induced adiabatic dissociation.

3.5. Absolute laboratory translational energy of collision-produced C_2H^+ ions

As mentioned in the introduction, when the collision induces an excitation of the molecule ions prior to their dissociation, or when the target atoms themselves are

excited by the collision, the excitation energy $\underline{E^*}$ is taken from the translational energy $\underline{V_o}$ of the incident ions. Thus, on the apparent mass scale, the peak of the collision produced C_2H^+ will be displaced by an amount E^*/V_o from its theoretical position at zero $\underline{E^*}$. This displacement was determined by measuring with a differential gaussmeter the variation of the magnetic field necessary for focussing either primary C_2^+ ions (mass 24.00) or collision-produced C_2H^+ ions (apparent mass $24.04\ (1 - E^*/V_o)$).

Since the position of the C_2^+ peak could be determined only at an electron energy higher than its appearance potential, it was checked in separate runs that the variation of the energy of the ionizing electrons had no noticeable effect on the position of the $C_2H_2^+$ peak, observed as reference; such an effect could have arisen from a variation - due to space charge - of the potential in the ionization chamber.

The value of E* thus obtained, with helium as a target gas, is shown in Figure 10-10 as a function of ionizing electron energy (lower curve). The range of E* obtained (4 to 6 eV) shows that no excitation of the target atoms takes place.

On the other hand, a simple calculation shows that the recoil energy of the target due to momentum conservation is perfectly negligible. Thus the measured E* is the energy

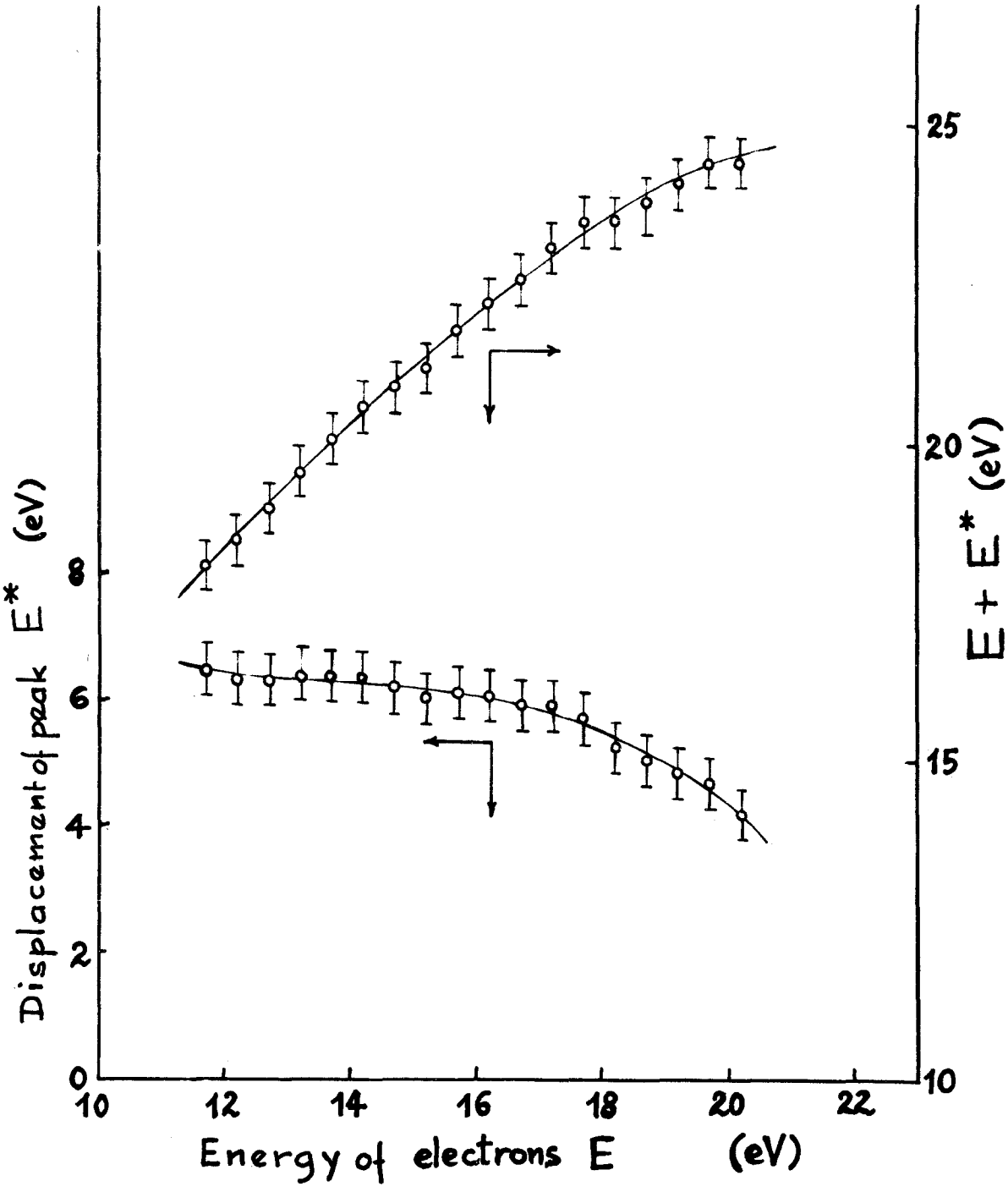

Figure 10-10. Lower curve: energy loss E* experienced by primary $C_2H_2^+$ ions during collisions leading to dissociation into C_2H^+ + H, as a function of electron energy E.
Upper curve: E + E* as a function of E.
Incident ion energy: 3000 eV, target: helium.

required for excitation of the $C_2H_2^+$ ions to their dissociative upper level.

It is now possible to determine the energy of this upper state, which occurs as intermediate during the collision-induced dissociation of ground-state $C_2H_2^+$ ions in low vibrational levels. Indeed, this energy is equal to the sum of the initial vibronic energy $\underline{E_o}$ of the ions and the excitation energy E*. An upper limit of $\underline{E_o}$ is the ionizing electron energy $\underline{E}$ ($\underline{E_o}$ being counted from the energy of ground-state C_2H_2 molecules). Further, when $\underline{E}$ tends towards the ionization threshold of acetylene, 11.4 eV, $\underline{E_o}$ tends towards $\underline{E}$.

The upper curve of Figure 10-10 represents $\underline{E}$ + $\underline{E}$* as a function of $\underline{E}$; extrapolation to $\underline{E}$ = 11.4 eV yields the energy of the upper state attained in the collision-induced dissociation of ground-state $C_2H_2^+$ ions:

$$E_o + E^* = 17.3 \pm 0.5 \text{ eV}$$

This value is consistent with both hypotheses: electronic excitation of these ions to an upper electronic state, or momentum transfer leading to $C_2H_2^+$ ions in the vibrational continuum of ground electronic state (adiabatic dissociation). We excluded the latter possibility from the results of Section 3.3, which will be confirmed by further evidence (see Chapter 11, process $C_2H_2^+ \longrightarrow H^+ + C_2H$).

It is concluded from these results that $C_2H_2^+$ ground-state ions are excited by collision with helium atoms to a state the energy of which, for an internuclear distance equal to the equilibrium internuclear distance of ground-state ions, is 17.3 ± 0.5 eV.

This upper state must either have a dissociation limit lower than or equal to 17.3 eV, or be predissociated. It cannot be the $^2\Sigma_u^+$ state, which lies too high and, in addition, could not be reached from the $X^2\Pi_u$ state by an allowed transition.

It can be the $^2\Sigma_g^+$ state, if this state is predissociated through the $^4\Sigma_g^-$ state, as discussed in Section 3.2.

It can also be one of the states of the configuration

$$(1\sigma_g)^2\ (1\sigma_u)^2\ (2\sigma_g)^2\ (2\sigma_u)^2\ (3\sigma_g)^2\ (1\pi_u)^2\ (3\ s\ 4\sigma_g)$$

such as the $^2\Delta_g$ state which is represented in Figure 10-8, or else the $^2\Phi_g$ or one of the $^2\Pi_g$ states of the configuration

$$(1\sigma_g)^2\ (1\sigma_u)^2\ (2\sigma_g)^2\ (2\sigma_u)^2\ (3\sigma_g)^2\ (1\pi_u)^2\ (1\pi_g)^1.$$

Both these configurations are easily attained from ground state

$$(1\sigma_g)^2\ (1\sigma_u)^2\ (2\sigma_g)^2\ (2\sigma_u)^2\ (3\sigma_g)^2\ (1\pi_u)^3,\ X^2\Pi_u$$

by an optically allowed, one-electron, transition. From

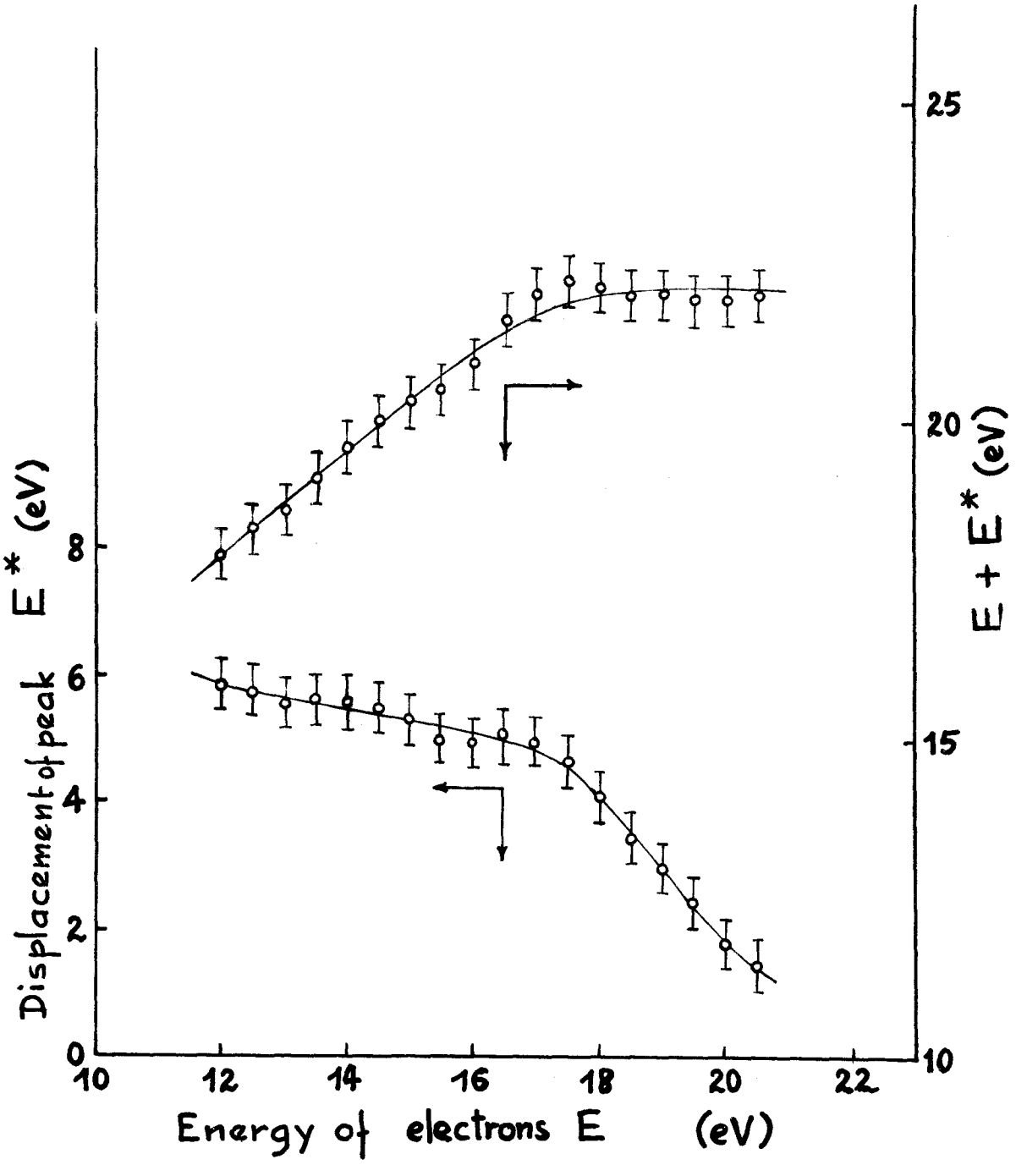

Figure 10-11. Lower curve: energy loss E* experienced by primary $C_2H_2^+$ ions during collisions leading to dissociation into $C_2H^+ + H$, as a function of electron energy E. Upper curve: E + E* as a function of E. Incident ion energy: 3000 eV, target: xenon.

known orbital energies, this $^2\Phi_g$ or $^2\Pi_g$ state is likely to lie in the vicinity of 18 eV.

From simple considerations, it can be found that the $^2\Phi_g$ state is predissociated by the $^2\Delta_g$ state (dissociating into C_2H^+ ($^1\Delta_g$) + H(^{2}S)), and the $^2\Pi_g$ state by the $^2\Delta_g$ state and by the $^2\Sigma_g^-$ state (dissociating into C_2H^+ ($^3\Sigma_g^-$) + H(^{2}S)), according to the rules recalled by Fiquet-Fayard.[13]

In fact, the dissociation of this $^2\Pi_g$ or $^2\Phi_g$ state may be shown to be much more rapid and efficient than through a predissociation, if it is taken into account that, for most substates of these states, the linear geometry is not the stable one, as discussed earlier.

Using xenon as a target, curves similar to those of Figure 10-10 were obtained (Figure 10-11). They lead to an energy of the upper state

$$E_o + E^* = 17.4 \pm 0.5 \text{ eV},$$

in agreement with the results obtained with helium as a target.

4. Conclusions

Two processes were discriminated for the collision-induced dissociation of $C_2H_2^+$ ions into C_2H^+ + H:

- a) electronic excitation of any vibrational level of the $X^2\Pi_u$ ground state, leading to an upper state, dissociative or predissociated, lying at 17.3 ± 0.5 eV; this state is proposed to be either the first $^2\Sigma_g^+$ state or the first $^2\Delta_g$ or the first $^2\Phi_g$ or $^2\Pi_g$ state of $C_2H_2^+$;

- b) dissociation - most probably by collision-induced predissociation or else by adiabatic momentum transfer - of vibrationally excited levels, lying between 17.2 and 17.8 eV, of the first $^2\Sigma_g^+$ state of $C_2H_2^+$; in the case of a collision-induced predissociation, the fragments $C_2H^+(^3\Sigma_g^-)$ + $H(^2S)$ would be obtained through the $^2\Sigma_g^-$ state of $C_2H_2^+$, or the fragments C_2H^+ ($^1\Delta_g$) + H (^2S) through the $^2\Delta_g$ state of $C_2H_2^+$.

References

1) R. Caudano, J. M. Delfosse, and J. Steyaert, Ann. Soc. Sci. Bruxelles, 76, 127 (1962); R. Caudano and J. M. Delfosse, Vth Intern. Conf. Phys. Electron. At. Coll., Leningrad, Abstr. Pap. 590 (1967); J. Phys. B (Proc. Phys. Soc.) 2, 813 (1968).

2) F. P. G. Valckx and P. Verveer, J. Physique, 27, 480 (1966).

3) D. G. Gibson and J. Los, Physica, 35, 258 (1967); D. G. Gibson, J. Los, and J. Schopman, Phys. Lett., 25A, 634 (1967); Vth Intern. Conf. Phys. Electron. At. Coll., Leningrad, Abstr. Pap. 594 (1967); Physica, 40, 385 (1968).

4) M. Vogler and W. Seibt, Z. Phys., 210, 337 (1968).

5) A. Valance, Thèse de Doctorat de Spécialité, Paris (1968).

6) J. Durup, P. Fournier, and Pham D., Intern. J. Mass Spectrom. Ion Phys., 2, 311 (1969).

7) J. B. Hasted, Physics of Atomic Collisions, Butterworths, London, 1964, chap. 12.

8) A. Henglein, Z. Naturf., 7a, 165 (1952).

9) C. E. Melton, M. M. Bretscher, and R. Baldock, J. Chem. Phys., 26, 1302 (1957).

10) S. E. Kuprijanov and A. A. Perov, Zh. Fiz. Khim., 42, 857 (1968) [Russ. J. Phys. Chem. 447 (1968)].

11) (a) M. I. Al-Joboury, D. P. May, and D. W. Turner, J. Chem. Soc., 616 (1965).
(b) C. Baker and D. W. Turner, Proc. Roy. Soc. A308, 19 (1968).

12) R. Botter, V. H. Dibeler, J. A. Walker, and H. M. Rosenstock, J. Chem. Phys., 44, 1271 (1966).

13) F. Fiquet-Fayard, J. Chim. Phys., 64, 320 (1967).

14) R. S. Mulliken, Can. J. Chem., 36, 10 (1958).

15) J. T. Tate, P. T. Smith, and A. C. Vaughan, Phys. Rev., 48, 525 (1935).

16) Pham D., Thèse de Doctorat, Paris (1965).

17) E. Lindholm, I. Szabo, and P. Wilmenius, Ark. Fys., 25, 417 (1963); see also E. Lindholm, Private communication quoted in ref. (18).

18) V. Čermak, J. Chem. Phys., 44, 3781 (1966).

19) P. M. Guyon and F. Fiquet-Fayard, J. Chim. Phys. 66, 32 (1969).

20) W. B. Maier, J. Chem. Phys. 42, 1790 (1965).

21) A. J. C. Nicholson, J. Chem. Phys., 43, 1171 (1965).

22) V. I. Vedeneev, L. V. Gurvich, V. N. Kondrat'yev, V. A. Medvedev, and Ye. L. Frankevich , "Bond Energies, Ionization Potentials and Electron Affinities" (English translation), Edward Arnold, London, 1966, Table 2.

23) J. Desesquelles, M. Dufay, and M. C. Poulizac, Phys. Lett., 27A, 96 (1968).

24) J. G. Larson and A. B. King, quoted in ref. (12).

25) J. Durup, 14th Annual Meeting on Mass Spectrom., Dallas, Texas, 1966, p. 190.

26) F. H. Field, J. L. Franklin, and F. W. Lampe, J. Am. Chem. Soc., 79, 2665 (1957).

Chapter 11

Collision-induced Dissociation of Acetylene Ions.

Part II. Process $C_2H_2^+ \longrightarrow H^+ + (C_2H)$

1. Introduction

In the preceding Chapter, the energetics of the collision-induced dissociation of fast $C_2H_2^+$ ions into $C_2H^+ + H$ was determined from the measurements of the translational energy of the fragments and from the study of the influence of ionizing electron energy, incident ion energy, delay between production of the ions and collision, and nature of the target used.

For purposes of comparing the dissociation mode of H^+ formation with that of the secondary C_2H^+ ions, the present study deals with the dissociation process of acetylene ions into $H^+ + (C_2H)$ on collision with helium by the same line of investigation mentioned in the proceding Chapter.

The successive appearance potentials of H^+ ions from acetylene were determined by Tate et al.[1] as

21.7 ± 1.0 eV and 25.6 ± 1.0 eV, and by Pham[2] as 20.1 ± 0.1 eV, 24.35 ± 0.2 eV, 26.8 ± 0.2 eV, and 30.9 ± 0.3 eV.

2. Results and Discussion

The observation of the process $C_2H_2^+ \longrightarrow H^+ + (C_2H)$ is difficult for two reasons related to the relatively small energy of the secondary H^+ ions ($V_o/26$, here 150 to 200 eV). Firstly, an extremely small magnet current has to be used for focussing these ions of "apparent mass" 0.04. Secondly, the H^+ beam intensity is drastically reduced by elastic scattering.

When xenon is used as a target gas, the scattering is so effecient that the signal is lost in the noise; direct experiments with H^+ ions produced in the ionization chamber and accelerated by a tension equal to 155 V showed that the ion beam intensity was reduced to 10 % by about 10^{-3} torr of xenon in the collision chamber, as shown in Figure 11-1.

Therefore, strong enough signals were obtained only at relatively high ion energies (4000 to 5000 eV) and using helium as a target gas. Higher energies could not be used owing to lack of insulation at very high tensions.

A registration of H^+ ions produced by $C_2H_2^+$-on-He

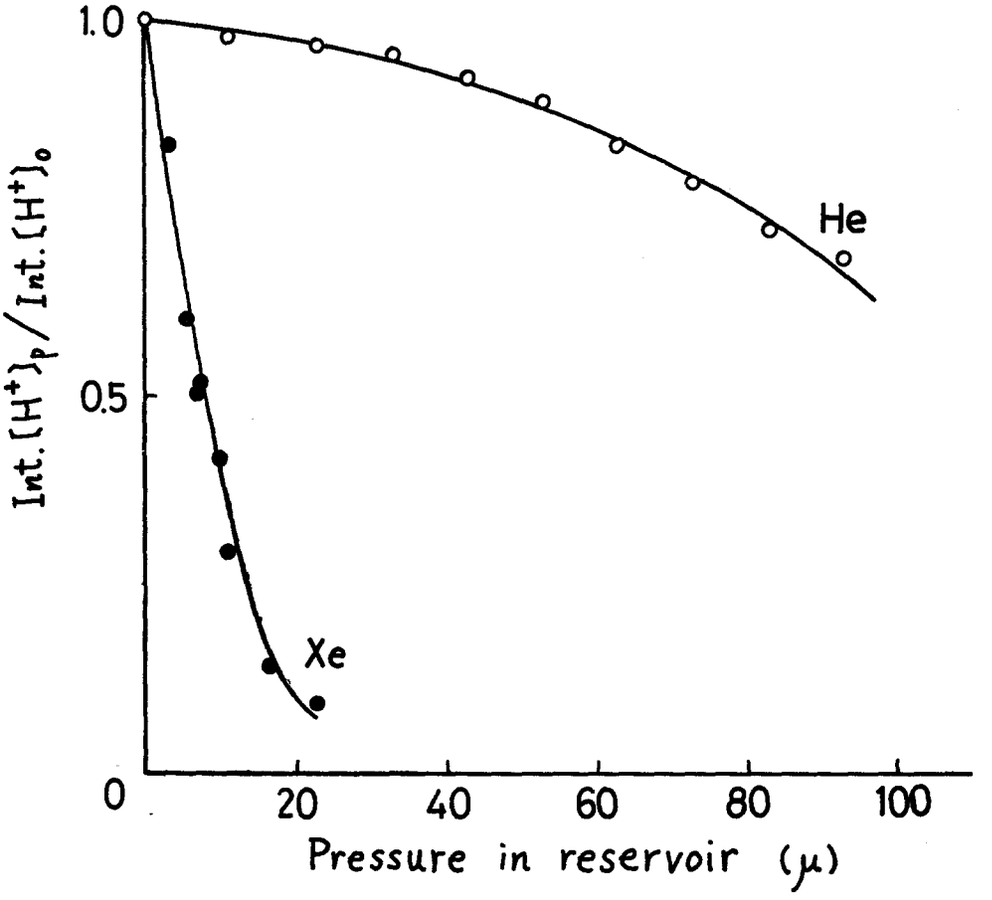

Figure 11-1. Pressure dependence of scattering effect of H^+ ions by target gases.
Incident ion energy: 155 eV, electron energy: 25 eV, target: helium or xenon.

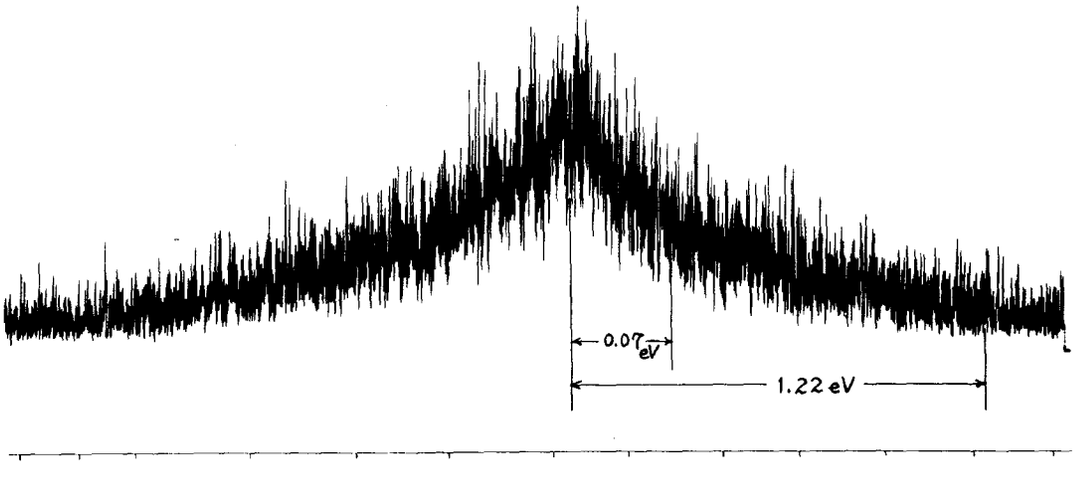

Figure 11-2. Registration of the $C_2H_2^+ \longrightarrow H^+$ peak.
Ion incident energy: 4000 eV, electron energy: 25 eV, target: helium, abscissa: magnet field (Gauss).

collisions is shown in Figure 11-2. The total translational energy of the fragments in the centre-of-mass system at half-height of the peak is 0.07 eV, and the maximum total translational energy in the centre-of-mass system, measured at the bottom of the peak, is about 1.2 eV.

The appearance curve of the collision-produced H^+ ions (Figure 11-3, upper curve) leads to an appearance potential of about 12.6 eV. The ratio of the heights of the collision-produced H^+ peak to the parent $C_2H_2^+$ peak (Figure 11-3, lower curve) smoothly increases with electron energy, indicating on the one hand that H^+ fragments probably appear at the ionization threshold (11.4 eV)[3] and, on the other hand, that the cross section for collision-induced dissociation into $H^+ + (C_2H)$ increases with an increasing vibrational energy of the incident $C_2H_2^+$ ions.

The most interesting feature is the effect of incident ion translational energy. Table 11-1 shows, at two ionizing electron energies, the effect of increasing the ion energy from 4000 to 5000 eV. The ratio of the areas of the secondary H^+ peak to parent $C_2H_2^+$ peak is found to <u>decrease</u>, at both electron energies, with increasing ion energy, in contrast with the behaviour observed for the dissociation into $C_2H^+ + H$ (cf. Section 3.3 in Chapter 10).

It must be stressed that the decrease of the cross section with increasing ion energy is still stronger than

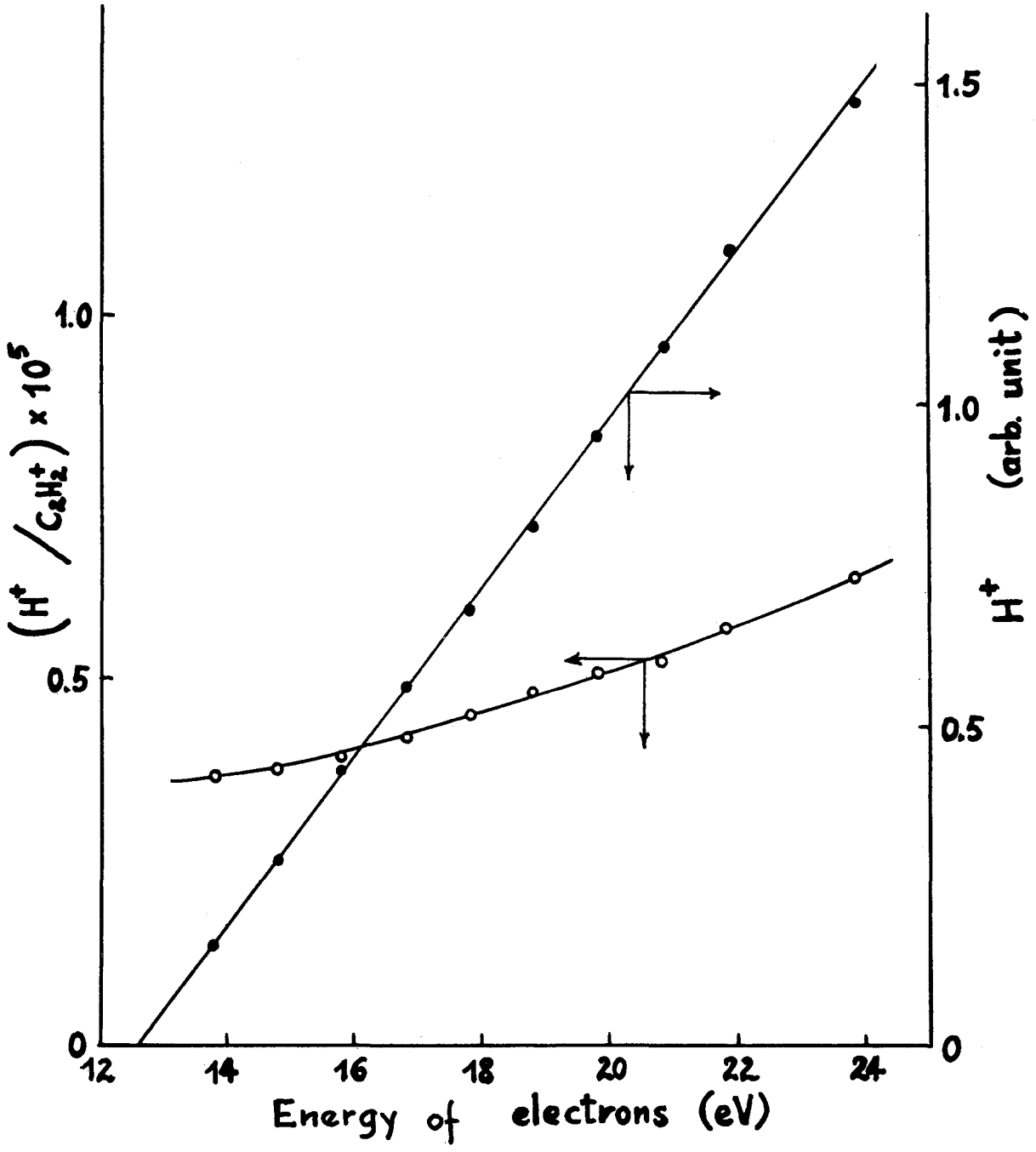

Figure 11-3. Upper curve: appearance curve of the $C_2H_2^+ \longrightarrow H^+$ peak. Lower curve: ratio of peak heights for $C_2H_2^+ \longrightarrow H^+$ and for $C_2H_2^+$, as a function of electron energy.

Ion incident energy: 5000 eV, target: helium.

Table 11-1. Process $C_2H_2^+ \xrightarrow{He} H^+ + (C_2H)$

Ionizing electron energy (eV)	Ratio of peak areas H^+ (coll.)/$C_2H_2^+$	
	V_o = 4000 eV	V_o = 5000 eV
16.5	2.6×10^{-5}	1.7×10^{-5}
19.5	3.8×10^{-5}	2.9×10^{-5}

indicated by the ratio given in Table 11-1. For, firstly the scattering of the secondary H^+ beam is much stronger at lower ion velocity. Secondly, the collimation of the beam gives rise to a discrimination which is very effective for secondary H^+ ions, part of which are formed with large excess kinetic energy, whereas it is much less effective for parent $C_2H_2^+$ ions, which are formed with only thermal velocities; this discrimination against high excess velocities transverse to the flight direction increases with decreasing ion velocity. On the contrary, as regards the effect of incident ion energy on the efficiency of the first dynode of the electron multiplier, an opposite tendency to previous effects may be expected: the negative

high tension of the multiplier being 2800 eV, the velocity of H^+ secondaries will vary from 7.69 to 7.74×10^7 cm s^{-1}, when V_o varies from 4000 to 5000 eV, whereas under the same conditions the velocity of $C_2H_2^+$ parent ions will vary from 2.29 to 2.45×10^7 cm s^{-1}; taking into account a threshold velocity equal to 5.5×10^6 cm s^{-1},[4] the ratio of the efficiencies of the electron multiplier for secondary H^+ to parent $C_2H_2^+$ will decrease by a factor 0.93 in the range V_o = 4000 to 5000 eV. This is quite unimportant compared to the variation given by Table 11-1.

Thus there is certainly a decrease, and probably a strong decrease, in the cross section for H^+ production by $C_2H_2^+$-on-He collisions when the ion energy increases in the range of 4000 to 5000 eV. This is indicative, either of an adiabatic dissociation process (ii), see introduction of Chapter 10, or of an electronic transition requiring only a very small energy. Since the same effect is observed at electron energies 16.5 and 19.5 eV, (see Table 11-1) and since the energetic threshold for production of $C_2H + H^+$ is equal to $D(C_2H\text{-}H) + I.P.(H) = 4.9 \pm 0.4$ eV[5] + 13.6 eV = 18.5 ± 0.4 eV, it is clear that the hypothesis of an electronic excitation has to be rejected.

It is concluded from these results that the collision-induced dissociation of $C_2H_2^+$ ions into $H^+ + (C_2H)$ is an

adiabatic process, viz. a momentum transfer from the proton to the target atom, leading to dissociation of electronically ground-state $C_2H_2^+$ ions.

This means that the $X^2\Pi_u$ ground state of $C_2H_2^+$ is adiabatically correlated with $H^+ + C_2H$ ($X^2\Pi_u$) rather than C_2H^+ ($^3\Pi_u$) + H (^2S) as represented in Figure 1 of Fiquet-Fayard's paper.[6] This provides an explanation of why the dissociation of ground-state $C_2H_2^+$ ions into C_2H^+ + H is necessarily an electronic transition and not an adiabatic process (see Chapter 10).

A consequence of this statement is that the energy of $C_2H^+(^3\Pi_u)$ + $H(^2S)$ is higher than that of C_2H ($X^2\Pi_u$) + H^+, and thus that the energy of the $^3\Pi_u$ state of C_2H^+ above its $^3\Sigma_g^-$ ground-state is more than I.P.(H) - I.P.(C_2H) = 13.6 - (11.25 ± 0.15) = 2.35 ± 0.15 eV.

References

1) J. T. Tate, P. T. Smith, and A. C. Vaughan, Phys. Rev., 48, 525 (1935).

2) Pham D., Thèse de Doctorat, Paris (1965).

3) A. J. C. Nicholson, J. Chem. Phys., 43, 1171 (1965).

4) B. L. Schram, A. J. H. Boerboom, W. Kleine, and J. Kistemaker, Proc. 7th Intern. Conf. Phenom. Ionized Gases, Beograd, 1966, Vol. 1, p. 170.

5) V. I. Vedeneev, L. V. Gurvich, V. N. Kondrat'yev, V. A. Medvedev, and Ye. L. Frankevich, "Bond Energies, Ionization Potentials and Electron Affinities" (English Translation), Edward Arnold, London, 1966, Table 2.

6) F. Fiquet-Fayard, J. Chim. Phys., 64, 320 (1967).

Chapter 12

Collision-induced Dissociation of Acetylene Ions. Part III. Processes $C_2H_2^+ \longrightarrow C_2^+$, CH_2^+, CH^+, and C^+

1. Introduction

The fragment ions to be produced through collision-induced dissociation processes of acetylene molecule ions ($C_2H_2^+$) are those given in the following schemes:

$$C_2H_2^+ \xrightarrow{M} \begin{cases} C_2H^+ + H \\ C_2^+ + (2H) \\ CH_2^+ + C \\ CH^+ + (CH) \\ C^+ + (CH_2) \end{cases}$$

Among them, the dissociation processes producing C_2H^+ and H^+ fragment ions were already mentioned in the proceding Chapters.

The present study is concerned with four other processes to produce C_2^+, CH_2^+, CH^+, and C^+ fragment ions. In order to investigate these dissociation processes, it would be

very desirable to have detailed knowledge of the potential energy surfaces of these systems as in the case of C_2H^+ formation, since it would permit a more definitive interpretation of the experimental results. Unfortunately no available information on these surfaces has been reported so far. Therefore, it is the purpose of this Chapter to show the results obtained by the variation of experimental parameters and to explain qualitatively some features of these dissociation processes.

Melton et al.[1] first observed the collision-induced dissociation processes of $C_2H_2^+$ ions into CH_2^+, CH^+, and C^+ fragments. Recently, Kuprijanov and Perov[2] reported the results of an investigation of the dissociation processes of $C_2H_2^+$ ions into C_2^+, CH^+, and C^+ fragments on collision with xenon atoms.

The appearance potentials of C_2^+, CH^+, and C^+ fragments from acetylene were determined by several researchers as follows,

C_2^+; 18.85 ± 0.15 eV,[3] 23.3 ± 0.5 eV,[4] 23.8 ± 0.3 eV,[5] and 23.6 eV,[6]

CH^+; 20.7 ± 0.2 eV,[3] 22.2 ± 0.5,[5] and 23.1 eV,[6]

C^+ ; 24.5 ± 1.0,[5,7] and 24.3 eV.[6]

2. Results and Discussion

2.1. Process $C_2H_2^+ \longrightarrow C_2^+ + (2H)$

From the equations (2) and (3) in Chapter 10, the apparent mass of C_2^+ ions produced in the collision chamber is expected to be $m^* = 22.15$, if $\underline{E}^*$ and $\underline{W}$ are equal to zero. A typical example of collision-induced peak of C_2^+ ions at ionizing electron energy of 20 eV is shown in the upper part of Figure 12-1, where the magnetic field was scanned in the vicinity of mass 22. On the other hand, when a target gas does not exist in the collision chamber, no peak is observed, as seen in the lower part of Figure 12-1 where the same magnetic field range was scanned.

Figure 12-2 shows the appearance curves of the collision-induced dissociation peak of C_2^+ ions and the acetylene molecule ions. The appearance potential of C_2^+ fragments lies between 11.5 and 12 eV, close to the appearance potential of acetylene molecule ions (11.40[8]). This indicates that ground-state $C_2H_2^+$ ions can participate in the production of C_2^+ fragments induced by collision with target atoms.

Relative cross sections for the production of C_2^+ fragments (for $W = 0$) are shown in Figure 12-3 as a function of ionizing electron energy. It appears that the

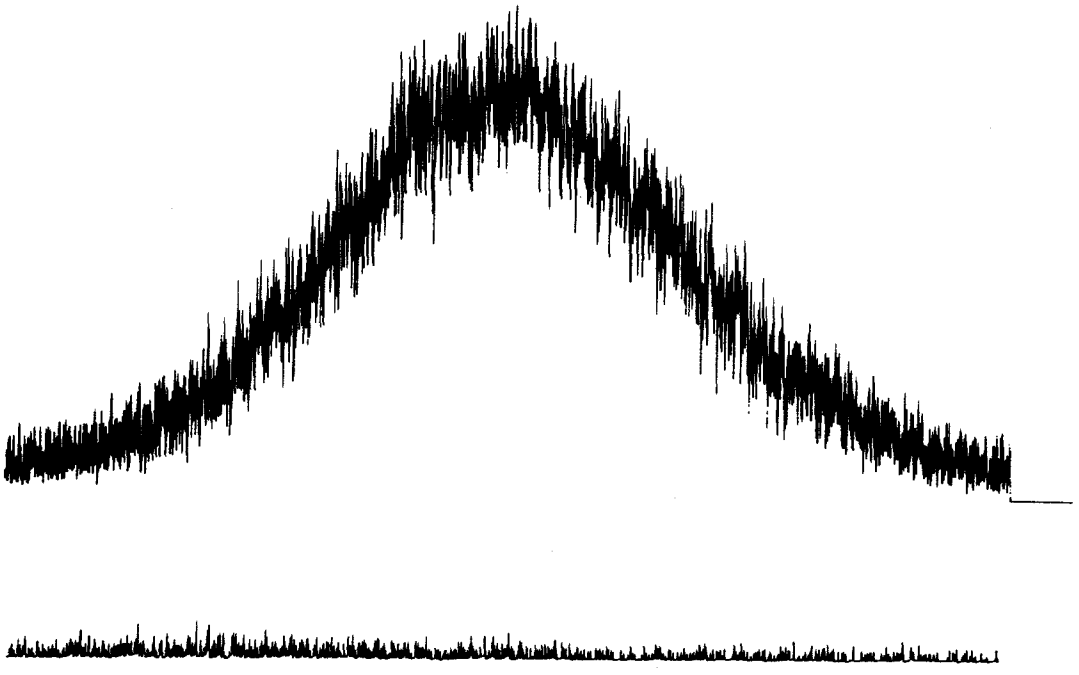

Figure 12-1. Registration of the $C_2H_2^+ \longrightarrow C_2^+$ peak.
Ion incident energy: 3000 eV, electron energy:
20 eV, abscissa: magnet field (Gauss).
Upper curve: target helium,
Lower curve: target absent.

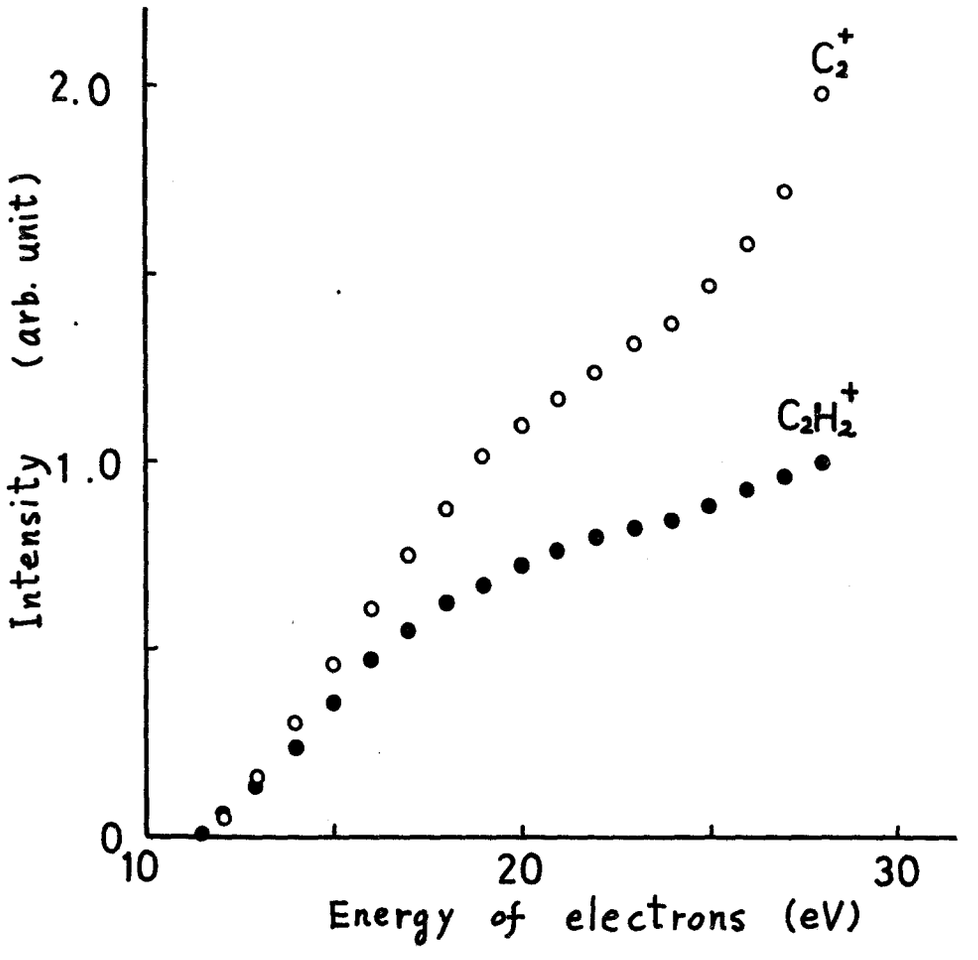

Figure 12-2. Appearance curves of the $C_2H_2^+$ peak and the $C_2H_2^+ \longrightarrow C_2H^+$ peak.
Ion incident energy: 3000 eV,
target: helium.

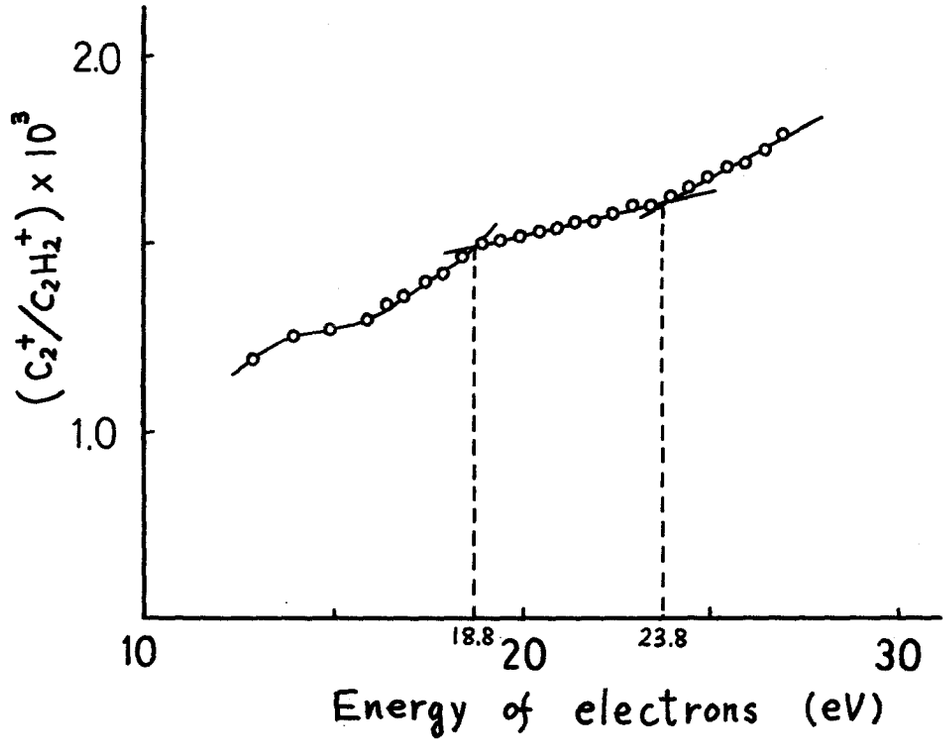

Figure 12-3. Ratio of peak heights for $C_2H_2^+ \longrightarrow C_2H^+$ and for $C_2H_2^+$ as a function of electron energy.

Incident ion energy: 3000 eV,

target: helium.

cross sections increase with increasing electron energy in the whole range studied. Further, the rate of the increase of the cross section with electron energy changes at about 19 and 24 eV. These inflection points closely agree with first and second appearence potentials of C_2^+ ions from acetylene which are 18.85[3] and 23.8 eV,[5] respectively.

Similar results were obtained with xenon as a target. However, the efficiency of the collision-induced dissociation, which was calculated on the same assumptions mentioned in section 3.1. of Chapter 10, is much lower for xenon than for helium as shown in Table 12-1.

The dependence of initial translational energy V_o of $C_2H_2^+$ primaries on the relative cross section of C_2^+ fragments is summarized in Table 12-2. For three different electron energies, the relative cross section increases remarkably with increasing incident translational energy, in agreement with the results of Kuprijanov and Perov.[2]

From the effect of target gas and the dependence of initial translational energy, it can be tentatively concluded that the main process of producing C_2^+ fragments by collision, which concerns ground-state $C_2H_2^+$ ions, is an electronic excitation.

It is not yet clear as to why the relative cross section of collision-induced C_2^+ ions shows the inflection

Table 12-1. Process $C_2H_2^+ \xrightarrow{M} C_2^+ + (2H)$

Ionizing electron energy (eV)	Ion current ratio $(C_2^+(coll.) / C_2H_2^+) / \sqrt{M}$	
	He	Xe
15	3.52×10^{-4}	0.35×10^{-4}
20	4.18×10^{-4}	0.58×10^{-4}
25	4.58×10^{-4}	0.73×10^{-4}

Table 12-2. Dependence of initial translational energy Vo of $C_2H_2^+$ primaries on the collision-induced dissociation cross section of C_2^+ fragments.
target : helium

Ionizing electron energy (eV)	Ratio of peak areas $C_2^+(coll.) / C_2H_2^+$		
	Vo = 1000eV	Vo = 3000eV	Vo = 5000eV
15	0.08×10^{-2}	0.77×10^{-2}	1.16×10^{-2}
20	0.17×10^{-2}	0.89×10^{-2}	1.33×10^{-2}
25	0.23×10^{-2}	1.03×10^{-2}	1.55×10^{-2}

points at the electron energies corresponding to the first and the second appearance potentials of C_2^+ ions from acetylene. More detailed studies on the effects of residence time of $C_2H_2^+$ primaries in the ionization chamber, of pressure in the collision chamber, and the displacement of dissociation peaks with the variation of ionizing electron energy will be needed before any definite conclusion can be drawn regarding the formation process of C_2^+ fragments.

2.2. Processes $C_2H_2^+ \longrightarrow CH_2^+$, CH^+, and C^+

Mass spectra of the present system in lower mass region between 5.5 and 7.6 are shown in Figure 12-4, using helium as a target gas. As seen in the upper spectrum of the Figure, six peaks corresponding to the following dissociation processes are observed at ionizing electron energy of 35 eV:

	Apparent mass	
$C_2H_2^+ \longrightarrow C^+$	5.54	(a)
$C_2H^+ \longrightarrow C^+$	5.76	(b)
$C_2^+ \longrightarrow C^+$	6.00	(c)
$C_2H_2^+ \longrightarrow CH^+$	6.50	(d)
$C_2H^+ \longrightarrow CH^+$	6.76	(e)
$C_2H_2^+ \longrightarrow CH_2^+$	7.56	(f)

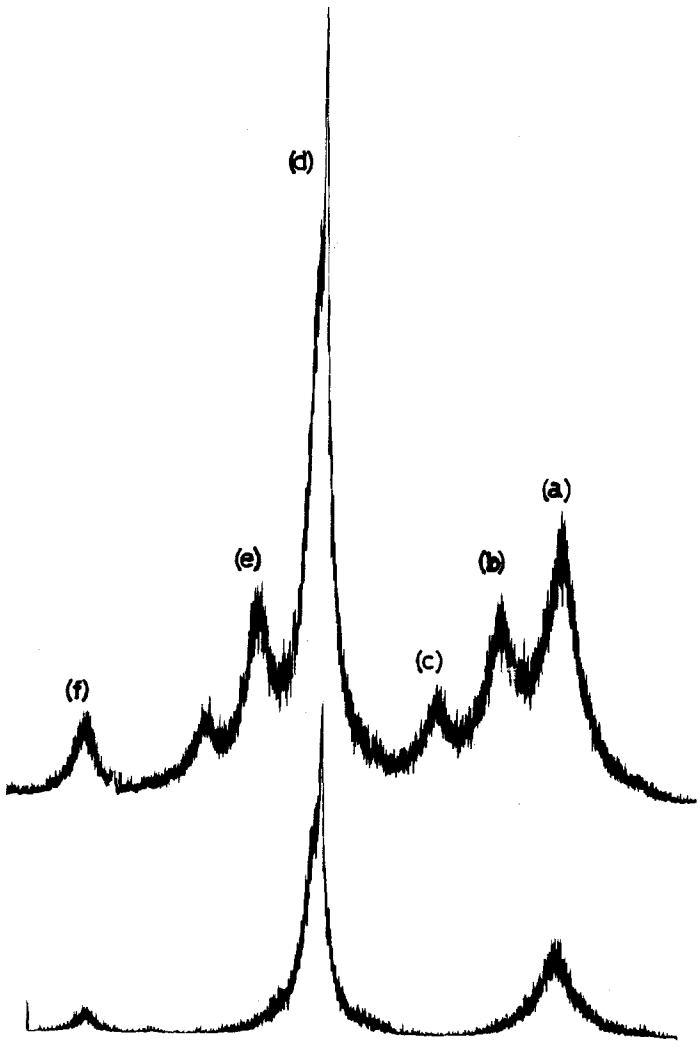

Figure 12-4. Registration of the $C_2H_2^+ \longrightarrow CH_2^+$, CH^+, and C^+ peaks.

Ion incident energy: 5000 eV, target: helium, abscissa: magnet field (Gauss).

Upper curve: electron energy 35 eV,

Lower curve: electron energy 16 eV.

In this spectrum, the small peak which lies between the peaks (e) and (f) is that of a doubly charged nitrogen atom (mass 7.00) as a standard. At ionizing electron energy of 16 eV, only three peaks produced from $C_2H_2^+$ primaries are found as shown in the lower spectrum of the Figure, because the primary ions of C_2H^+ and C_2^+ are not produced at this electron energy.

The appearance curves of these collision-induced fragments are shown in Figure 12-5. The appearance potentials of CH_2^+, CH^+, and C^+ fragments are found to be about 13.0, 11.8, and 12.2 eV, respectively. As seen in Figure 12-6, the ratios of the heights of these collision-induced peaks to the parent $C_2H_2^+$ peak increase gradually with increasing electron energy.

The results obtained with xenon as a target gas are similar to those with helium. However, the relative cross sections with xenon are considerably smaller than those obtained with helium in the whole electron energy range studied, as summarized in Table 12-3. This result seems to indicate that these dissociation processes induced by collision also take place predominantly through an electronic excitation. Although further discussion about these processes is impossible because of the limited quantity of available data, it should be pointed out that the ratio of the cross section for C^+ or CH_2^+ formation to

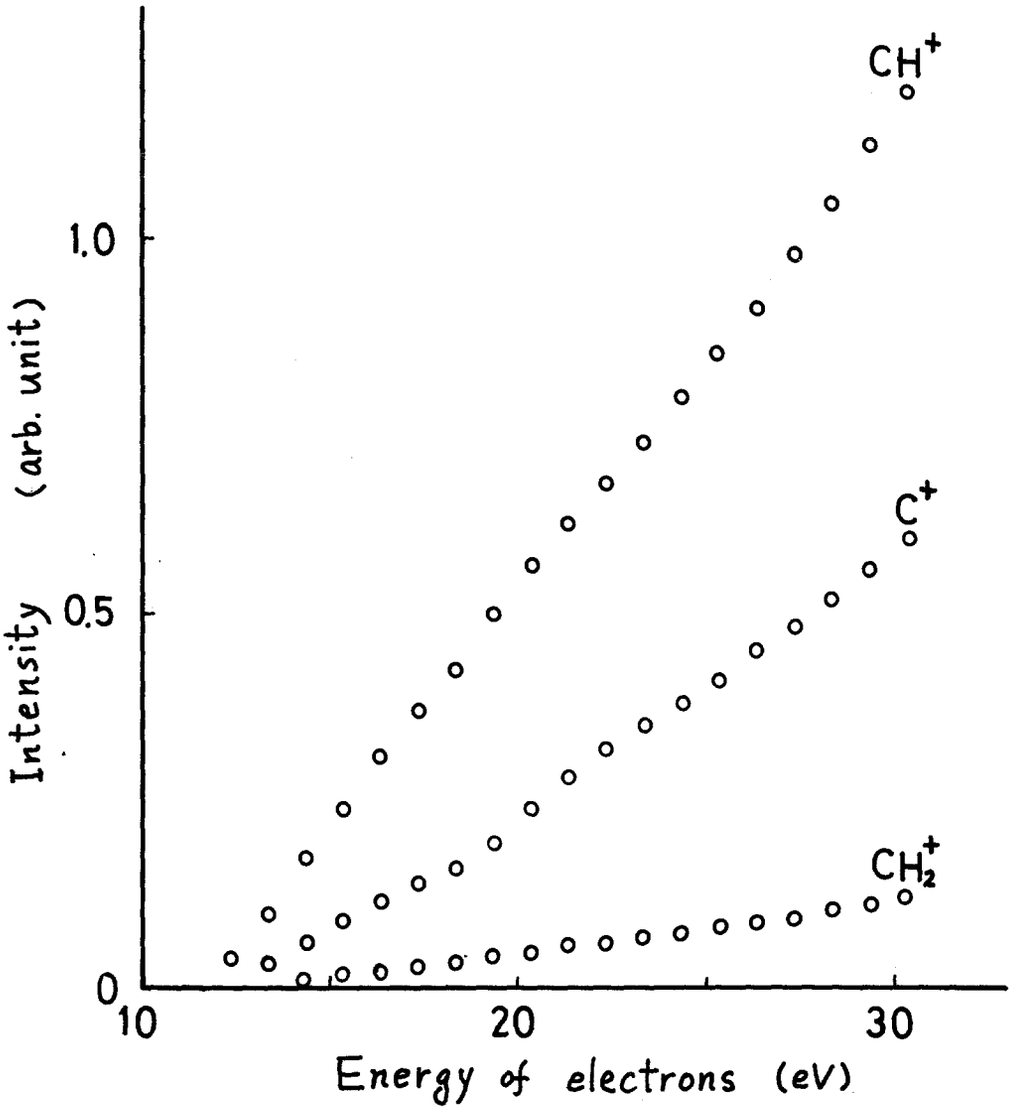

Figure 12-5. Appearance curves of the $C_2H_2^+ \longrightarrow$ CH_2^+, CH^+, and C^+ peaks.

Incident ion energy: 3000 eV, target: helium.

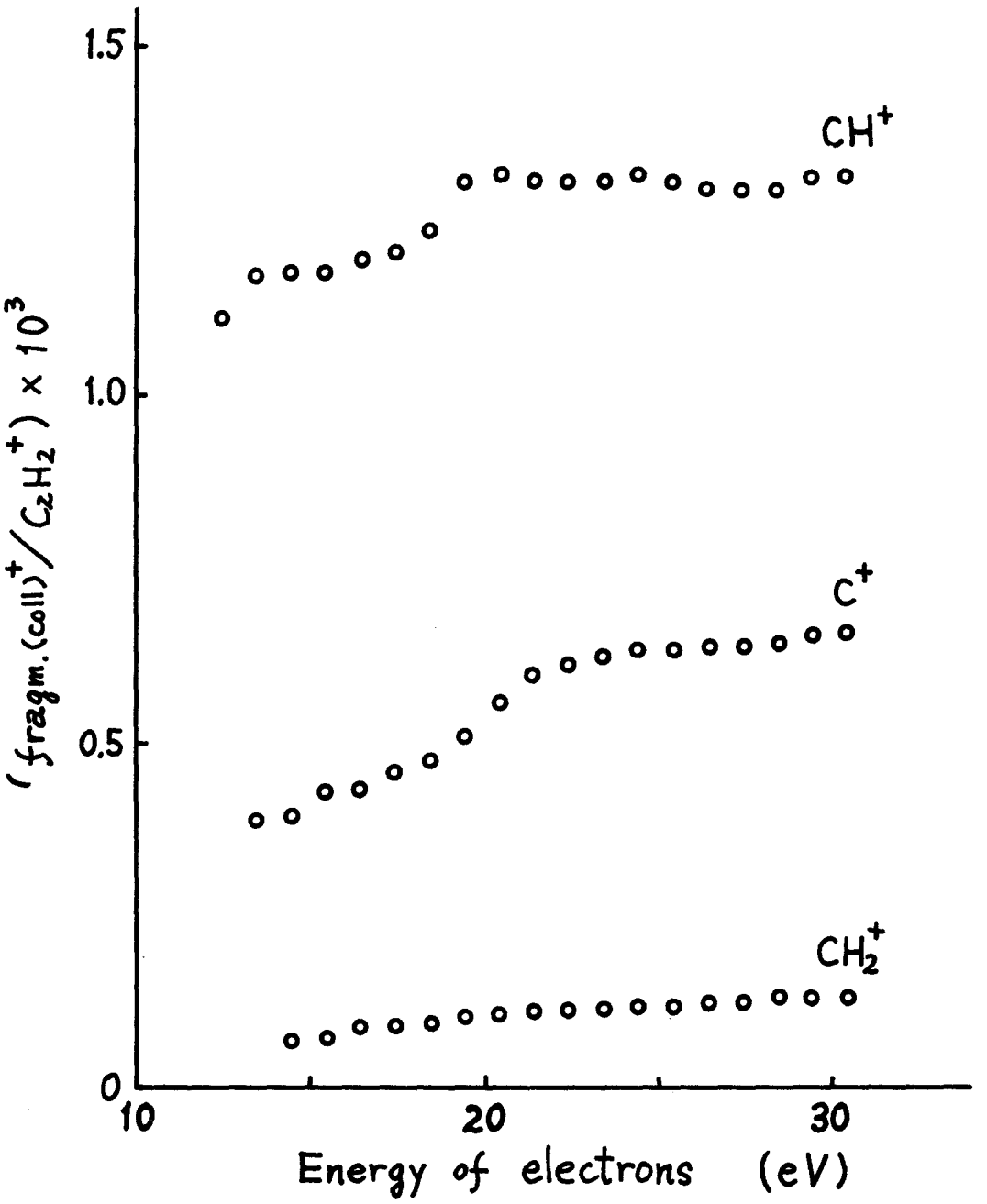

Figure 12-6. Ratios of peak heights for $C_2H_2^+ \longrightarrow CH_2^+$, CH^+, and C^+ and for $C_2H_2^+$ as a function of electron energy.

Incident ion energy: 3000 eV, target: helium.

Table 12-3. Processes $C_2H_2^+ \xrightarrow{M}$ C^+, CH^+, and CH_2^+

Vo = 3000 eV

fragment ion	target gas	Ion current ratio (frag.$^+$(coll)/ $C_2H_2^+$) $/\sqrt{M}$			
		15 eV	20 eV	25 eV	30 eV
C^+	He	0.97×10^{-4}	1.26×10^{-4}	1.48×10^{-4}	1.54×10^{-4}
	Xe	0.11×10^{-4}	0.13×10^{-4}	0.15×10^{-4}	0.16×10^{-4}
CH^+	He	2.75×10^{-4}	3.06×10^{-4}	3.06×10^{-4}	3.08×10^{-4}
	Xe	0.40×10^{-4}	0.46×10^{-4}	0.50×10^{-4}	0.49×10^{-4}
CH_2^+	He	0.16×10^{-4}	0.24×10^{-4}	0.27×10^{-4}	0.31×10^{-4}
	Xe	0.02×10^{-4}	0.04×10^{-4}	0.05×10^{-4}	0.05×10^{-4}

Table 12-4. Ratio of the cross section for C^+, CH^+, and CH_2^+ formations

Vo = 3000 eV

fragment ion	target gas	Cross section ratio $\sigma(\text{frag.}^+) / \sigma(CH^+)_{He}$			
		15 eV	20 eV	25 eV	30 eV
C^+	He	0.35	0.41	0.48	0.50
	Xe	0.04	0.04	0.05	0.05
CH^+	He	1.00	1.00	1.00	1.00
	Xe	0.16	0.15	0.16	0.16
CH_2^+	He	0.06	0.08	0.08	0.10
	Xe	0.00_7	0.01_3	0.01_6	0.01_6

that for CH^+ formation with helium at each electron energy, increases with increasing electron energy, whereas the ratio of the cross section for CH^+ formation with xenon to that with helium is almost constant, as shown in Table 12-4. These results may suggest that the formation process of CH^+ fragments is different from that of C^+ or CH_2^+ fragments.

It can be concluded from the results mentioned in Part 4 that the studies on collision-induced dissociation of fast ions provide available information for investigating a correlation between the electronic levels of molecule ions and those of their dissociative fragments. Measurements of collision-induced dissociation cross sections obtained by the variation of relevant parameters (initial state of molecule ions, their incident velocity, their time of flight, and the kind of target) allow a distinction to be made between the transition due to electronic excitation and that due to vibrational excitation. Precise measurements of the inelastic energy loss of the center-of-mass of molecule ions on collision, as a function of ionizing electron energy, may give the value of the energy of the upper dissociative level of excited molecule ions attained in the collision. Further, the identification of dissociation processes due to vibrational excitation may provide important knowledge on the adiabatic correlations of electronic states of non-symmetric molecule ions with their fragments.

The line of investigations described in the present Part may also lead to interesting and important results which will give rise to extensive development in the studies of primary processes in radiation-induced reactions.

References

1) C. E. Melton, M. M. Bretscher, and R. Baldock, J. Chem. Phys., 26, 1302 (1957).

2) S. E. Kuprijanov and A. A. Perov, Zh. Fiz. Khim., 42, 857 (1968); (Russ. J. Phys. Chem., 42, 447 (1968)).

3) Pham D., Thèse de Doctorat, Paris (1965).

4) F. H. Coats and R. C. Anderson, J. Am. Chem. Soc., 77, 895 (1955).

5) P. Kusch, A. Hustrulid, and J. T. Tate, Phys. Rev., 52, 843 (1937).

6) J. Momigny and E. Derouane, "Advances in Mass Spectrometry", Vol. 4, p. 607, Institute of Petroleum, London, 1968.

7) V. H. Dibeler, F. L. Mohler, and R. M. Reese, J. Research Natl. Bur. Standards, 38, 617 (1947).

8) A. J. C. Nicholson, J. Chem. Phys., 43, 1171 (1965).

P A R T 5

SUMMARY

Studies on the initiating species of radiation-induced polymerization of nitroethylene and on the formation processe of ions under the influence of radiation were described in Parts 2, 3 and 4. The experimental results will be now summarized.

PART 2. RADIATION-INDUCED POLYMERIZATION OF NITROETHYLENE

Chapter 1. Solution Polymerization at Low Temperature

The radiation-induced polymerization of nitroethylene was carried out in tetrahydrofuran solution at -78°C. The kinetic order of the rate of polymerization was 1.0 in reference to the dose rate and the monomer concentration. The molecular weight of the polymer obtained was independent of both the conversion and the dose rate, and increased linearly with the increase of the monomer concentration. The G value of the initiation, G_i, which was given by the quotient G(-monomer)/ $\overline{DP}$, did not change with the changes of the conversion, the dose rate or the monomer concentration.

The polymerization was strongly retarded by the addition of a small amount of hydrogen chloride. In the copolymerization of nitroethylene with acrylonitrile, the

monomer reactivity ratios were determined as follows:

$$r_1(NE) = 63 \pm 15, \quad r_2(AN) = 0.01 \pm 0.01 .$$

These results indicate that the polymerization proceeds by an anionic mechanism. Furthermore, the kinetic considera tion led to the conclusion that all of the energy absorbed in the system contributes effectively to the initiation of polymerization.

Chapter 2. Bulk Polymerization at Room Temperature

The radiation-induced polymerization of nitroethylene in bulk was studied at 10°C. The high polymer yield ($G(-\text{monomer}) \simeq 4.7 \times 10^4$) and the strong retardation effect by hydrogen bromide indicate that the polymerization prodeeds even at room temperature by an anionic mechanism involving free ions. The calculated G_i value of 2.3 (average) for this monomer is much larger than the value (about 0.1) obtained for various cationic polymerizations of hydrocarbons. This difference may be explained in terms of the large dielectric constant and high electron affinity of this monomer. By the competitive kinetic method based on the retarding effect of hydrogen bromide, the propagation rate constant at 10°C was estimated to be about 4×10^7 M^{-1} sec^{-1}.

Chapter 3. Dose Rate Dependence of Bulk Polymerization at Room Temperature

The polymerization of extremely dried nitroethylene in bulk was studied as a function of dose rate. The experimental results indicate that the technique of drying the monomer is very important in anionic polymerization as well as in cationic polymerizations reported by many researchers. The observed value of G(-monomer), which lay in the range between 1.68×10^4 and 1.90×10^5, was about 10 times as large as that in the normally dried one. The rate of polymerization was found to be proportional to the square-root of dose rate. This indicates that the termination reaction takes place by charge recombination between the propagating anions and positively recharged species. By the kinetic analysis based on bimolecular termination, the propagation rate constant at 20°C was estimated. The calculated values of propagation rate constant lie in the range between 1.7×10^4 and 5.3×10^4 M^{-1} sec^{-1}. These values are considerably smaller than the estimated value in Chapter 2. However, taking into consideration that the value in Chapter 2 is un upper limit, these values obtained in the present study seem to be reasonable, despite the uncertainity of the value of termination rate constant.

Chapter 4. Studies on Initiating Species

For the purpose of studying the initiating species of the radiation-induced polymerization of nitroethylene, the electron spin resonance (ESR) measurements of irradiated 2-methyltetrahydrofuran (MTHF) glass containing nitroethylene were carried out at -196°C, and also the negative ions from nitroethylene formed by the electron impact were measured by means of a mass spectrometer. In ESR measurements, MTHF glass containing 1.5 mole % nitroethylene gave no spectrum due to the trapped electrons, but showed a new complex spectrum superposed on the spectrum of MTHF radicals. This new complex spectrum was bleached out by photoirradiation of visible light. This spectrum is thought to be due to anion radicals formed through the electron capture by added nitroethylene. The MTHF glass containing 0.15 mole % nitroethylene showed spectra of both trapped electrons and the nitroethylene anion radicals after the irradiation. When the irradiated glassy mixture was maintained at -196°C in the dark, the signal intensity of the trapped electrons gradually decreased and that of the nitroethylene anion radicals increased with the keeping time. This indicates that the nitroethylene molecule has an ability as a strong electron acceptor.

In mass spectra of negative ions formed from nitroethylene, the parent negative ion was observed at a pressure of 2.6×10^{-6} mmHg. The appearance potential of this ion was found to be about 0 eV. This also indicates that nitroethylene is a strong electron acceptor in accordance with the result of ESR measurements. It was suggested from these results that the anion radicals of nitroethylene were readily formed by the capture of electrons and these species were responsible for the initiation process of the radiation-induced anionic polymerization of nitroethylene.

Chapter 5. Investigations on Postpolymerization

Radiation-induced postpolymerization of nitroethylene in 2-methyltetrahydrofuran glass was studied and discussed in reference to the results obtained from ESR measurements described in Chapter 4. No postpolymerization occurred at the temperature below $-150^{\circ}C$. In the temperature range between $-135^{\circ}C$ and $-78^{\circ}C$, the polymer yield decreased with the rising temperature of the postpolymerization. The polymer yield increased linearly with the increase of the preirradiation dose in the range below 0.9×10^{6}r. The mean value of G(-monomer) was obtained as 2.73×10^{2}, and the G_i value for chain initiation was estimated to be about 1.3. The following correlations were observed between the results

of the postpolymerization and ESR measurements: (i) the postpolymerization started in the temperature range between -140°C and -135°C where the ESR spectrum due to the anion radicals of nitroethylene disappeared, and (ii) the polymer yield of the postpolymerization decreased with the photo-irradiation at -196°C before warming the samples, while at the the same time the photo-bleachability of the anion radicals was observed in the glassy mixture by the ESR method. It was concluded from these results that the radiation-induced postpolymerization was initiated by the anion radicals of nitroethylene formed by the capture of electrons.

Chapter 6. Reaction Mechanisms in Polymerization

In order to clarify the characteristics of radiation-induced polymerization, the reaction mechanism of radiation-induced polymerization of nitroethylene, described in the preceding Chapters, was summarized and discussed in comparison with the results of other monomers obtained by several workers.

Compared with catalytic polymerizations, the characteristics of radiation-induced polymerization appear to be as follows:

(1) coexistence of radical and ionic polymerizations and contribution of ion radicals to the initiation process, and

(2) propagation by free ions.

The first of these characteristics was studied in the radiation-induced copolymerization of p-chlorostyrene (Cl-St) with styrene (St). The monomer reactivity ratio (MRR) at 9°C was almost the same as that obtained by conventional free radical initiators and the MRR at -78°C coincided with that by cationic catalysts. When the copolymerization was carried out at -40°C, the intermediate value of the MRR between 9°C and -78°C was obtained. Furthermore, the copolymer composition curve at -40°C approached the cationic one by the addition of a small amount of DPPH which is a typical radical scavenger, and it was almost consistent with the free radical composition curve by the addition of triethylamine as a cation scavenger. It was suggested from these results that the cationic and free radical species, coexisting in the initiation process, were contributed equally at -40°C.

In the radiation-induced polymerization of nitroethylene, the anion radicals appeared to contribute to the initiation process as mentioned in Chapters 4 and 5. Similar results were also obtained in the study of the electronic spectra of nitroethylene.

The results described above indicate that ionic and free radical species, which are capable of initiating the polymerizations, coexist in the irradiated system, and the

contribution of ion radicals for the initiation process is very important in radiation-induced ionic polymerizations.

Another distinctive feature of radiation-induced polymerization seems to be the propagation by free ions as previously pointed out. Recent extensive studies in radiation-induced polymerization have provided experimental evidence of propagation by free ions. Measurements of radiation-induced electroconductivity have also established the presence of free ions in the polymerization system.

As shown in the preceding Chapters, the radiation-induced polymerization of nitroethylene proceeds by an anionic mechanism involving free ions. In order to compare the results obtained in the present studies with those of cationic polymerization, the propagation rate constant in various systems were summarized. Although the quantitative comparison of these values may be present difficulties because of the different polymerization conditions and estimation methods, the concept seems to be established that the propagation rate constant for free ions is very large for both cationic and anionic propagations.

To conclude, it is shown from the results obtained in Part 2 that the radiation-induced polymerization of nitroethylene is initiated by the anion radicals of nitroethylene, propagated by free anionic species, and terminated by

charge recombination between tne propagating anions and the positively recharged species.

PART 3. MASS SPECTROMETRIC STUDY ON NEGATIVE ION-MOLECULE REACTIONS OF NITROETHYLENE

Chapter 7. Formation of Negative Ions

The use of mass spectrometry to detect and identify transient intermediates produced by ionizing radiation has provided new insight into the mechanism of radiation chemistry.

In order to obtain some information on the initiating species of radiation-induced anionic polymerization of nitroethylene, the formation of negative ions from nitroethylene was studied by means of a mass spectrometer. The ionization efficiency curves of several negative ions from nitroethylene were measured as a function of the impact electron energy. From these curves, the appearance potentials and the apparent energy width of the resonance electron capture processes were obtained. The most interesting result was that the existence of the parent negative ion, of which the appearance potential is about 0 eV and the width of the resonance capture is very narrow, was confirmed at low

source pressure. This indicates that the nitroethylene molecule has an ability to capture easily thermal electrons by nondissociative process. Furthermore, the lifetime of the parent ion and the cross section of the parent ion formation were estimated to be 14 μsec and 1.3×10^{-16} cm^2, respectively.

Chapter 8. Dimer Negative Ion Formation by Ion-molecule Reaction

From the point of view of studying the initial process of the polymerization, particular attention was paid to the formation process of the dimer negative ion of nitroethylene. The ionization efficiency curve of the dimer ion was in close agreement with that of the parent negative ion. Furthermore, the plots of the intensity ratio of the dimer ion to the parent ion vs. the source pressure of nitroethylene gave a linear relation. It is evident from these results that the precursor of the dimer negative ion is the parent negative ion, and the dimer ion is formed by the ion-molecule reaction of the parent ion with neutral molecule. From results of the pressure dependence, the rate constant of this ion-molecule reaction was estimated to be 3.2×10^{-13} cm^3 $molecule^{-1} sec^{-1}$. The estimated rate constant was discussed in comparison with the theoretical value based on the modified collision theory.

Chapter 9. Formation of the Parent and the Dimer Negative Ions at Higher Electron Energies

The formation processes of the parent and the dimer negative ions of nit. ethylene at higher electron energies above 20 eV were studied under higher source pressure. At pressures less than 10^{-4} torr, the intensity of the parent negative ion appeared to be of second order with respect to the pressure in all the electron energies above 25 eV. A three-boby process obviously occurred under these conditions, indicating that the parent negative ion is stabilized by collision. At source pressures above 10^{-4} torr, the intensity of the parent negative ion was revealed to be higher than second order dependence with respect to the pressure. In order to obtained some information on the parent ion formation at higher pressure, the effects of added rare gases in the ionization chamber were studied at the electron energy of 100 eV. At a constant pressure of nitroethylene of 10^{-5} torr, second order dependence of added gas pressure on the ion intensity was observed in all cases of used rare gases, and the relative intensities were found to increase in the order ; neon, argon, krypton and xenon. At a constant pressure of rare gases (10^{-3} torr), the intensity of the parent ion was proportional to the pressure of nitroethylene. The formation process of the parent ion was discussed on the

basis of experimenta_ results mentioned above.

For the dimer negative ion at electron energy of 100 eV, the ion intensity wa found to be of fourth order with respect to the nitroethylene pressure less than 10^{-4} torr and to be higher than fourth order at pressures above 10^{-4} torr. However, the intensity ratio of the dimer ion to the parent ion showed second order dependence with respect to the pressure in the whole pressure range examined. This may indicate that the dimer negative ion formed initially by ion-molecule reaction is in vibrationally excited states, and requires collisional stabilization. The effect of added rare gases on the dir r ion formation were also examined and discussed.

It is concluded from the results mentioned in Part 3 that the precursor of the dimer negative ion is the parent negative ion formed by the capture of thermal or near-thermal energy electrons and that the dimer ion, which leads to the trimer ion through a consecutive reaction, is produced by the ion-molecule reaction between the parent ion and the neutral molecule. Furthermore, it seems probable that the process of collisional stabilization of the product ions is very important at hig er electron energies. These findings give rise to the suggestion that the precursor of the radiation-induced polymerization of nitroethylene is the parent negative ion.

PART 4. MASS SPECTROMETRIC STUDY ON PRIMARY PROCESSES IN RADIATION-INDUCED REACTIONS

Chapter 10. Collision-induced Dissociation of Acetylene Ions. Part I. Process $C_2H_2^+ \longrightarrow C_2H^+ + H$

It has been recognized that the role of ionic fragmentation processes in radiation chemistry is very important, although the details of these processes, especially in polyatomic molecules, are not yet clear. One of the most useful methods of studying these processes is to excite fast ground-state or metastable-state ions into the dissociative states of molecule ions by collision with atomic or molecular targets. In Part 4, the fragmentation processes of acetylene molecule ions induced by collision with rare gas atoms were investigated.

For the first part of the present work, the dissociation processes of $C_2H_2^+$ ions into C_2H^+ ions were studied in Chapter 10. The collision-induced dissociation cross section of C_2H^+ fragment ions were measured by the variation of relevant parameters such as ionizing electron energy, incident ion energy, delay between production of the ions and collision, and nature of the target used. From the result obtained, two processes were discriminated for the collision-induced

dissociation of $C_2H_2^+$ ions into C_2H^+ fragment ions as follows:

- a) electronic excitation of any vibrational level of the $X^2\Pi_u$ ground state, leading to an upper state, dissociative or predissociated, lying at 17.3 ± 0.5 eV; this state is proposed to be either the first $^2\Sigma_g^+$ state or the first $^2\Delta_g$ or the first $^2\Phi_g$ or $^2\Pi_g$ state of $C_2H_2^+$;

- b) dissociation - most probably by collision-induced predissociation or else by adiabatic momentum transfer - of vibrationally excited levels, lying between 17.2 and 17.8 eV, of the first $^2\Sigma_g^+$ state of $C_2H_2^+$; in the case of a collision-induced predissociation, the fragments $C_2H^+(^3\Sigma_g^-)$ + $H(^2S)$ would be obtained through the $^2\Sigma_g^-$ state of $C_2H_2^+$, or the fragments C_2H^+ $(^1\Delta_g)$ + H (^2S) through the $^2\Delta_g$ state of $C_2H_2^+$.

Chapter 11. Collision-induced Dissociation of Acetylene Ions. Part II. Process $C_2H_2^+ \longrightarrow H^+ + (C_2H)$

In order to compare the dissociation mode of H^+ ion formation with that of C_2H^+ ions, the collision-induced dissociation process of acetylene ions into H^+ + (C_2H) was studied by the use of helium as a target. Similar measurements to those in Chapter 10 were carried out. The most interesting feature was the effect of incident ion translational energy. The cross section for the formation

of H^+ fragment ions was found to decrease with increasing ion energy, in contrast to the behavior observed in the formation of C_2H^+ fragment ions.

It was concluded from the results obtained that the collision-induced dissociation of $C_2H_2^+$ ions into $H^+ + (C_2H)$ is an adiabatic process, viz. a momentum transfer from the proton to the target atom, leading to dissociation of electronically ground-state $C_2H_2^+$ ions.

This means that the $X^2\Pi_u$ ground state of $C_2H_2^+$ is adiabatically correlated with $H^+ + C_2H$ ($X^2\Pi_u$) rather than C_2H^+ ($^3\Pi_u$) + H (^2S) as represented in Figure 1 of Fiquet-Fayard's paper. Thus an explanation can be found why the dissociation of ground-state $C_2H_2^+$ ions into $C_2H^+ + H$ is necessarily an electronic transition and not an adiabatic process (see Chapter 10).

A consequence of this statement is that the energy of $C_2H^+(^3\Pi_u) + H(^2S)$ is higher than that of C_2H ($X^2\Pi_u$) + H^+, and thus that the energy of the $^3\Pi_u$ state of C_2H^+ above its $^3\Sigma_g^-$ ground -state is more than I.P.(H) - I.P.(C_2H) = 13.6 - (11.25 $\pm$ 0.15) = 2.35 $\pm$ 0.15 eV.

Chapter 12. Collision-induced Dissociation of Acetylene Ions. Part III. Processes $C_2H_2^+ \longrightarrow C_2^+$, CH_2^+, CH^+, and C^+

By the same line of investigation, the collision-induced dissociation of acetylene molecule ions was studied on four processes to produce C_2^+, CH_2^+, CH^+, and C^+ fragment ions.

For the dissociation process on C_2^+ fragment ions, it was tentatively concluded from the effects of target and of initial translational energy that the main process of producing C_2^+ fragments by collision, which concerns ground-state $C_2H_2^+$ ions, is an electronic excitation. For the other three dissociations on CH_2^+, CH^+, and C^+ fragment ions, the processes through an electronic excitation also seemed to be probable.

It can be concluded from the results mentioned in Part 4 that the studies on collision-induced dissociation of fast ions provide available information for investigating a correlation between the electronic levels of molecule ions and of their dissociative fragments. Measurements of collision-induced dissociation cross sections obtained by the variation of relevant parameters (initial state of

molecule ions, their incident velocity, their time of flight, and the kind of target) allow a distinction to be made between the transition due to electronic excitation and that due to vibrational excitation. Precise measurements of the inelastic energy loss of the centre-of-mass of molecule ions on collision, as a function of ionizing electron energy, may give the value of the energy of the upper dissociative level of excited molecule ions attained in the collision. Further, the identification of dissociation processes due to vibrational excitation may provide important knowledge on the adiabatic correlations of electronic states of non-symmetric molecule ions with their fragments.

The line of investigation described in the present Part may also lead to interesting and important results which will give rise to extensive development in the studies of primary processes in radiation-induced reactions.

LIST OF PUBLICATIONS

Chapter 1 Kobunshi Kagaku (Chemistry of High Polymers, Japan), 24, 79 (1967).

Chapter 2 Trans. Faraday Soc., 63, 376 (1967).

Chapter 3 J. Polymer Sci. B, 7, 371 (1969).

Chapter 4 J. Polymer Sci. B, 4, 629 (1966); ibid., 5, 329 (1967).

Chapter 5 J. Polymer Sci. A-1, in press.

Chapter 6 Kobunshi Kagaku, 24, 649 (1967); Proceedings of 2nd Tihany Symp. on Rad. Chem., p. 451, Akadémiai Kiadó, Budapest, 1967.

Chapter 7 J. Phys. Chem., to be published.

Chapter 8 Preprints of IUPAC Intern. Symp. on Macromol. Chem., Budapest, 1969.

Chapter 9 J. Phys. Chem., to be published.

Chapter 10 and

Chapter 11 J. Chem. Phys., 51, 3465 (1969).

Chapter 12 Unpublished.

Other publications not included in the present thesis.

Original papers

The Studies on the Cationic Polymerization of Alkyl Vinyl Ethers by Heterogeneous Catalysts.
I. The Polymerization of Isobutyl Vinyl Ether Catalyzed by Metal Sulfate-Sulfuric Acid Complexes.
Kobunshi Kagaku, 18, 561 (1961).

Radiation-induced Polymerization of Formaldehyde.
Part 1. Experimental Results.
Makromol. Chem., 76, 196 (1964).

Part 2. Kinetic Consideration.
Proceedings of 4th Japan Conference on Radioisotopes, 4, 305 (1963);
Annual Report of Japan Assoc. Rad. Res. Polymers, 3, 139 (1961).

Part 3. Copolymerization with other aldehydes.
Proceedings of 5th Japan Conference on Radioisotopes, 5, 238 (1963).

Studies on Radiation-induced Ionic Polymerization.
Part 1. Solution Polymerization of Styrene at Low Temperature.
Intern. J. Appl. Rad. Isotopes, 17, 513 (1966).

Part 2. Effect of Solvent on the Polymerization of Isobutene at Low Temperature.

Intern. J. Appl. Rad. Isotopes., 17, 595 (1966).

Cationic Polymerization of Isobutyl Vinyl Ether Initiated by the Species Derived from Aldehydes or Ketones and Maleic Anhydride.

J. Polymer Sci. B, 4, 509 (1966).

Reviews

Radiation-induced Polymerization of Formaldehyde.

Nippon Kagakusen-i Kenkyusho Koen Shu (Annual Report of the Research Institute for Chemical Fibers, Japan), 18, 65 (1961); Genshiryoku Kogyo (Nuclear Engineering, Japan), 7, (No. 12) 31 (1961).

Radiation-induced Polymerization.

Shikizai Kyokai-shi (Journal of the Japan Society of Colour Material), 35, 543 (1962).

Radiation-induced Polymerization of Aldehydes and Ketones.

Industrial Uses of Large Radiation Sources, Vol. 1, p.219, Intern. Atomic Energy

Agency, Vienna, 1963.

Radiation-induced Solution Polymerization at Low Temperature. Nippon Kagakusen-i Kenkyusho Koen Shu, 22, 71, (1965).

Radiation-induced Polymerization by Free Ions. Kobunshi (High Polymers, Japan), 16, 922 (1967).

Cationic Polymerization. Kogyo Kagaku Zasshi (Journal of the Chemical Society of Japan, Industrial Chemistry Section), 70, 1859 (1967).